

AD-A248 943



EXCC 987

(2)

PL-TR-91-2194

**DATA ANALYSIS SUPPORT FOR THE SHUTTLE
POTENTIAL AND RETURN ELECTRON
EXPERIMENT (SPREE) ON THE TETHERED
SATELLITE SYSTEM 1 (TSS-1) FLIGHT**

**T. T. Luu
J. R. Lilley
V. A. Davis
I. Katz**



**Maxwell Laboratories, Inc.
S-CUBED Division
P.O. Box 1620
La Jolla, California 92038-1620**

June 24, 1991

Scientific Report No. 1

Approved for public release; distribution unlimited



**Phillips Laboratory
Air Force Systems Command
Hanscom Air Force Base, Massachusetts 01731-5000**

92-09495



92 4 13 086

"This technical report has been reviewed and is approved for publication"


MARILYN R. OERHARDT, CAPT, USAF
Contract Manager


E. G. MULLEN
Branch Chief


RITA C. SAGALYN
Director, Space Physics Division

This document has been reviewed by the ESD Public Affairs Office (PA) and is releasable to the National Technical Information Service (NTIS).

Qualified requestors may obtain additional copies from the Defense Technical Information Center. All others should apply to the National Technical Information Service.

If your address has changed, or if you wish to be removed from the mailing list, or if the addressee is no longer employed by your organization, please notify GL/IMA, Hanscom AFB, MA 01731. This will assist us in maintaining a current mailing list.

Do not return copies of this report unless contractual obligations or notices on a specific document requires that it be returned.

REPORT DOCUMENTATION PAGE			Form Approved OMB No. 0704-0188	
<small>Public reporting burden for this collection of information is estimated to average 1 hour per response, including the time for reviewing instructions, searching existing data sources, gathering and maintaining the data needed, and completing and reviewing the collection of information. Send comments regarding this burden estimate or any other aspect of this collection of information, including suggestions for reducing this burden, to Washington Headquarters Services, Directorate for Information Operations and Reports, 1215 Jefferson Davis Highway, Suite 1204, Arlington VA 22202-4302, and to the Office of Management and Budget, Paperwork Reduction Project (0704-0188), Washington, DC 20503.</small>				
1. AGENCY USE ONLY (Leave blank)		2. REPORT DATE June 24, 1991		3. REPORT TYPE AND DATES COVERED Scientific Report No. 1
4. TITLE AND SUBTITLE "Data Analysis Support for the Shuttle Potential and Return Electron Experiment (SPREE) on the Tethered Satellite System 1 (TSS-1) Flight"			5. FUNDING NUMBERS F19628-90-C-0133 PE 63410F PR 2822 TA01 WUAK	
6. AUTHOR(S) T. T. Luu V. A. Davis J. R. Lilley I. Katz				
7. PERFORMING ORGANIZATION NAME(S) AND ADDRESS(ES) Maxwell Laboratories, Inc. S-Cubed Division P. O. Box 1620 La Jolla, CA 92038-1620			8. PERFORMING ORGANIZATION REPORT NUMBER SSS-DPR-91-12627	
9. SPONSORING/MONITORING AGENCY NAME(S) AND ADDRESS(ES) Phillips Laboratory Hanscom Air Force Base, MA 01731-5000 Contract Manager: Capt. M. Oberhardt/PHE			10. SPONSORING/MONITORING AGENCY REPORT NUMBER PL-TR-91-2194	
11. SUPPLEMENTARY NOTES				
12a. DISTRIBUTION/AVAILABILITY STATEMENT Approved for public release; distribution unlimited			12b. DISTRIBUTION CODE	
13. ABSTRACT (Maximum 200 words) This report describes the first year of a scientific study of the interactions between the first flight of the Tethered Satellite System (TSS-1) and the ionosphere to increase understanding of the structure and current characteristics of high-voltage sheaths in the ionosphere. The investigations described here include a determination of the tether current and voltages, an evaluation of the shuttle orbiter ion collection, the ion current detected by the SPREE instrumentation, and the effect of the subsatellite thrusters on the surrounding neutral densities.				
14. SUBJECT TERMS tether, TSS-1, shuttle, current collection, SPREE			15. NUMBER OF PAGES 126	
			16. PRICE CODE	
17. SECURITY CLASSIFICATION OF REPORT Unclassified	18. SECURITY CLASSIFICATION OF THIS PAGE Unclassified	19. SECURITY CLASSIFICATION OF ABSTRACT Unclassified	20. LIMITATION OF ABSTRACT SAR	

TABLE OF CONTENTS

<u>Section</u>	<u>Page</u>
1. INTRODUCTION.....	1
2. CALCULATION OF TSS-1 USING EPSAT (SPECIAL VERSION).....	3
2.1 Introduction.....	3
3. CALCULATIONS OF ION CURRENT COLLECTED BY SHUTTLE ORBITER.....	11
4. CALCULATIONS OF ION CURRENT COLLECTED BY THE SPREE INSTRUMENT	13
5. OBSTRUCTION OF CURRENT OF SPREE INSTRUMENTS DUE TO RMS AND CAMERA.....	85
5.1 Objectives	85
5.2 Procedure	85
5.3 Run Cases	85
5.4 Parameters	86
5.6 Results.....	89
6. CALCULATIONS OF ION CURRENT COLLECTED BY SHUTTLE ORBITER.....	103
6.1 Ion Current Collected as a Function of Orientation.....	103
6.2 Results.....	108
6.3 Ion Current Collected as a Function.....	109
7. NEUTRAL DENSITIES ABOUT TSS-1 SUBSATELLITE	111

1. INTRODUCTION

This interim report covers the period June 15, 1990, to June 23, 1991, and describes the scientific progress on Contract F19628-90-0133 entitled "Data Analysis Support for the SPREE Instruments on the TSS-1 Shuttle Flight." The objective of this contract is a scientific study of the interactions between the first flight of the Tethered Satellite System (TSS-1) and the ionosphere to increase understanding of the structure and current characteristics of high-voltage sheaths in the ionosphere.

During the first year of this contract, we investigated the tether current and voltages, the shuttle orbiter ion collection, the ion current detected by the SPREE instrument, the effect of the subsatellite thrusters on the neutral densities, and provided support for the TSS-1 program.

The technical staff who contributed to the research described in this report are I. Katz, J. R. Lilley, Jr., T. T. Luu, and V. A. Davis.

Accession For	
NTIS GRA&I	<input checked="checked" type="checkbox"/>
DTIC TAB	<input type="checkbox"/>
Unannounced	<input type="checkbox"/>
Justification	
By _____	
Distribution/	
Availability Codes	
Dist	Avail and/or Special
A-1	



2. CALCULATION OF TSS-1 USING EPSAT (SPECIAL VERSION)

2.1 INTRODUCTION

Calculations of the tether current and voltages over the mission were performed using a specially modified version of EPSAT (Environment-Power System Analysis Tool). The model consisted of an orbiter with the subsatellite extended 20 km out of the bay. Collection of electrons was the product of the 1-sided thermal flux and $2\pi r^2$ times the minimum of the space-charge-limited or magnetic-limited collection radii. The ion collection is just the space-charge-limited ion collection to a sphere with effective area that of the engine bells.

The first calculations examined the effect of subsatellite paint resistance on the tether currents. It is uncertain whether the subsatellite paint will be 8K Ω , the highest impedance in the tether circuit, or whether it will have negligible bulk resistance at the operating potentials. With the core gun on, using a perveance of 3.8×10^{-6} , tether currents were calculated for the mission duration of different sphere and tether resistances. The results were surprisingly insensitive to the paint resistance. When the total resistance, tether plus subsatellite paint, was 10K Ω , the peak current was about 60 percent of that for an assumed 2K Ω resistance. Peak subsatellite potentials differed little, because they occur at low plasma density when low ionospheric currents cause the resistive voltage drop to be negligible.

The other sequence of EPSAT studies examined orbiter potentials when the tether is connected to the orbiter chassis through a large resistance. The resistances studied were between 25K Ω and 350K Ω . The calculations showed that the orbiter would charge only at low plasma density, again because the resistive voltage drop is small due to low tether currents. However, orbiter potentials as large as -2200 V resulted when the total tether, subsatellite, and shunt resistance was 35K Ω .

The FPSAT Model

Problem Name: spree2		Object Definition		>HELP<							
-----Axial Views of System-----											
View Front		Drafting View		Axonometric View of System							
View Side				View Direction:							
View Top				Theta 0.0							
				Phi 0.0							
				Axonometric View							
Create Another Object			Delete An Object								
Object	Solar Array	Position			Dimensions			Orientation			
		Len(Z)	Width(Y)	Hght(X)	Len(Z)	Width(Y)	Hght(X)	Theta	Phi	Twist	
nose	no	-14.0	0.0	0.0	4.00	4.00	8.00	0.	0.	0.	surf_spec.
body	no	0.0	0.0	0.0	8.00	8.00	20.00	0.	0.	0.	surf_spec.
wing	no	5.0	0.0	0.0	1.00	30.00	10.00	0.	0.	0.	surf_spec.
tail	no	7.5	0.0	8.0	5.00	1.00	5.00	0.	0.	0.	surf_spec.
engines	no	10.5	0.0	0.0	8.00	8.00	1.00	0.	0.	0.	surf_spec.
spree	no	0.0	0.0	8.0	1.00	1.00	1.00	0.	0.	0.	surf_spec.
subsat	no	0.0	0.0	0.0	1.02	1.02	1.02	0.	0.	0.	surf_spec.

The conducting surfaces are spree, engines, and subsat.

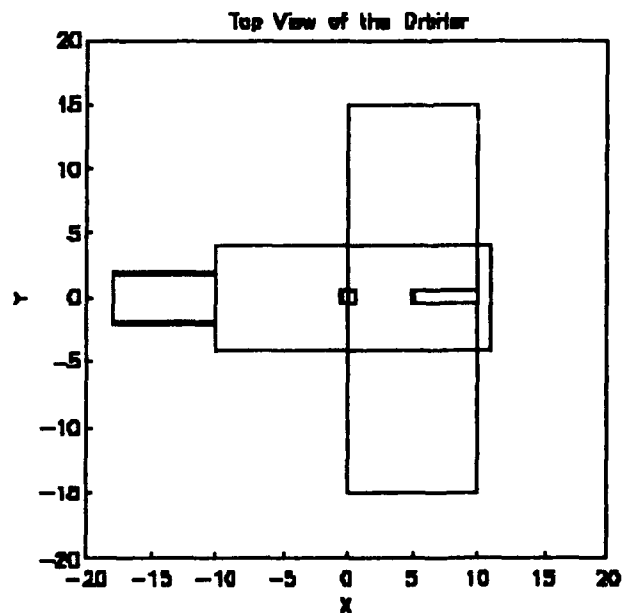


Figure 2.1 The EPSAT model of the shuttle orbiter.

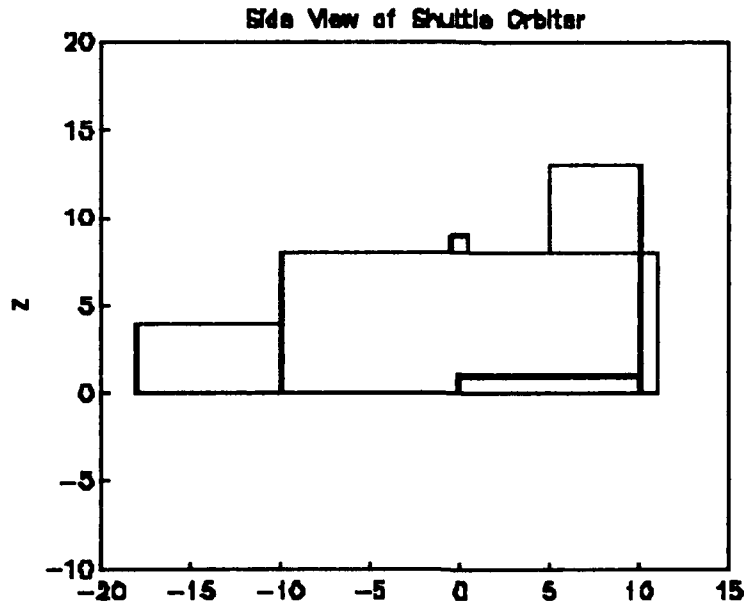


Figure 2.2 Side view of the EPSAT Orbiter model.

The model was oriented with the subsatellite away from the earth.

Update	Object_Orientation			

	Rotation from Body to (Ram) Space Frame			
	X(Velocity Direction)		Y	Z(Down)
Rotation Axis	1.000		0.000	0.000
Rotation Angle	1.800E+02			

Stabilization	gravity			

	Spin Stabilization			
	X(body)		Y(body)	Z(body)
Rotation Axis	1.000		1.000	1.000
Rotation Rate	0.000E+00			

Time_into_Mission	9.420E+04			
	Vector_from_System_Center_to_Point		Velocity Vector	
Point	Body		Space	
	Body		Space	
Altitude	0.000E+00	X 7.407E+05	N 7.407E+05	X 7.425E+03 N -3.150E+03
Latitude	0.000E+00	Y 5.679E+06	E -5.679E+06	Y -6.193E-08 E 7.053E+03
Longitude	0.000E+00	Z -9.587E+06	D 9.587E+06	Z -7.083E-01 D 7.083E-01

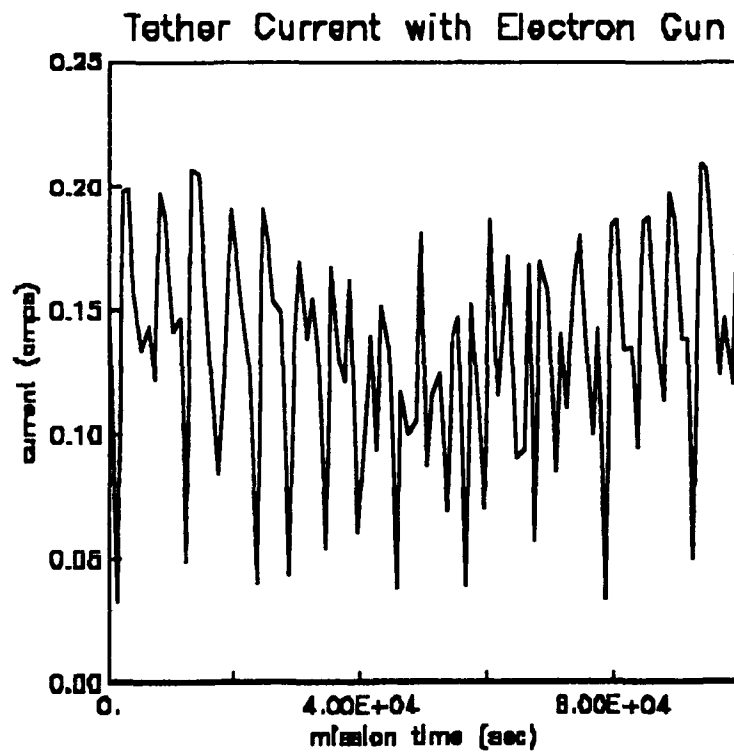


Figure 2.3

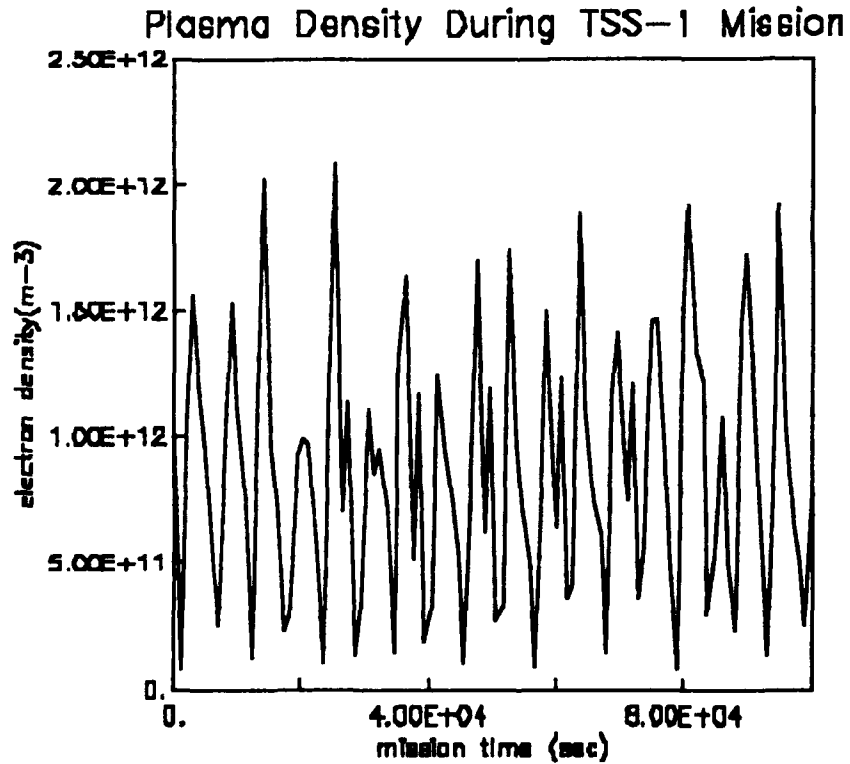


Figure 2.4

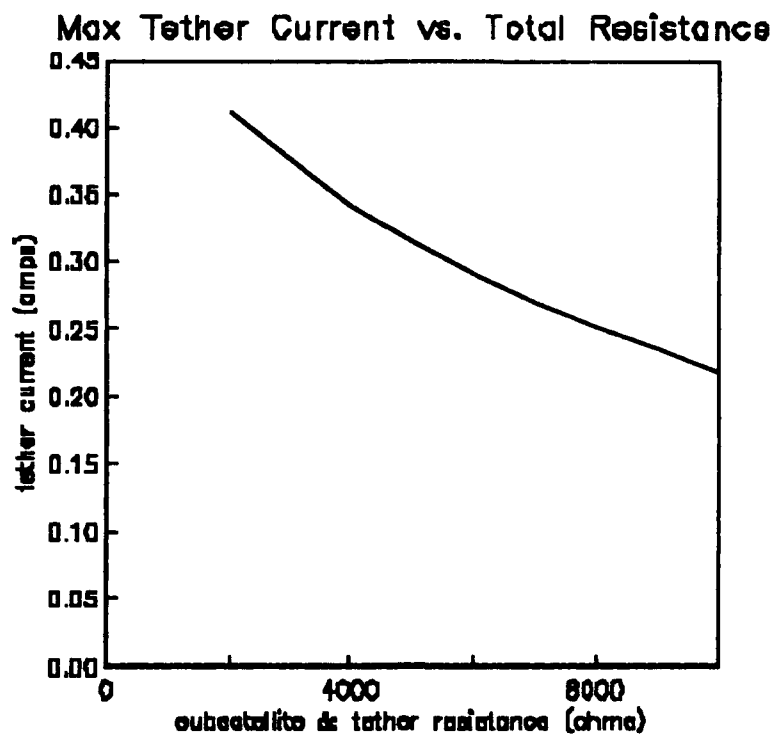


Figure 2.5

Results for a low current time on orbit.

No gun, 35K Ω impedance.

Update		Floating Potentials						
<hr/>								
Max Iterations	15	Plasma Thermal Currents						
Max Current	1.000E-03	Ion	9.6263E-06					
Voltage tol	1.000E-02	Electron	-6.4821E-04					
	Altitude	399.	Magnetic Field (B)					
Mission Time	1.010E+03	Latitude	25.3	North	0.163			
Unvrsl Time	1.010E+03	Longitude	58.6	East	-3.595E-02			
Angle between velocity and solar array	24.5	Down	-0.210					
<hr/>								
Object	Location	Radius	Bias Voltage	V X B Voltage	Floating Potential	Current		
nose	-14.0	0.0	2.0	3.6	0.000E+00	0.000E+00	-2222.	0.
body	0.0	0.0	4.0	7.8	0.000E+00	4.163E-01	-2222.	0.
wing	5.0	0.0	0.5	7.4	0.000E+00	-3.181E-01	-2222.	0.
tail	7.5	0.0	10.5	2.4	0.000E+00	1.777E+00	-2220.	0.
engines	10.5	0.0	4.0	3.6	0.000E+00	4.142E-01	-2222.	1.745E-02
spree	0.0	0.0	8.5	0.7	0.000E+00	1.359E+00	-2221.	2.445E-03
subsat	0.0	0.0*****	0.7	0.000E+00	4.140E+03	1272.	-1.990E-02	

3.8E-6 Perveance, 10K Ω Impedance.

Update		Floating Potentials	
Max Iterations	15	Plasma Thermal Currents	
Max Current	1.000E-03	Ion	9.6263E-06
Voltage tol	1.000E-02	Electron	-6.4821E-04
	Altitude	399.	Magnetic Field (B)
Mission Time	1.010E+03	Latitude	25.3
Unvrsl Time	1.010E+03	Longitude	58.6
Angle between velocity and solar array	24.5	North	0.163
		East	-3.595E-02
		Down	-0.210

Object	Location	Radius	Bias Voltage	V X B Voltage	Floating Potential	Current
nose	-14.0 0.0 2.0	3.6	0.000E+00	0.000E+00	-340.5	0.
body	0.0 0.0 4.0	7.8	0.000E+00	4.163E-01	-340.1	0.
wing	5.0 0.0 0.5	7.4	0.000E+00	-3.181E-01	-340.8	0.
tail	7.5 0.0 10.5	2.4	0.000E+00	1.777E+00	-338.7	0.
engines	10.5 0.0 4.0	3.6	0.000E+00	4.142E-01	-340.1	3.235E-02
spree	0.0 0.0 8.5	0.7	0.000E+00	1.359E+00	-339.2	7.671E-04
subsat	0.0 0.0*****	0.7	0.000E+00	4.190E+03	3519.	-3.311E-02

The orbital parameters used for the EPSAT study.

Update		Orbit Generator			

Orbit Parameters					
Name	Value	Name	Value	Mission Start	
Time Span	24.00	Num of Pts	200	Day	335.
Apogee	400.00	Perigee	400.00	Time	0.
Inclination	28.00	Mean Anomaly	0.00	Year	1991.
Arg of Perigee	0.00	Rt. Ascension	0.00		

Path Used orbit					

Quantity	Average		Minimum	Maximum	
Altitude	4.004E+02		3.926E+02	4.100E+02	
Longitude	1.750E+02		6.035E-02	3.566E+02	
Latitude	5.350E-01		-2.798E+01	2.798E+01	

Point on Path					
Time	Unvrs. Time	Latitude	Longitude	Velocity	
9.620E+04	7880.	4.073E+02	1.478E+01	1.171E+02	7.725E+03

Plasma conditions at one time during the mission.

Update	Ambient Plasma		

Mission Parameters			
Start Day	335.	Sunspot Number	100.
Time into Mission	9.420E+04		

Orbital Position Variables			
Name	Value	Name	Value
Altitude	402.27	Day of Year	336.
Latitude	14.78	Universal Time	7.200E+06
Longitude	117.07	Sunspot Number	100.

IRIS6 Output			
Species	Density	Species	Density
atomic_oxygen	1.498E+12	atomic_hydrogen	2.99E+11
helium	3.111E+10	molecular_oxygen	2.567E+05
nitric_oxide	0.000E+00	Electron	1.809E+12
Electron Temperature	9.388E-02	Ion Temperature	8.261E-02

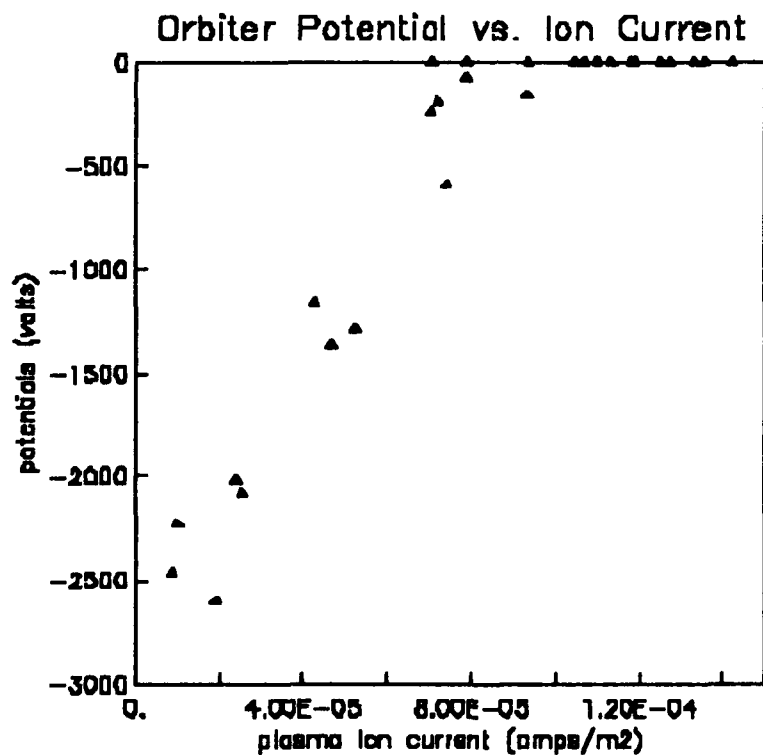


Figure 2.6

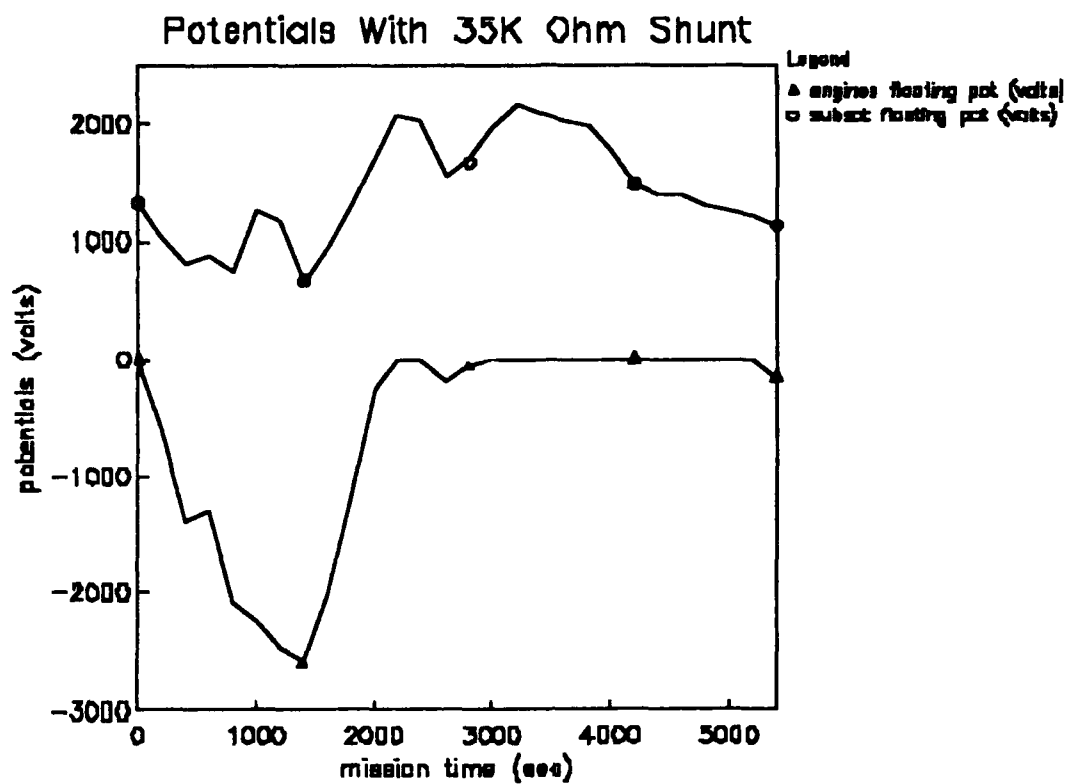


Figure 2.7

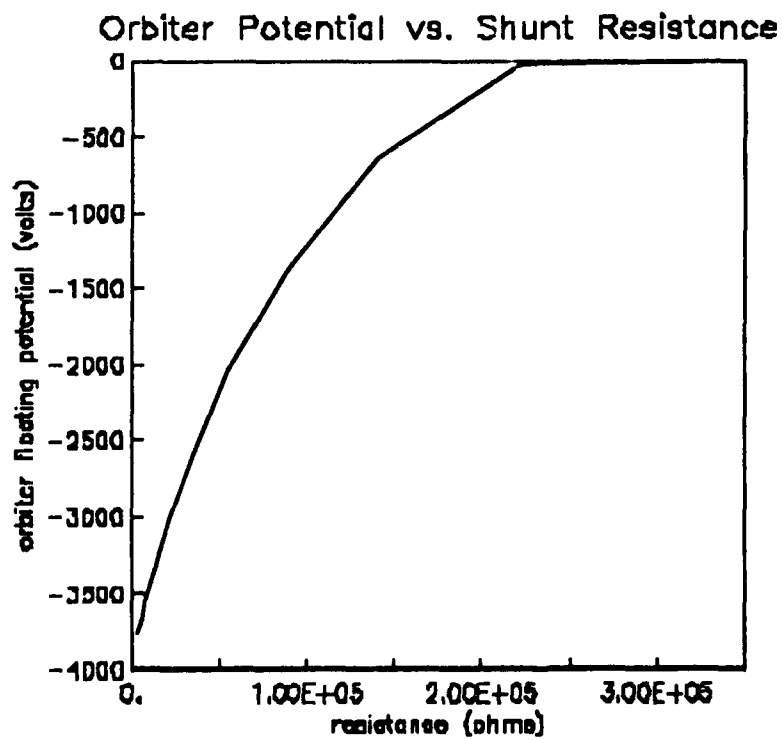


Figure 2.8

3. CALCULATIONS OF ION CURRENT COLLECTED BY SHUTTLE ORBITER

Using NASCAP/LEO, the collected ion (oxygen) currents were calculated as a function of voltage, plasma density, and the orientation of the shuttle orbiter with respect to the ram. The ion currents were found by varying the conducting surface potentials (the engine nozzles), computing the ion wake formed behind the moving shuttle, calculating the resulting spatial plasma potentials, and then pushing ions from an equipotential plasma sheath.

The shuttle model was made using PATRAN. The model coordinate system is such that the tail rises in the +x direction, the nose is in the +z direction, and starboard side of the shuttle is the +y direction. For the purposes of this calculation, only the engines nozzles were considered conducting (aluminum in the figure). The calculations used a nested, cubical grid with a mesh size of 1.645 meters. The plasma temperature for all of the calculations was 0.1 eV. The surface potentials of the insulating surfaces were defined to be -0.5 volts to simplify the calculations.

The varied parameters were the potential of the conducting surfaces (-10, -100, -300, and -1000 volts), the plasma density (10^{11} and 10^{12} ions/meter³), and the shuttle orientation with respect to its velocity 7500 meters/sec (cargo bay 45 degrees into the ram and into the wake). The corresponding shuttle velocity vectors in model coordinates are (5303, 0, -5303) meters/sec for the bay facing in the ram direction and (-5303, 0, 5303) meters/sec for the bay facing in the wake direction.

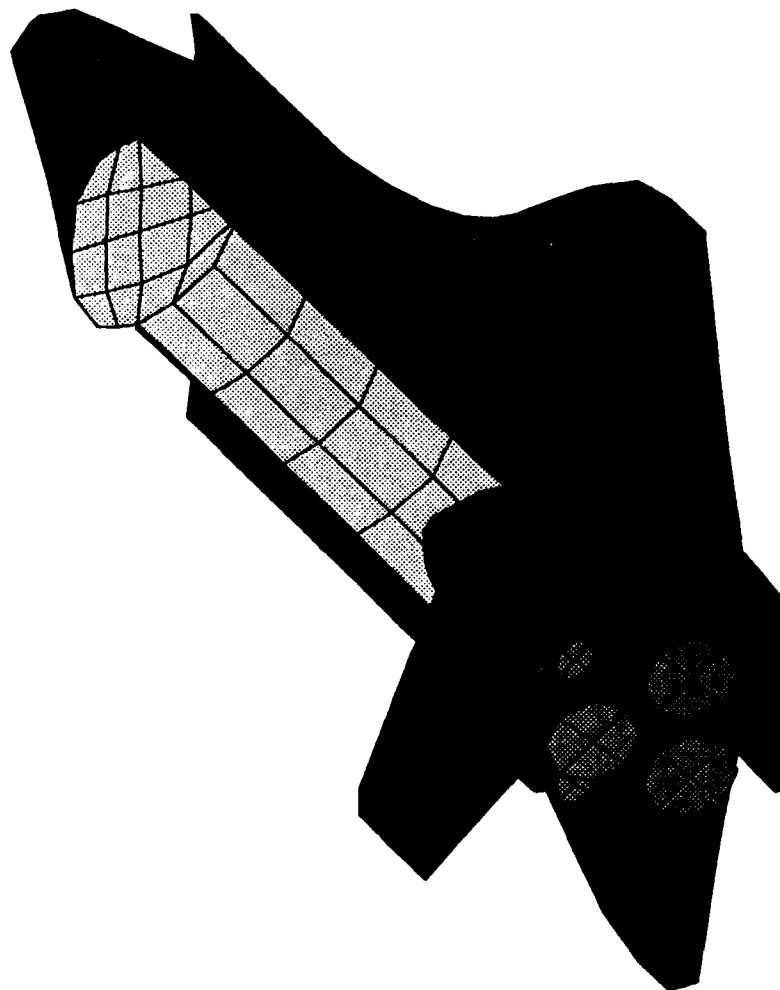
The results of the calculations follow:

Bay into the ram (shuttle velocity was (5303, 0, -5303) meters/sec)

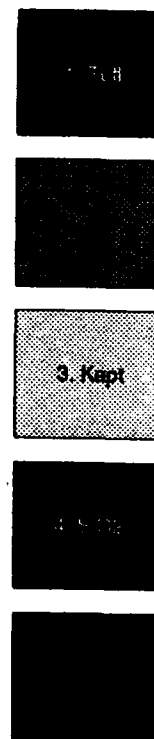
Conductor potential (volts)	Current (amps) at density	
	10^{11}	10^{12}
-10	4.1E-03	4.1E-02
-100	8.9E-03	8.9E-02
-300	1.5E-02	1.5E-01
-1000	2.3E-02	2.1E-01

Bay into the wake (shuttle velocity was (-5303, 0, 5303) meters/sec)

Conductor potential (volts)	Current (amps) at density 10^{**11}	(ions/meter**3) 10^{**12}
-10	4.0E-15	1.4E-13
-100	1.9E-03	2.2E-02
-300	5.0E-03	4.7E-02
-1000	1.9E-02	1.4E-01



COLOR LEGEND



4. CALCULATIONS OF ION CURRENT COLLECTED BY THE SPREE INSTRUMENT

Using NASCAP/LEO, ion (oxygen) currents were calculated as a function of voltage and the orientation of the SPREE instrument with respect to the flowing plasma. The currents calculated were the total current to each of the detector entrance screens, the current that entered the detector within 10 degrees of the surface normal, and the weighted (by particle current) average angle of particles striking the detector entrance.

The ion currents were found by varying the surface potentials of the detector cases, computing the ion wake formed by the moving instrument, calculating the resulting spatial plasma potentials, and then pushing ions from an equipotential plasma sheath. The particle velocity and current were used, saved, and postprocessed to compute the calculated currents.

The SPREE model was made using PATRAN. The model coordinate system is such that the detectors rise in the +y direction with the base plate in the x-z plane. The detector with screen 2 is higher in z than the detector with screen 1. The potentials were applied to the case of the detectors and their screens. The calculations used a nested, cubical grid with a mesh size of 0.04 meters. The plasma temperature for all of the calculations was 0.1 eV. The surface potentials of all of the surfaces other than the case of the detector were defined to be -0.5 volts to simplify the calculations.

The varied parameters were the potential of the conducting surfaces (-100, -300, and -1000 volts) and the SPREE orientation with respect to the flowing plasma (or orbiter velocity of 7500 meters/sec). Two orientations were studied. In case 1, the flow direction corresponds to the orbiter nose up 45 degrees and the cargo bay into the ram. Case 2 arises when the orbiter is oriented with the wings parallel to the flow (shuttle moving to port or starboard). The corresponding SPREE velocity vectors in model coordinates are (0, 5303, -5303) meters/sec for case 1 and (7500, 0, 0) meters/sec for case 2.

The results of the calculations follow:

Case 1 Nose up, cargo bay into the ram. (SPREE velocity was (0, 5303, -5303) meters/sec.) In this orientation, the low-Z detector is the aft detector.

AFT DETECTOR

<u>Voltage (volts)</u>	<u>-100</u>	<u>-300</u>	<u>-1000</u>
Total current (μ A)	4.88	1.15	1.61
Current within 10 degrees (μ A)	.0303	.055	0.
Weighted average angle detected (degrees)	43.8	64.9	59.4

FORWARD DETECTOR

<u>Voltage (volts)</u>	<u>-100</u>	<u>-300</u>	<u>-1000</u>
Total current (μ A)	2.43	.694	2.71
Current within 10 degrees (μ A)	.0962	0.	.073
Weighted average angle detected (degrees)	43.4	49.3	41.7

Case 2 Orbiter moving sideways. (SPREE velocity was (7500, 0, 0) meters/sec.) In this orientation, the low-Z detector is looking towards its wake and the high-Z detector is looking upstream.

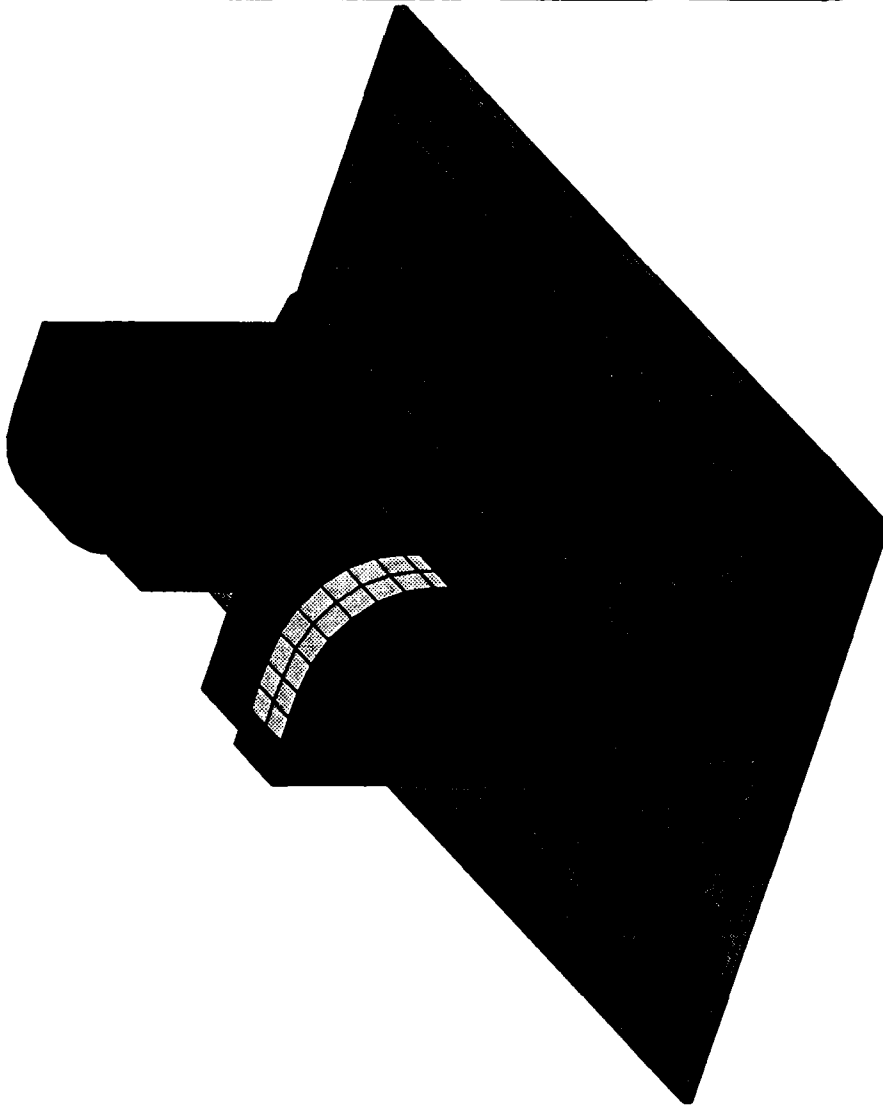
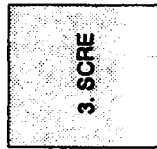
LOW-Z DETECTOR (DETECTOR 1), WAKE VIEW

<u>Voltage (volts)</u>	<u>-100</u>	<u>-300</u>	<u>-1000</u>
Total current (μ A)	5.14	4.93	3.84
Current within 10 degrees (μ A)	.102	0.	0.
Weighted average angle detected (degrees)	47.5	67.0	56.7

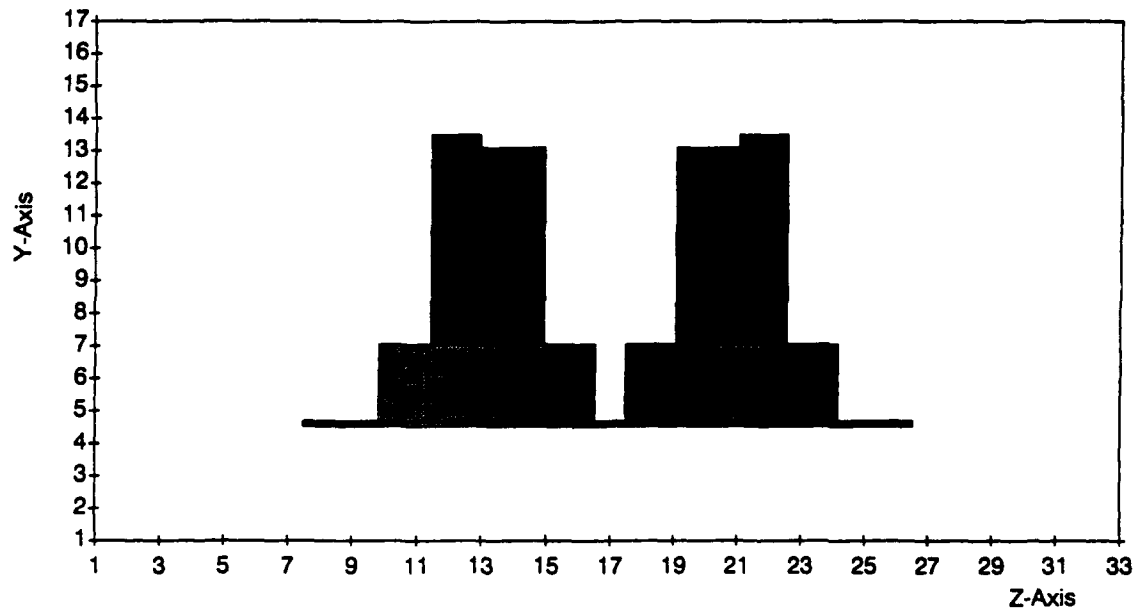
HIGH-Z DETECTOR (DETECTOR 2), RAM VIEW

<u>Voltage (volts)</u>	<u>-100</u>	<u>-300</u>	<u>-1000</u>
Total current (μ A)	2.43	5.18	4.03
Current within 10 degrees (μ A)	.098	0.	0.
Weighted average angle detected (degrees)	43.1	72.6	59.4

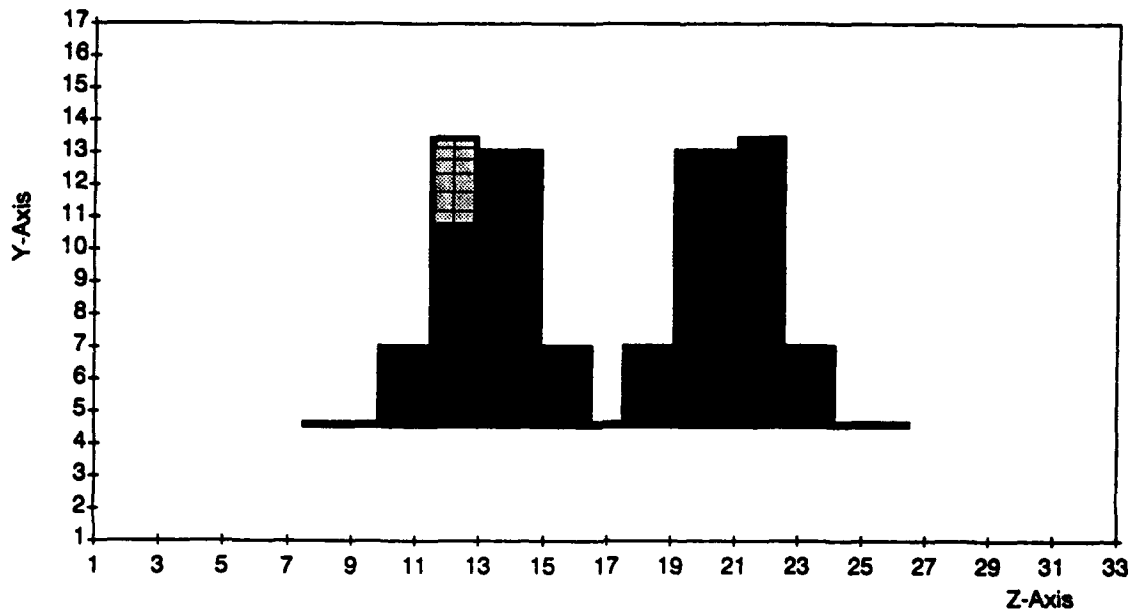
COLOR LEGEND



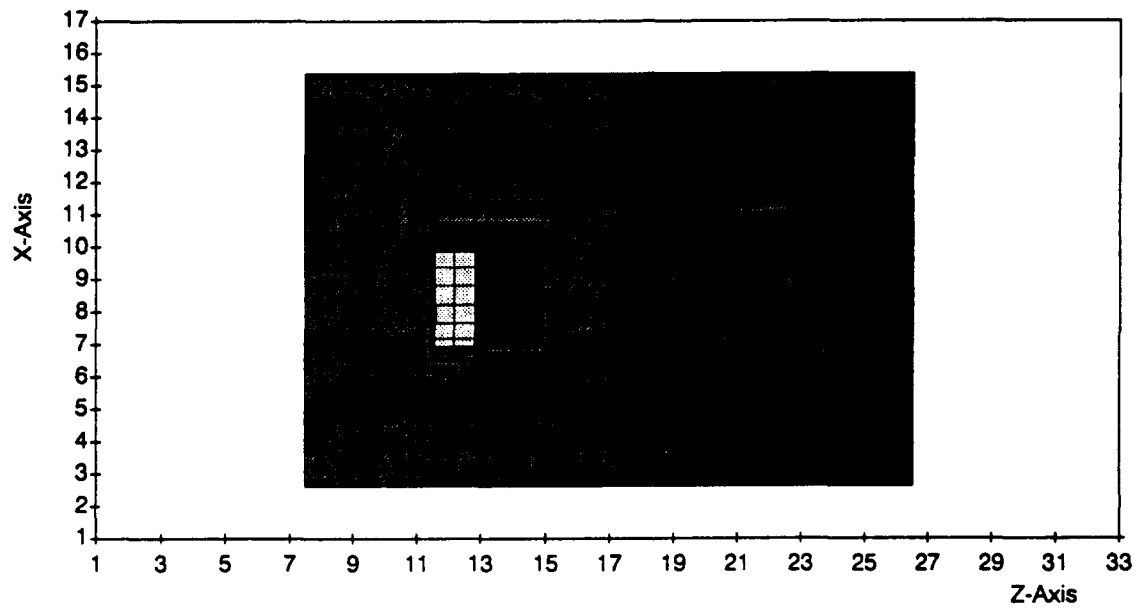
Positive X View



Negative X View

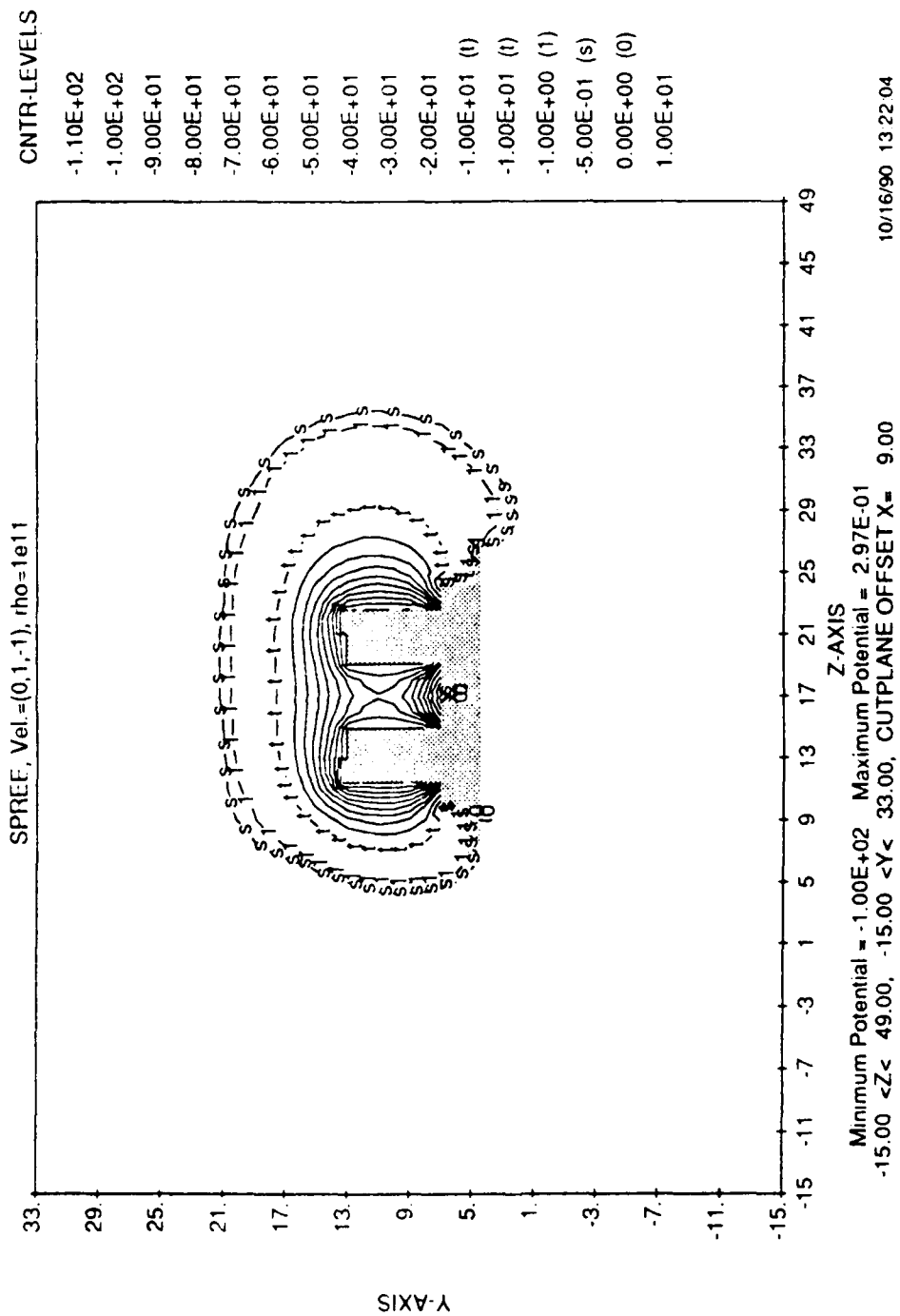


Positive Y View

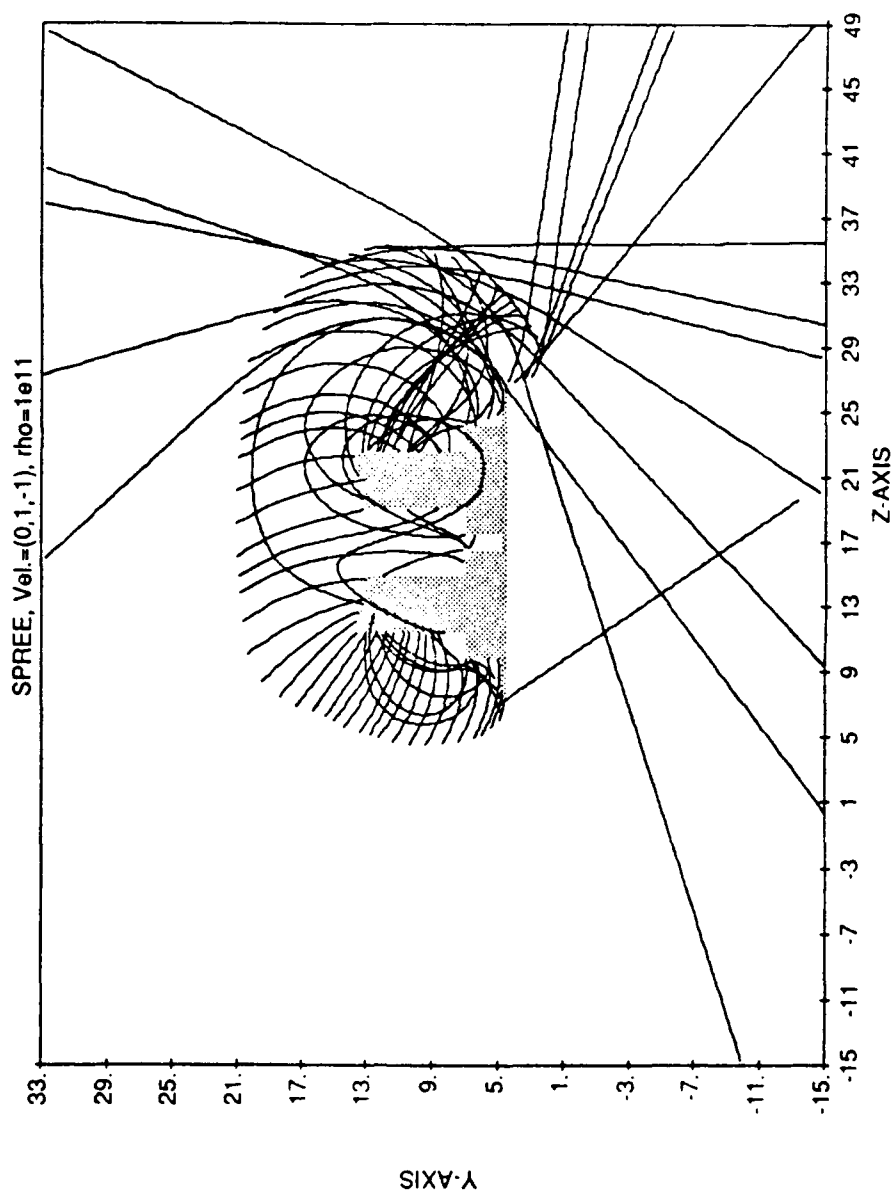


SPREE Case I

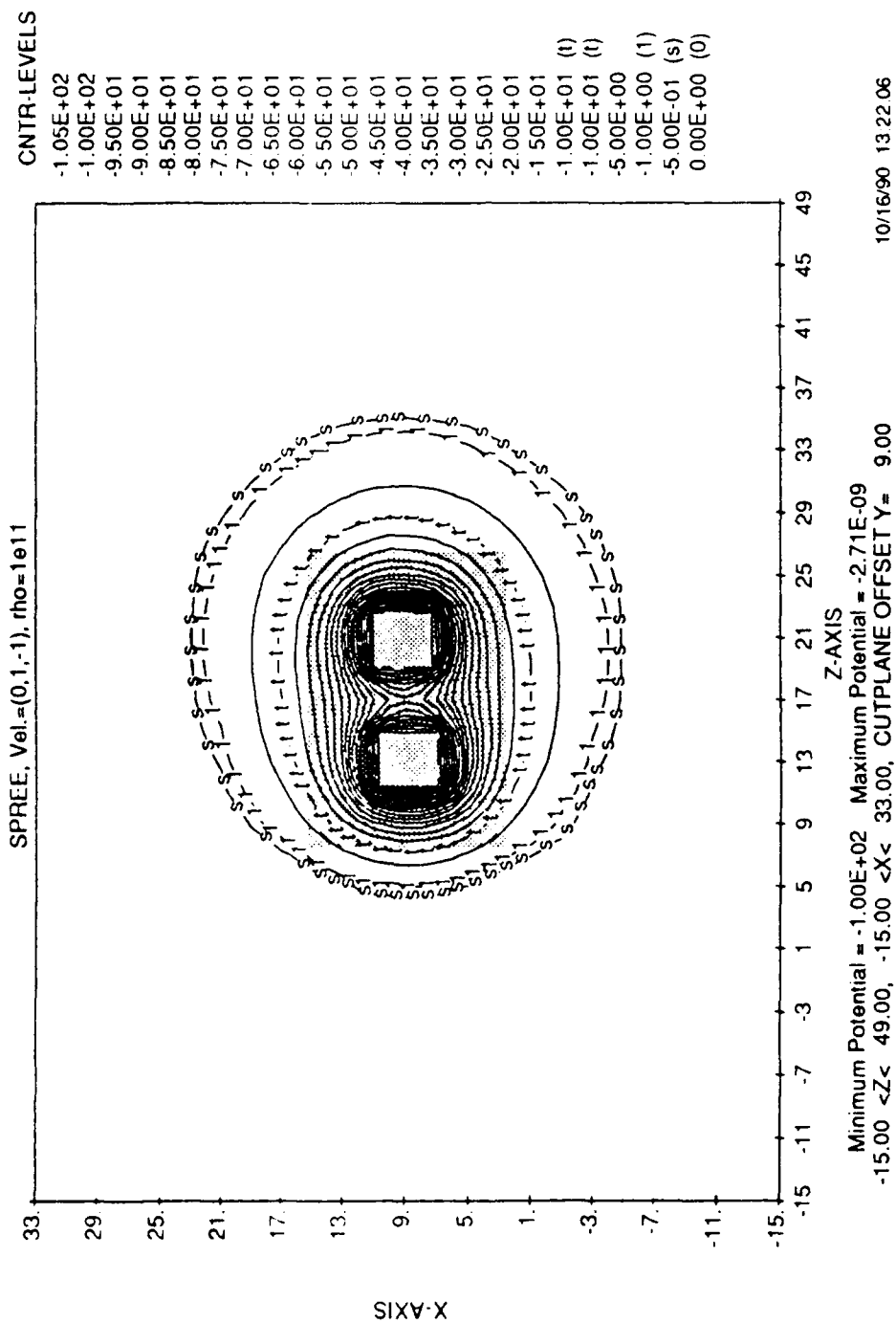
-100 V

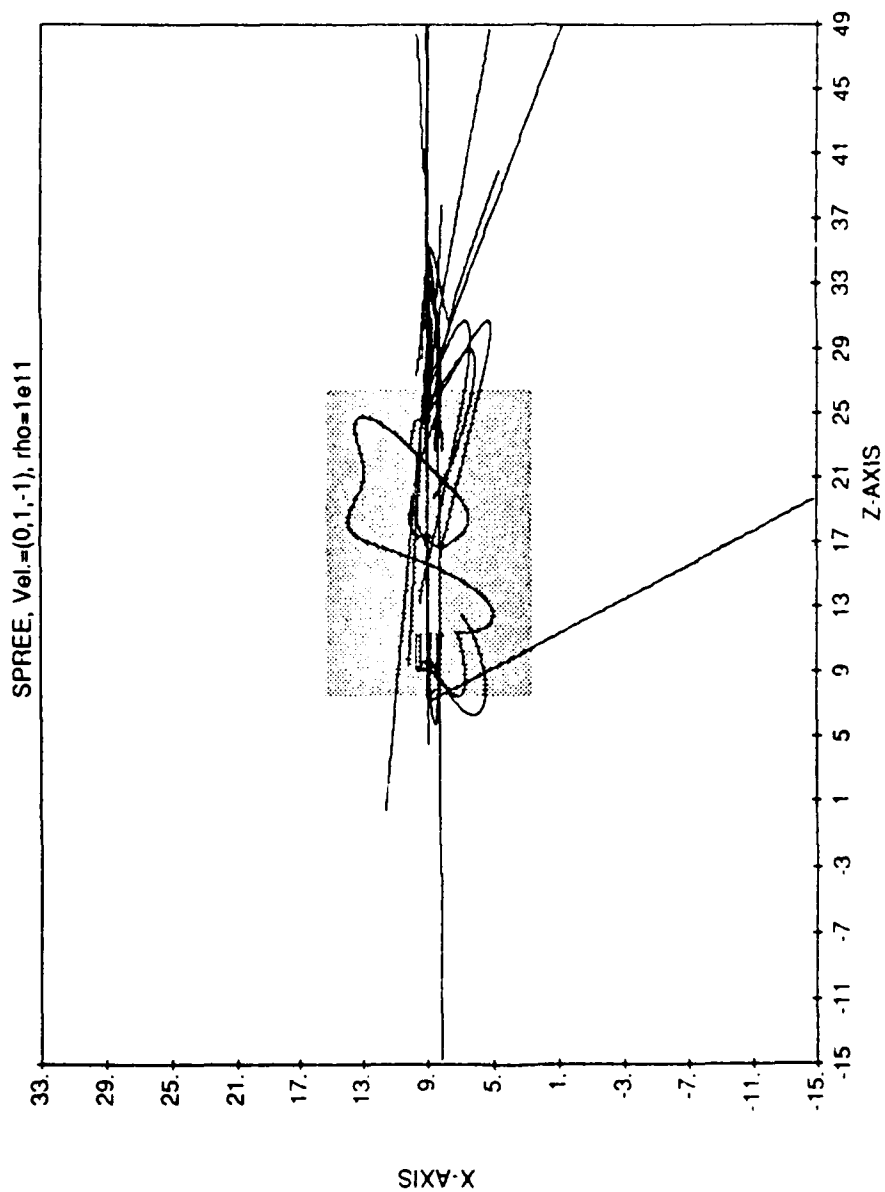


10/16/90 13 22 04

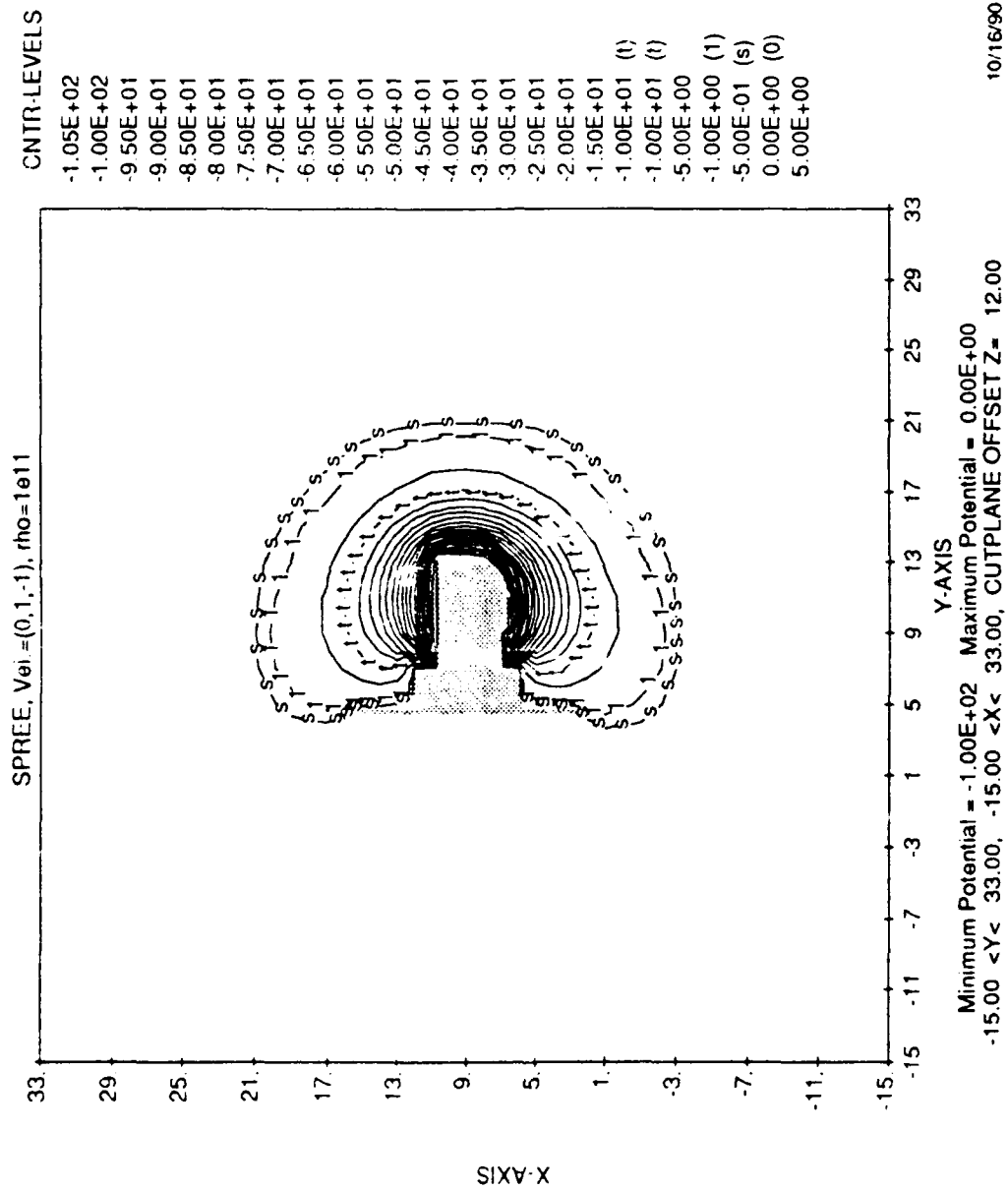


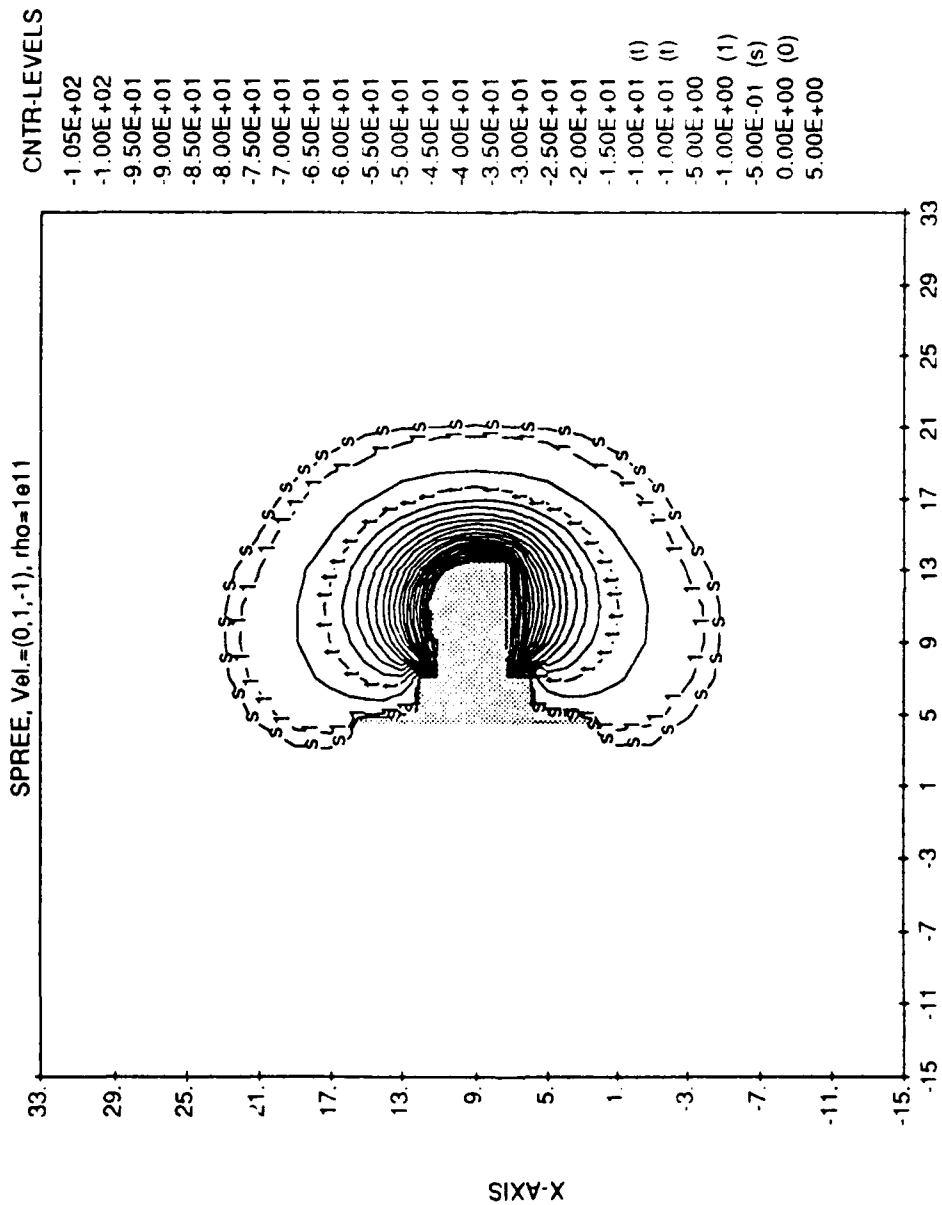
10/17/90 14:51:13



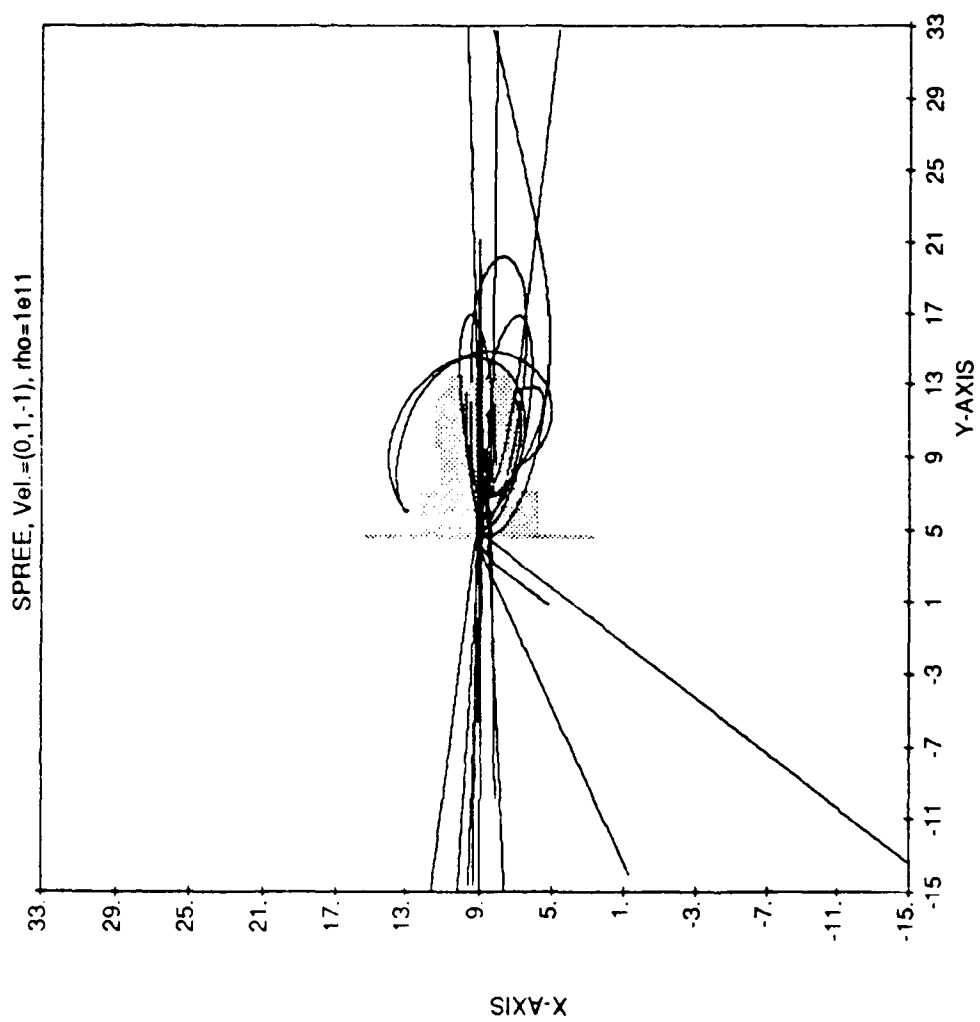


10/17/90 14 51 14





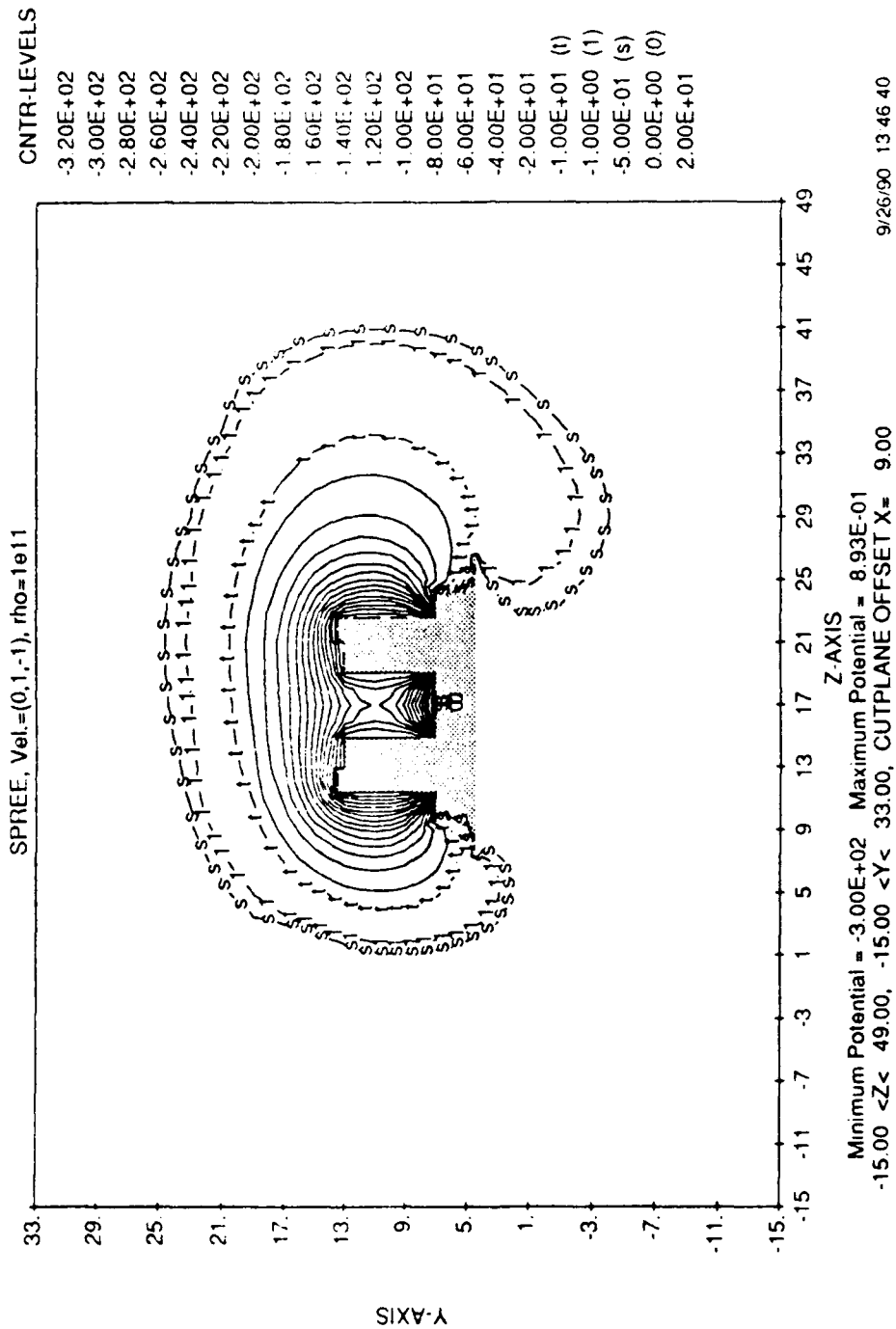
10/16/90 13 22.09

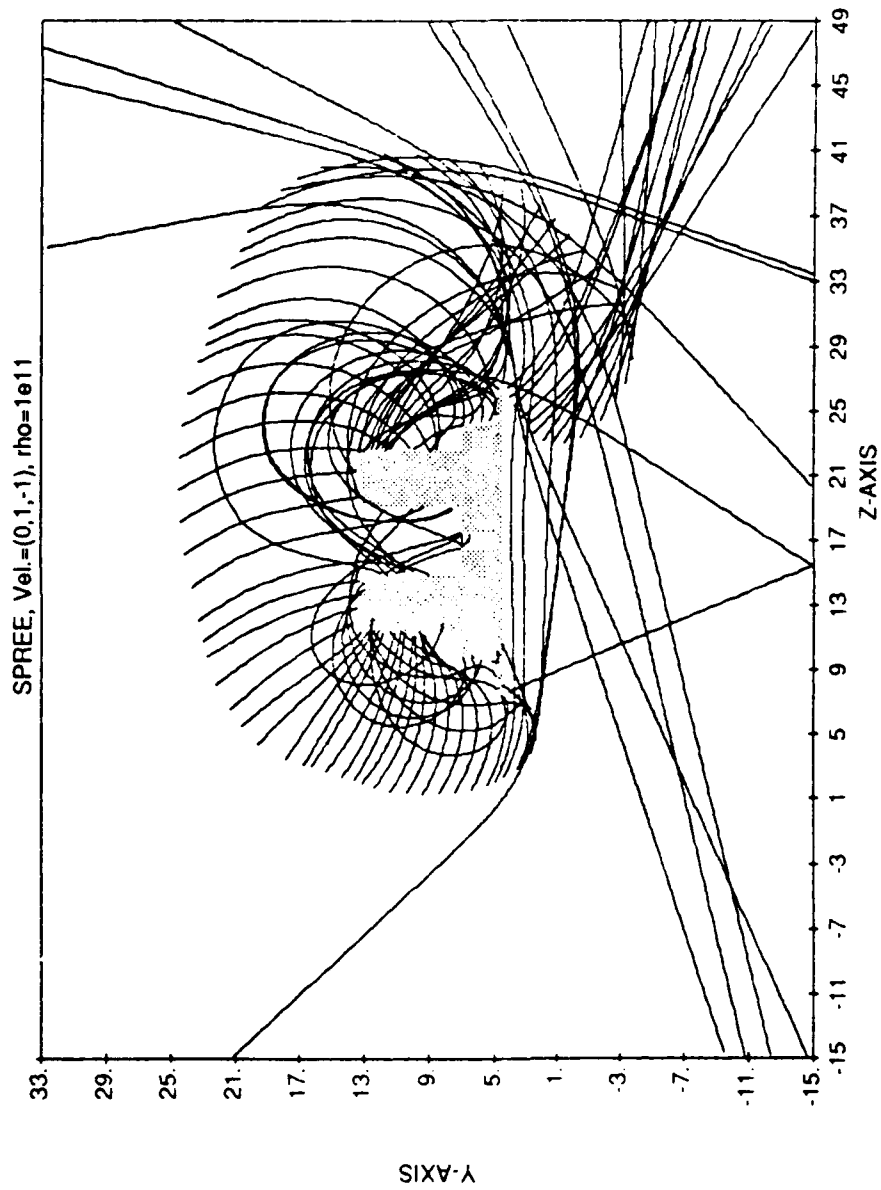


10/17/90 14 51:15

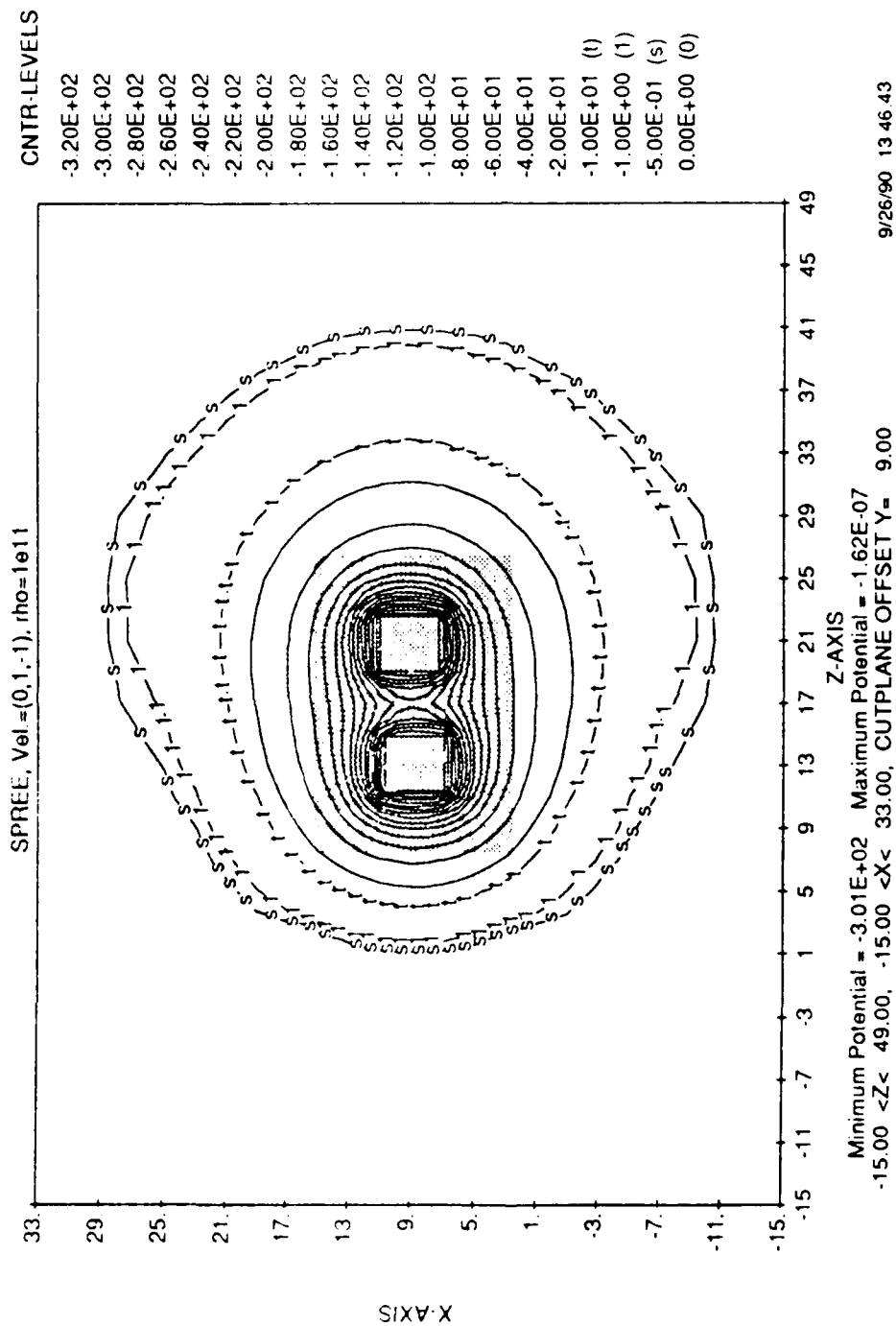
SPREE Case 1

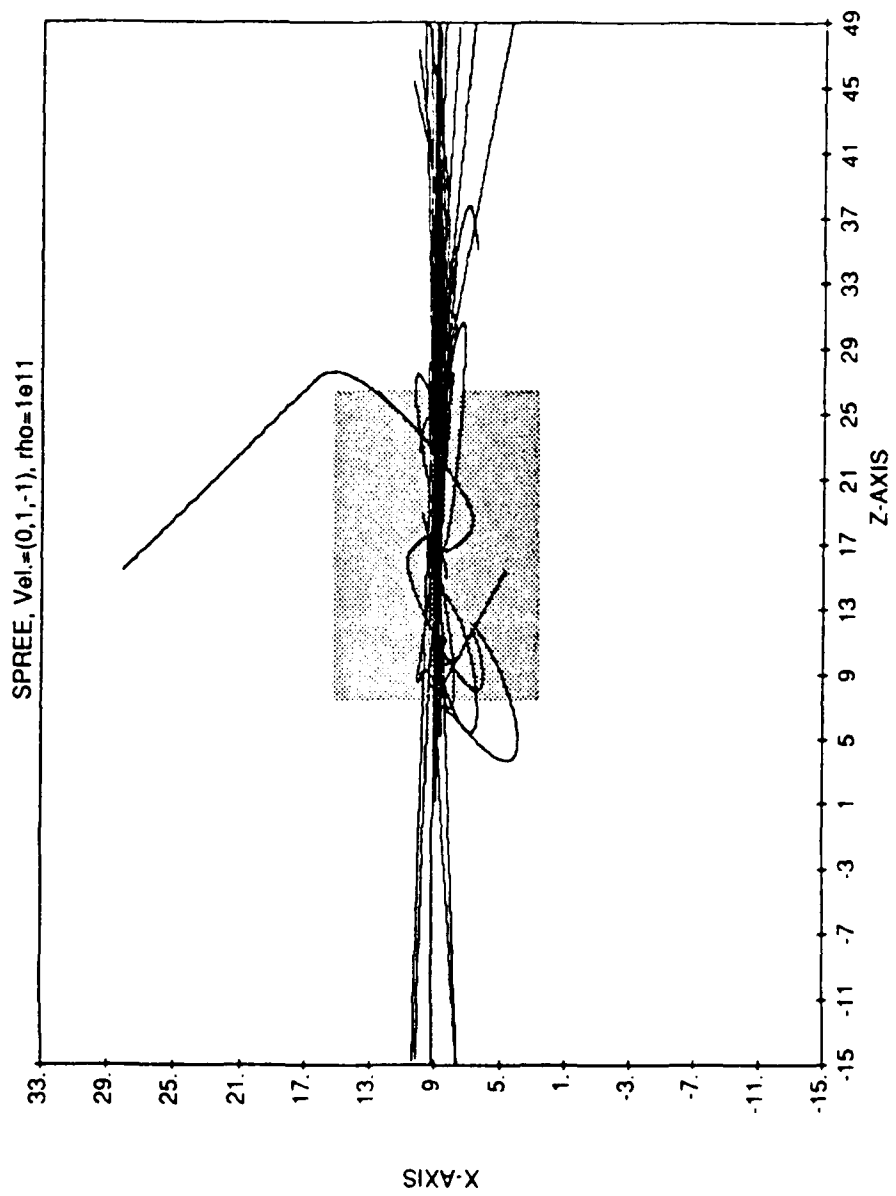
-300 V



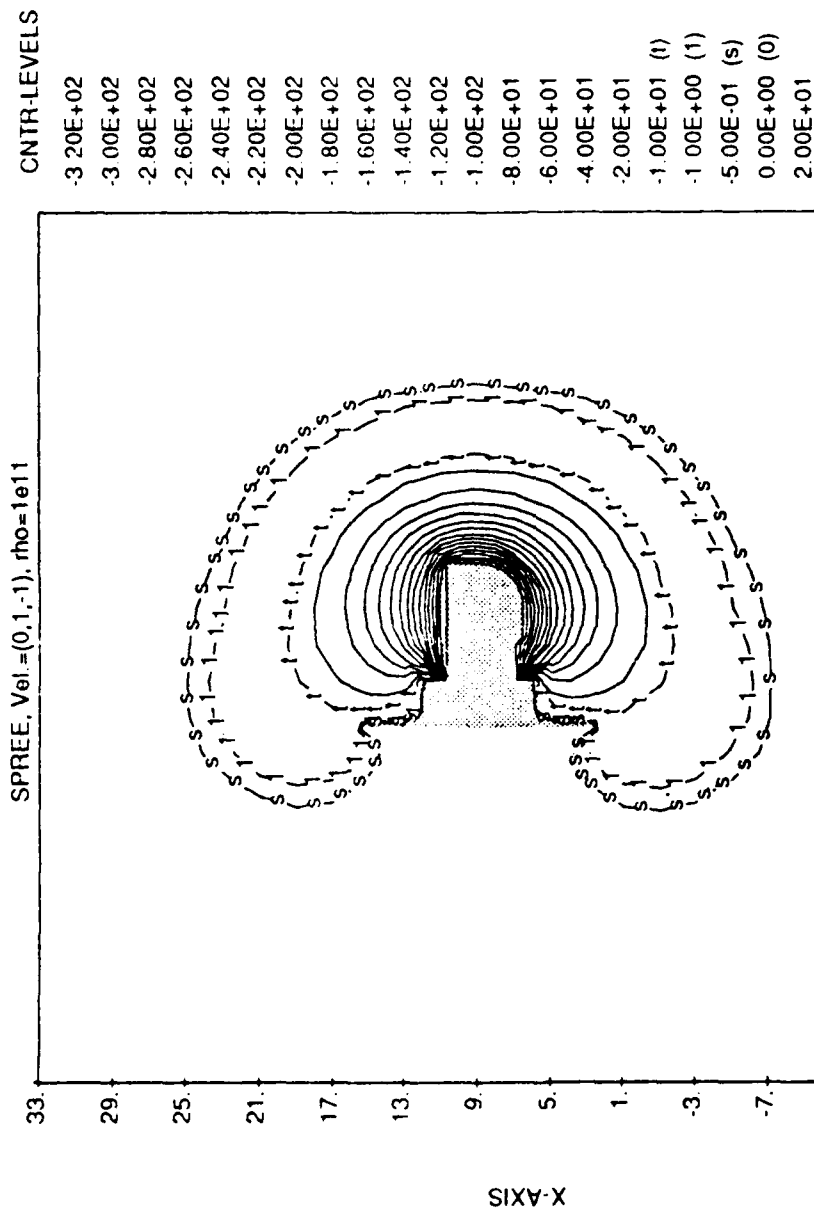


10/17/90 16 51 36

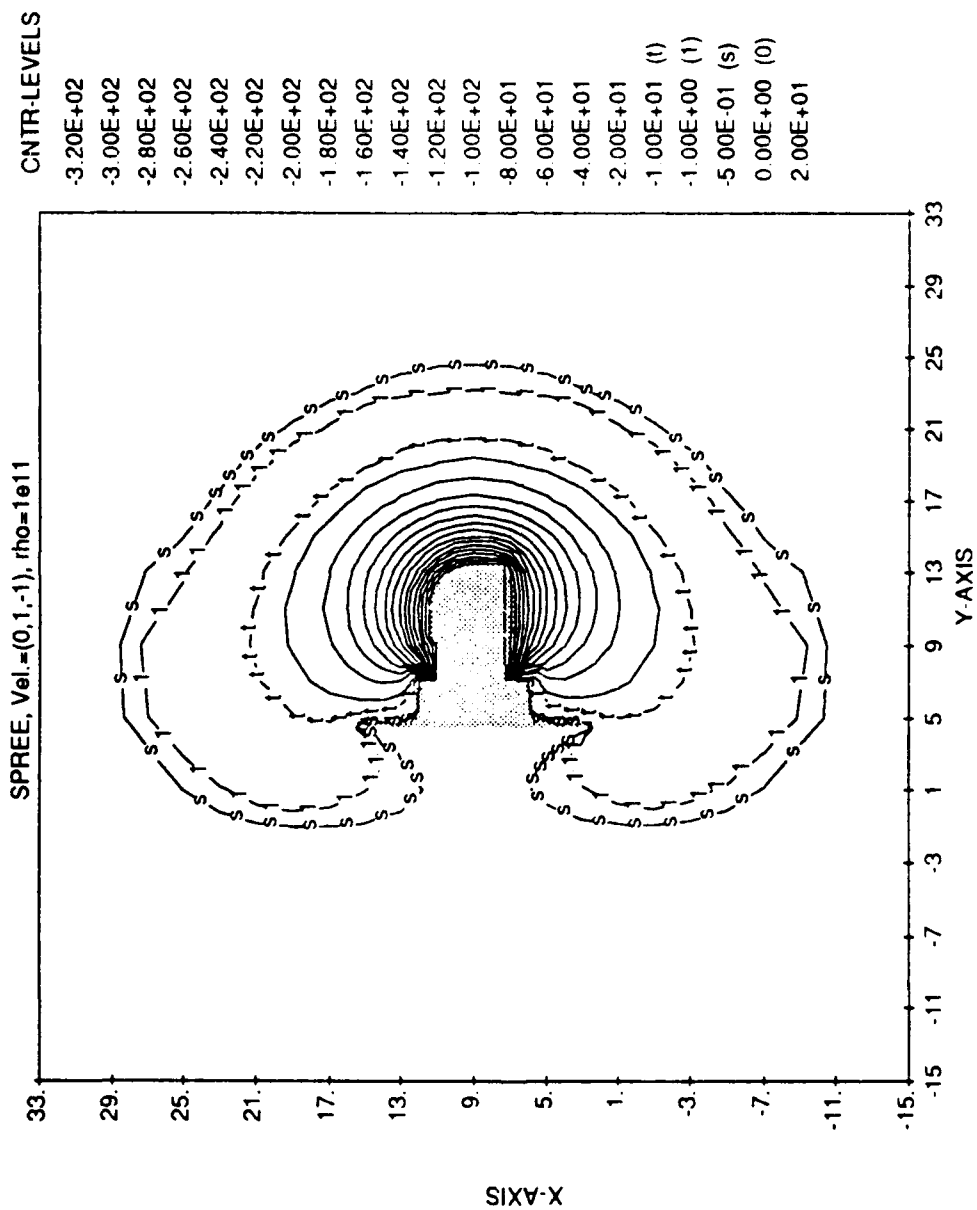




10/17/90 16 51 38

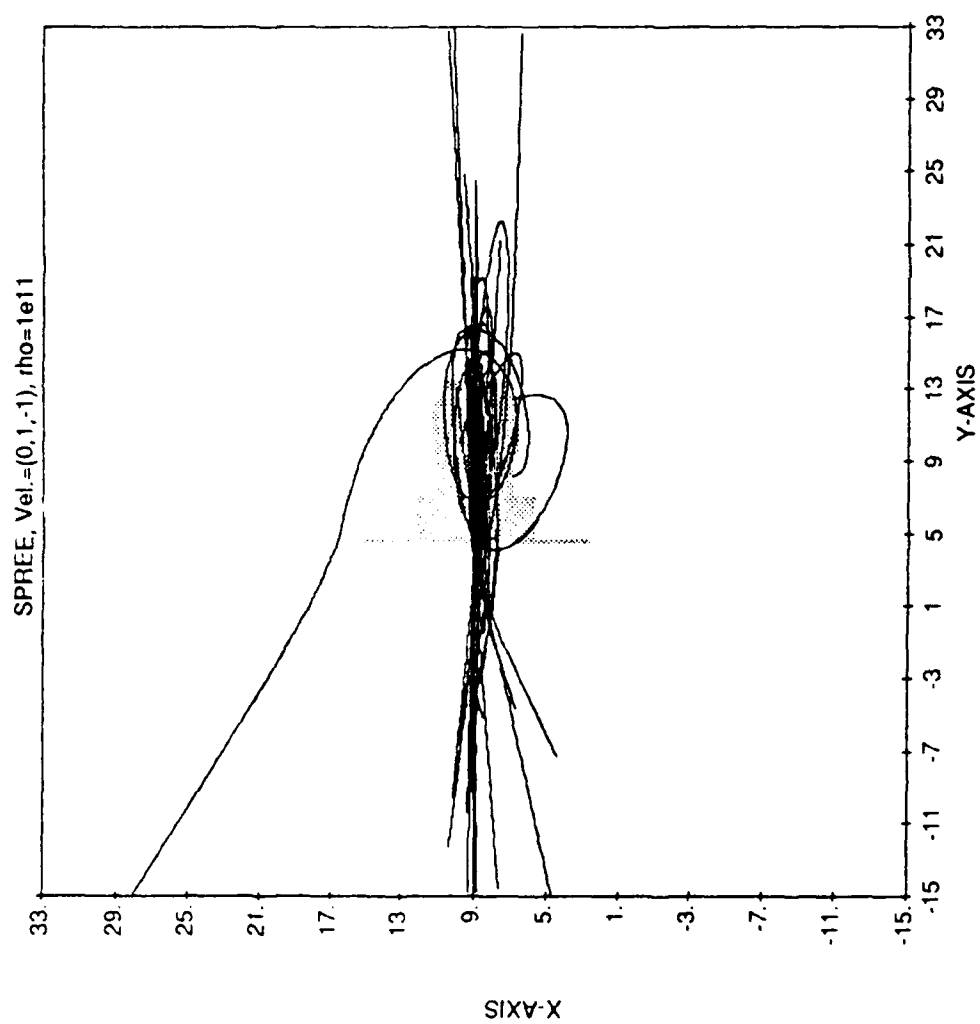


9/26/90 13 46 45



Minimum Potential = -3.00E+02 Maximum Potential = 0.00E+00
 -15.00 <Y< 33.00, -15.00 <X< 33.00, CUTPLANE OFFSET Z= 22.00

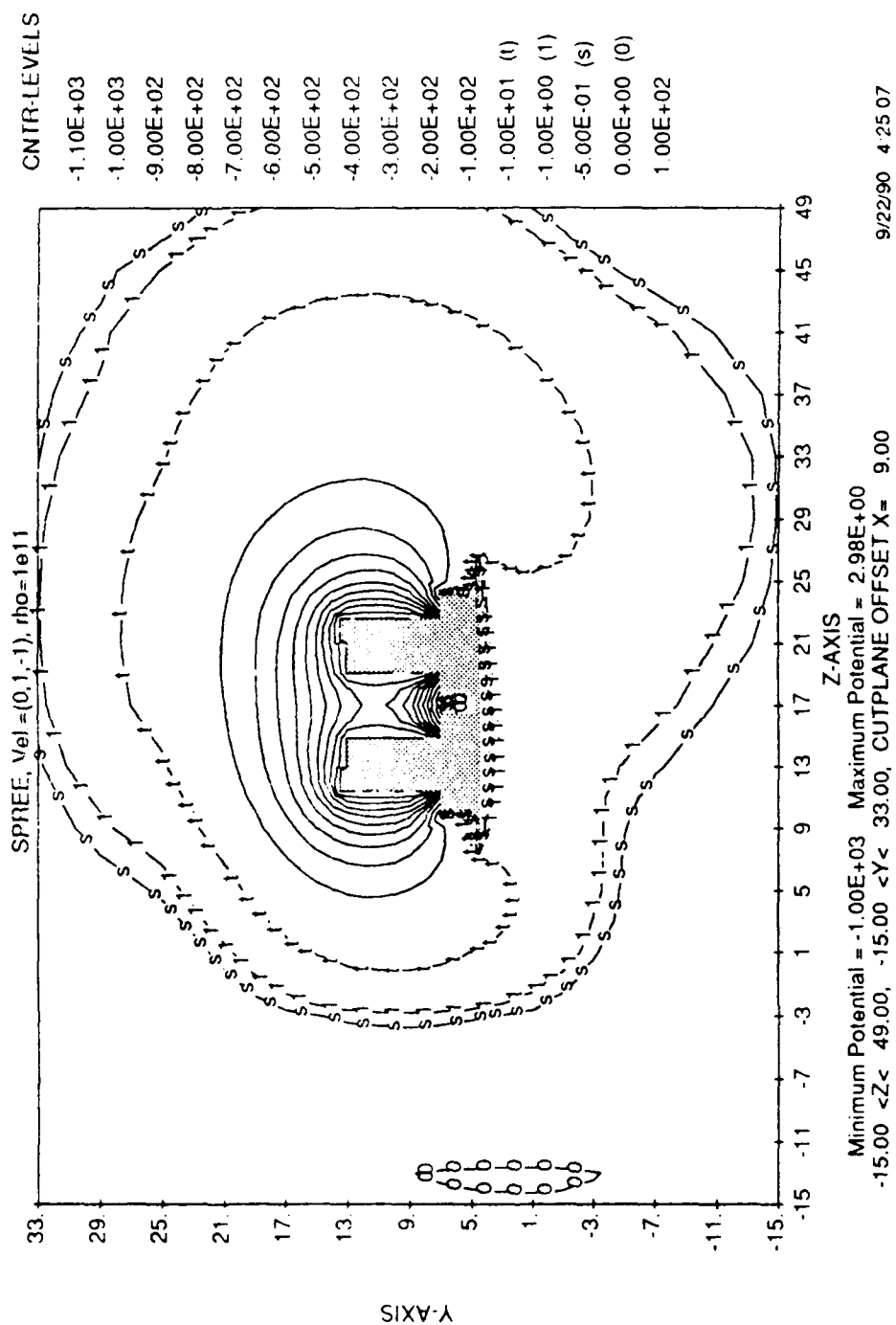
9/26/90 13 46 47



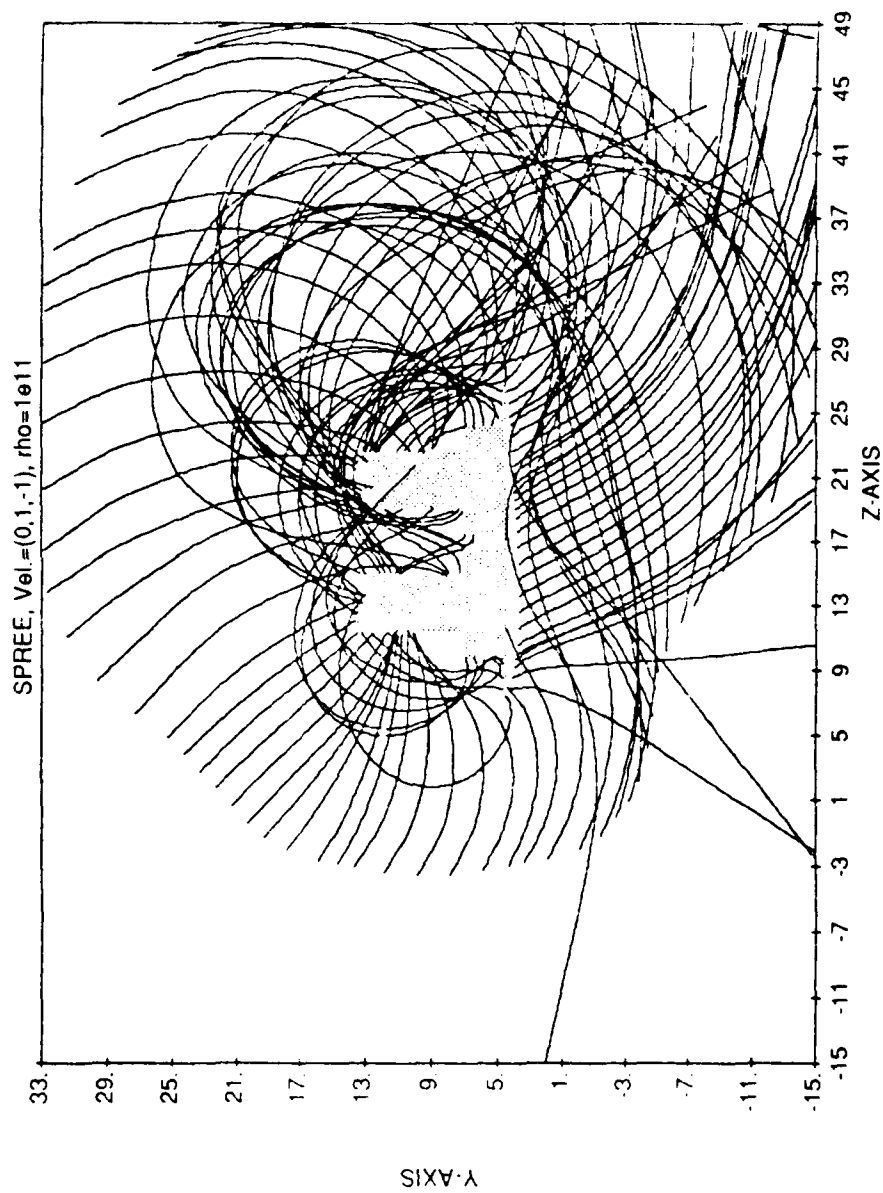
10/17/90 16:51:39

SPREE Case 1

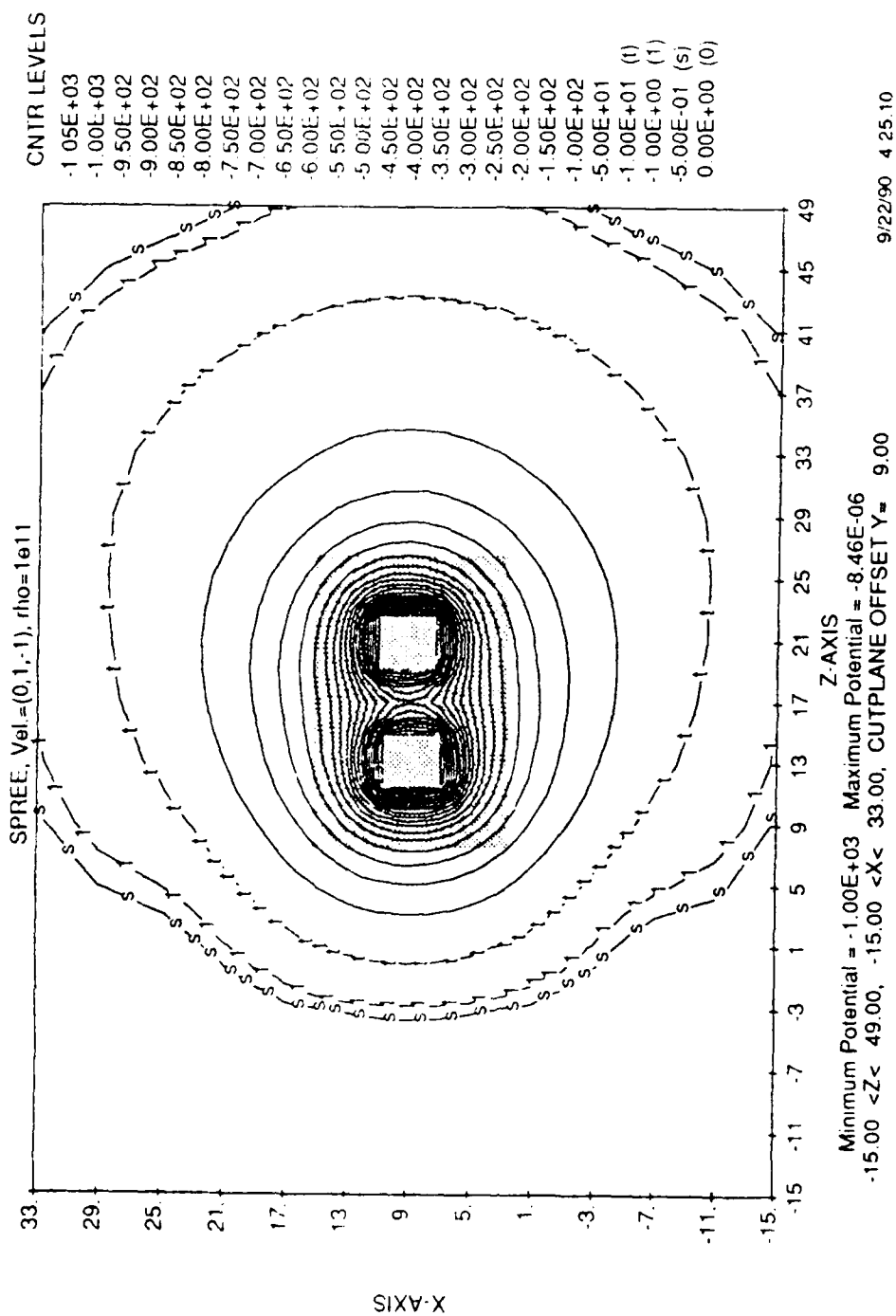
-1000 V

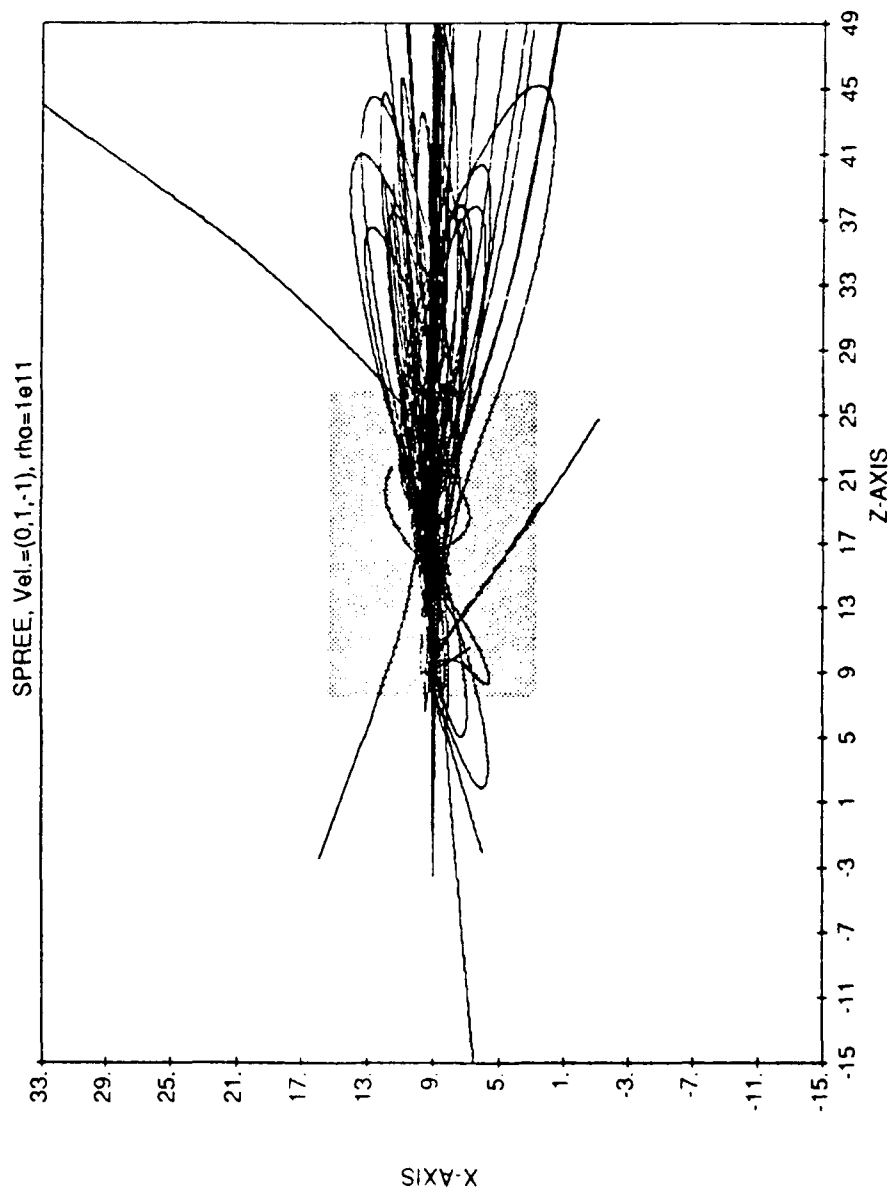


9/22/90 4 25 07

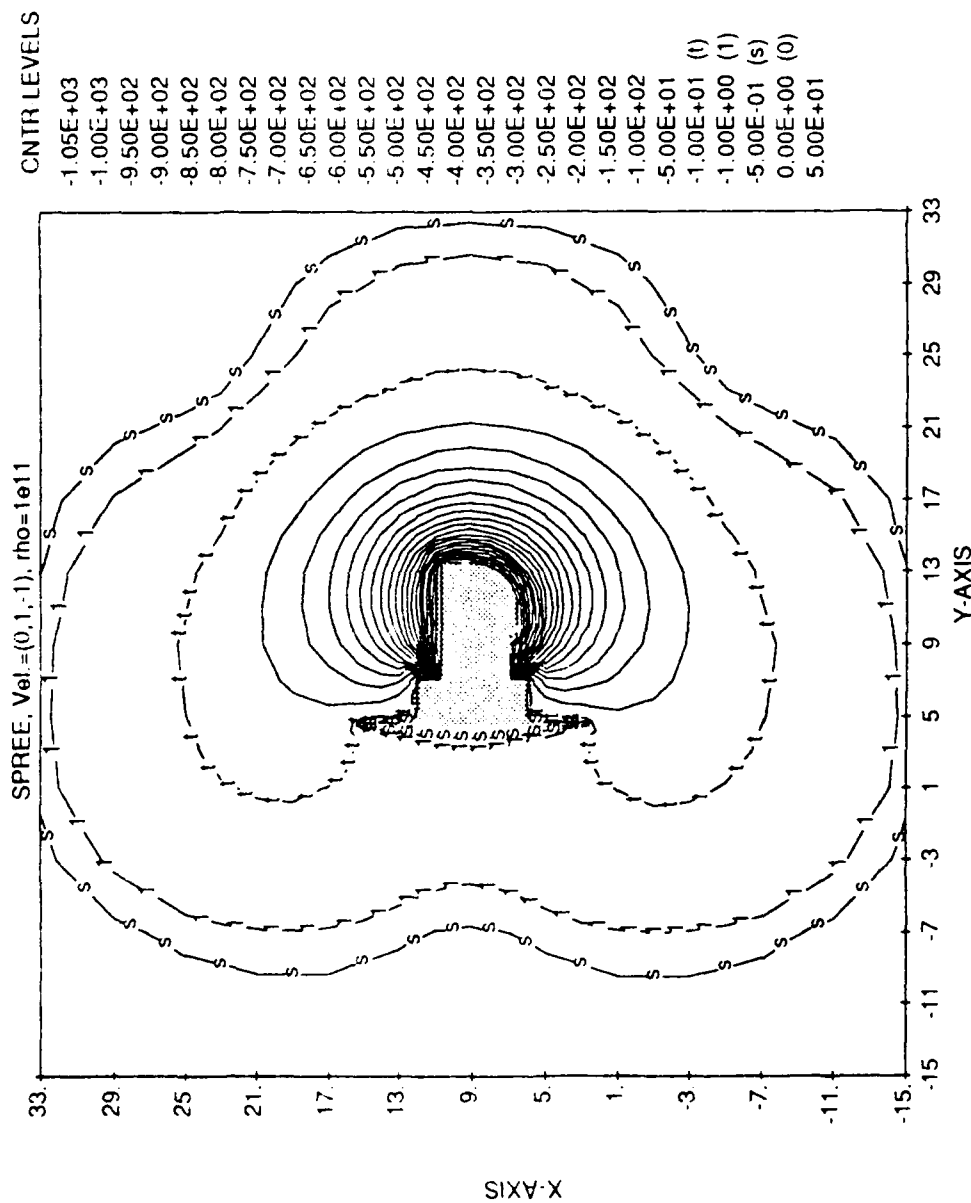


10/17/90 17 26 11



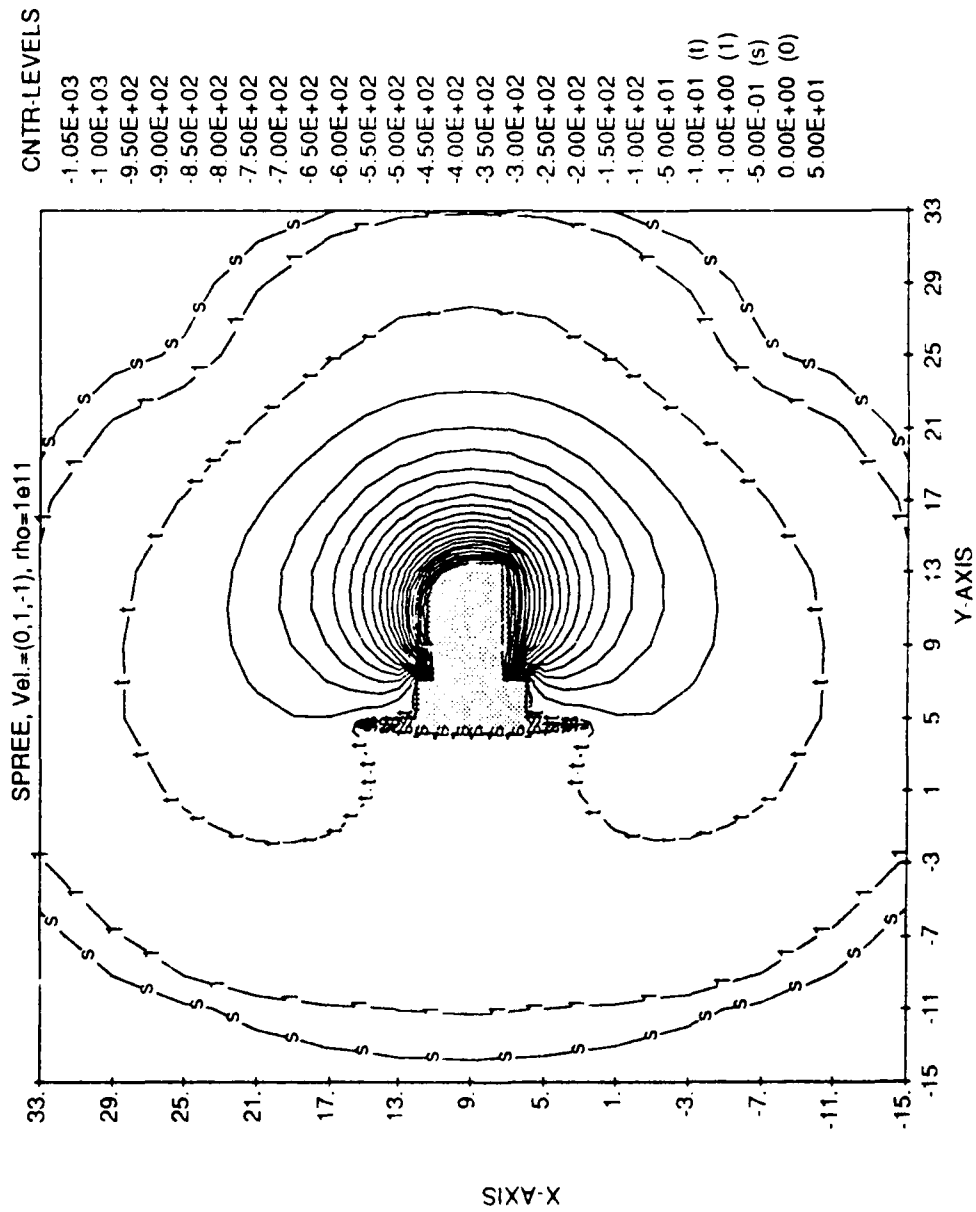


10/17/90 17 26 12



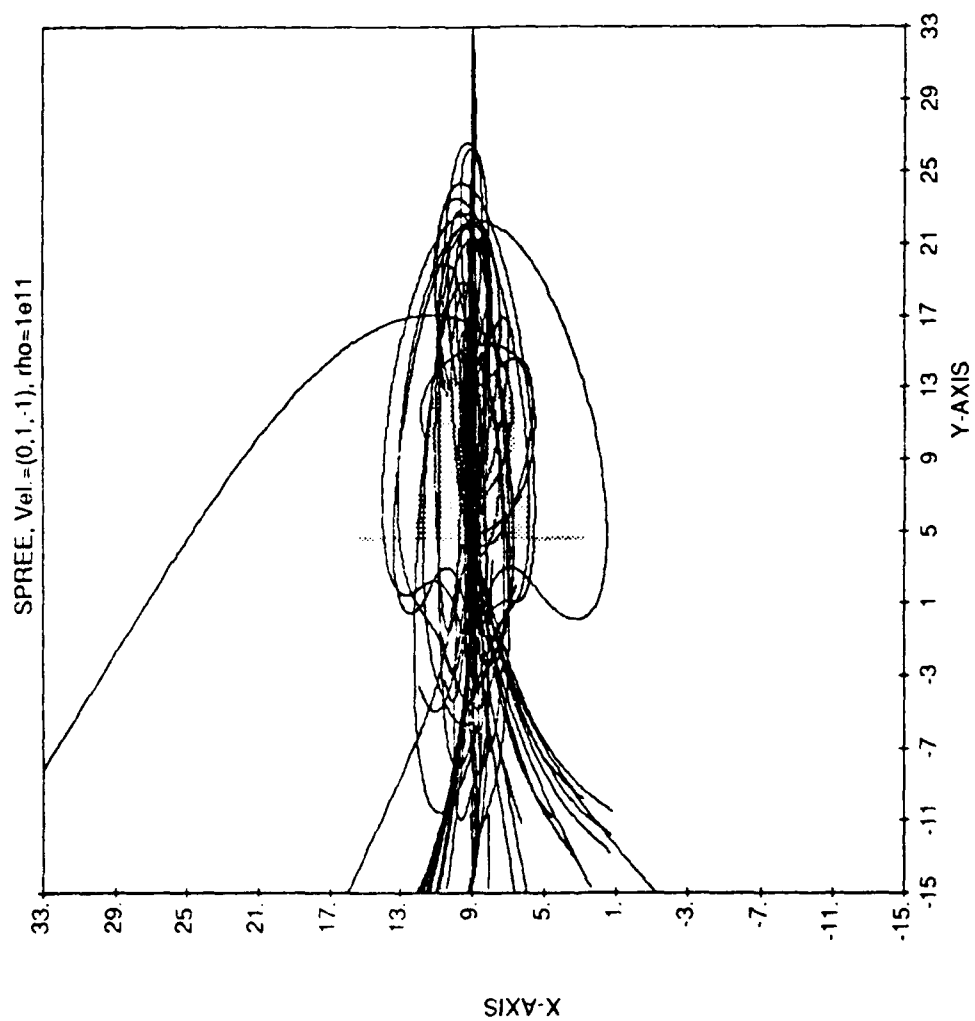
Minimum Potential = -1.00E+03 Maximum Potential = 0.00E+00
 -15.00 <Y< 33.00, -15.00 <X< 33.00, CUTPLANE OFFSET Z= 12.00

9/22/90 4 25 12



Minimum Potential = -1.00E+03 Maximum Potential = 0.00E+00
 -15.00 <Y< 33.00, -15.00 <X< 33.00, CUTPLANE OFFSET Z= 22.00

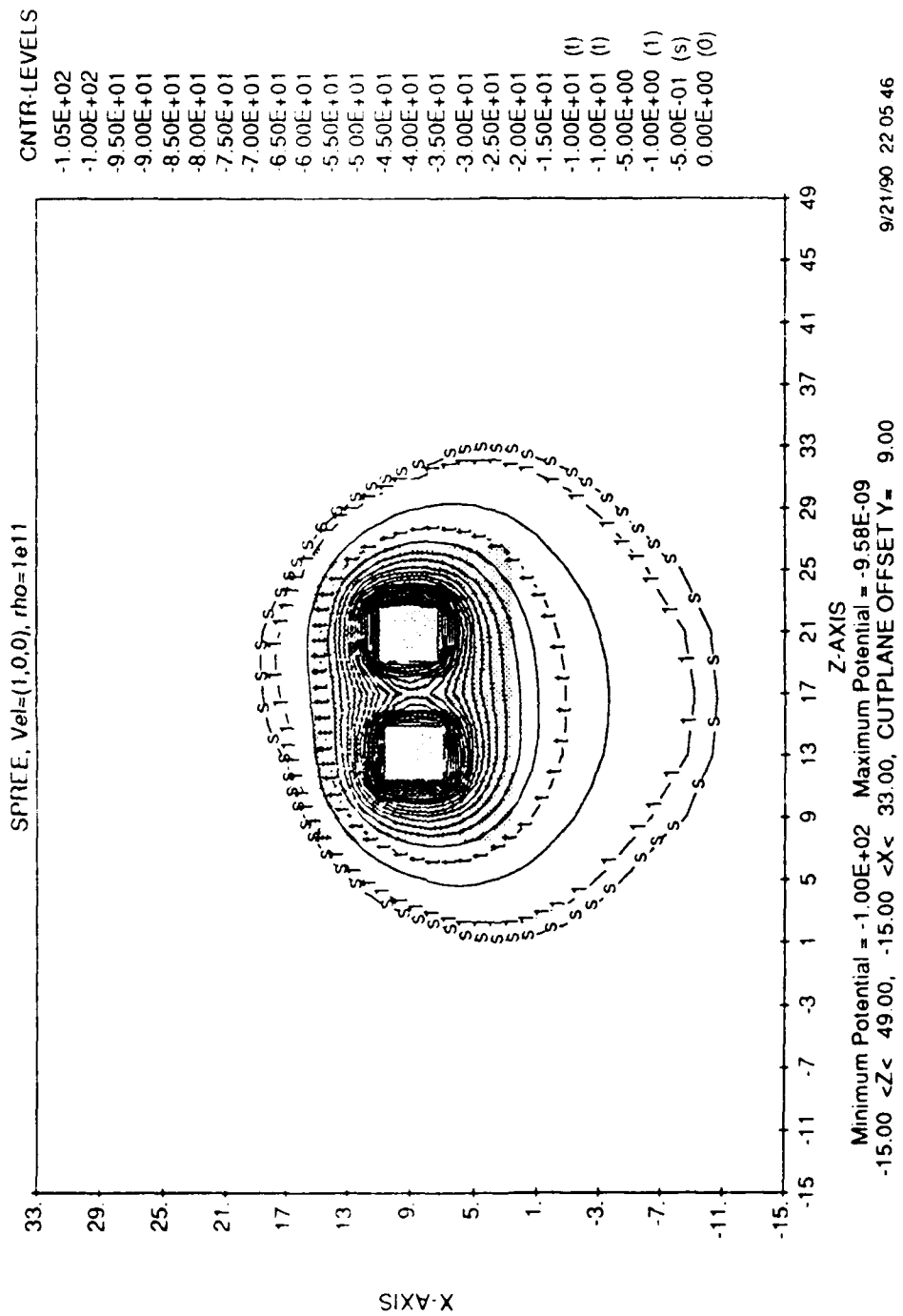
9/22/90 4 25 14

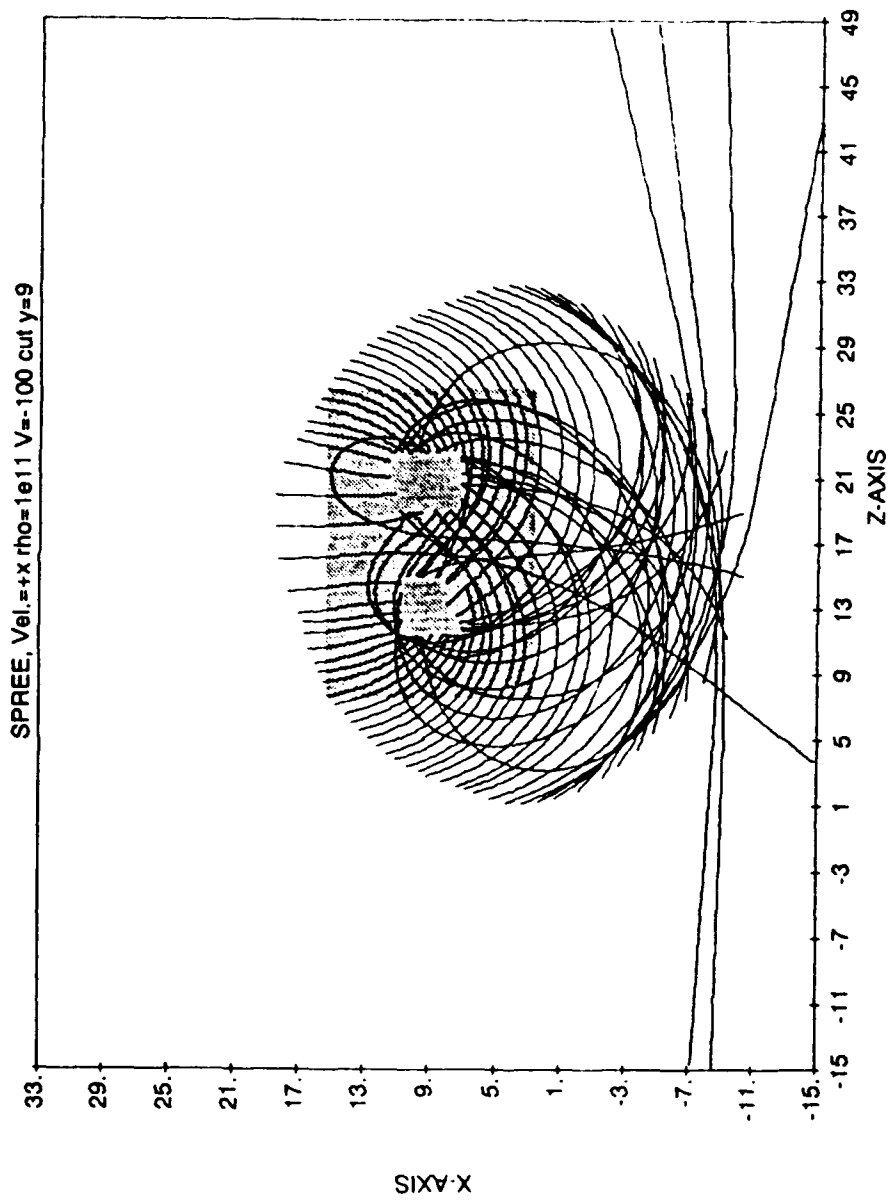


10/17/90 17 26.13

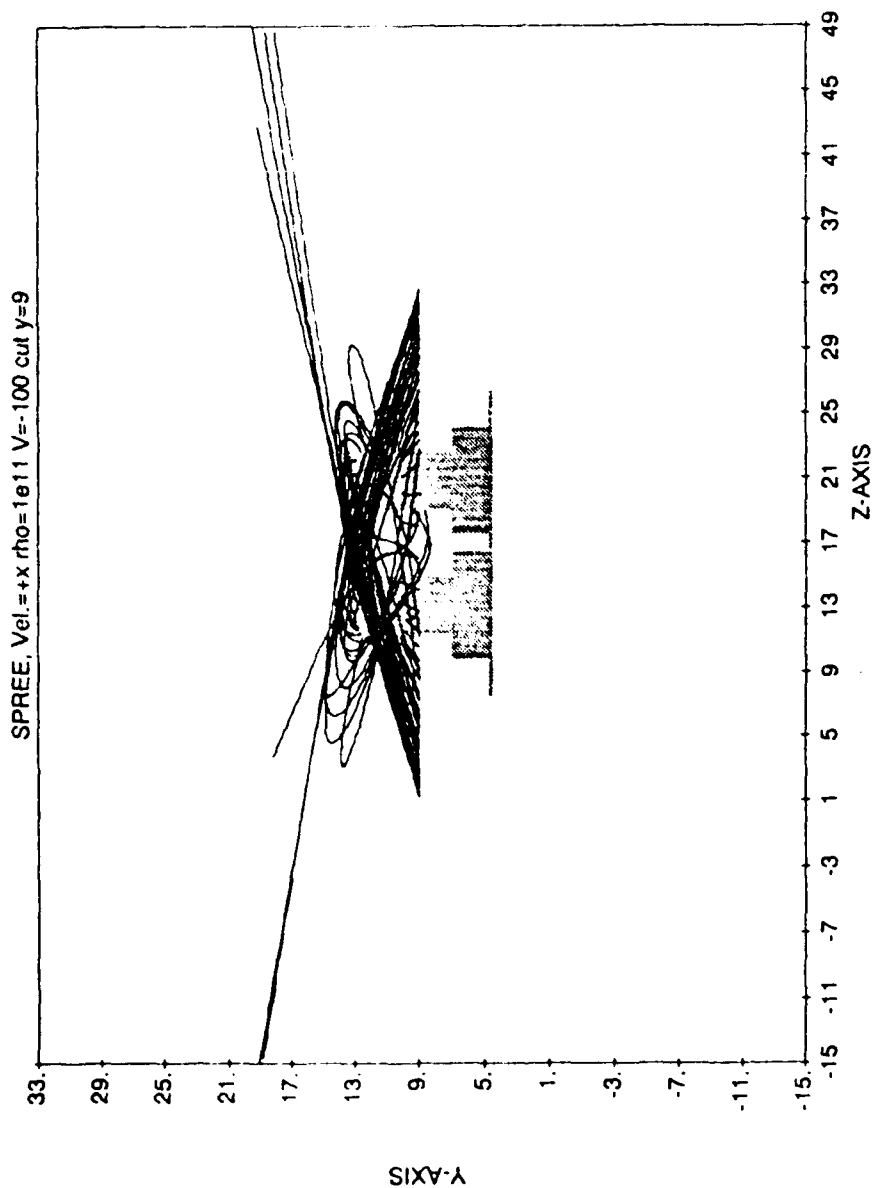
SPREE Case 2

-100 V

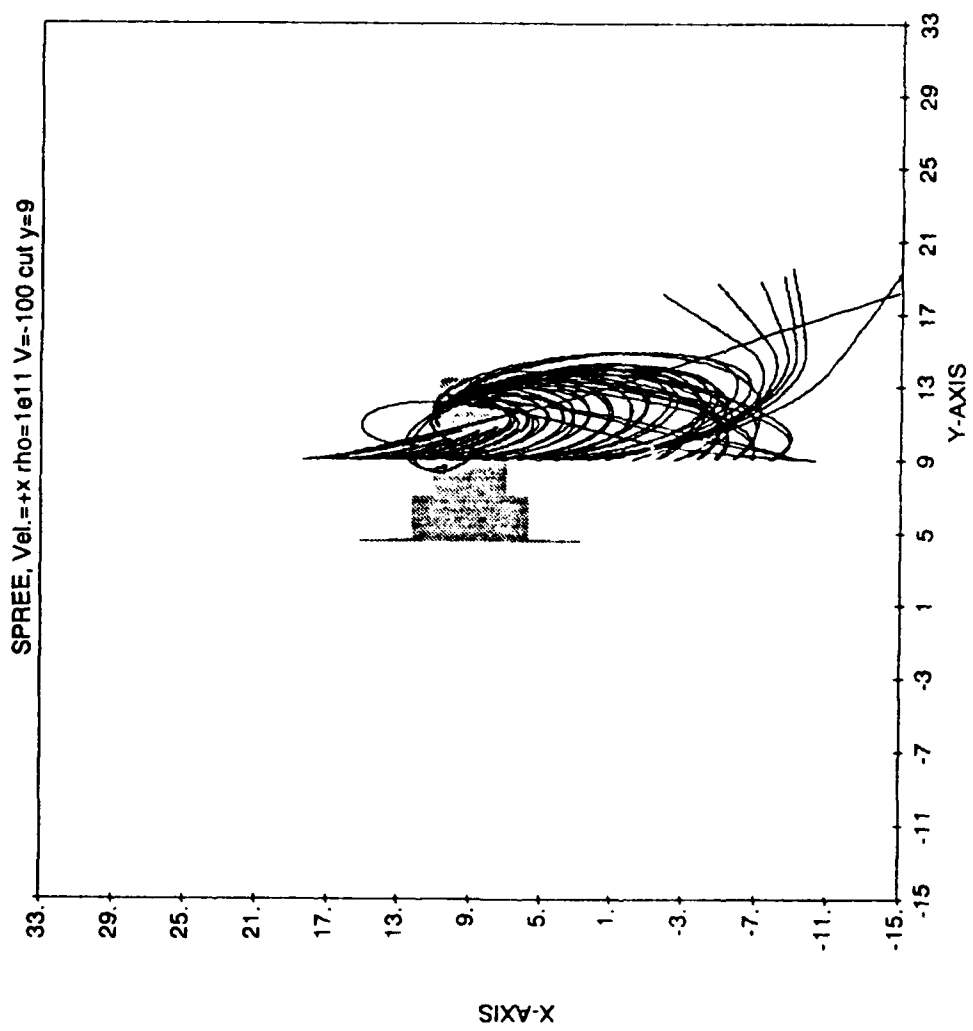




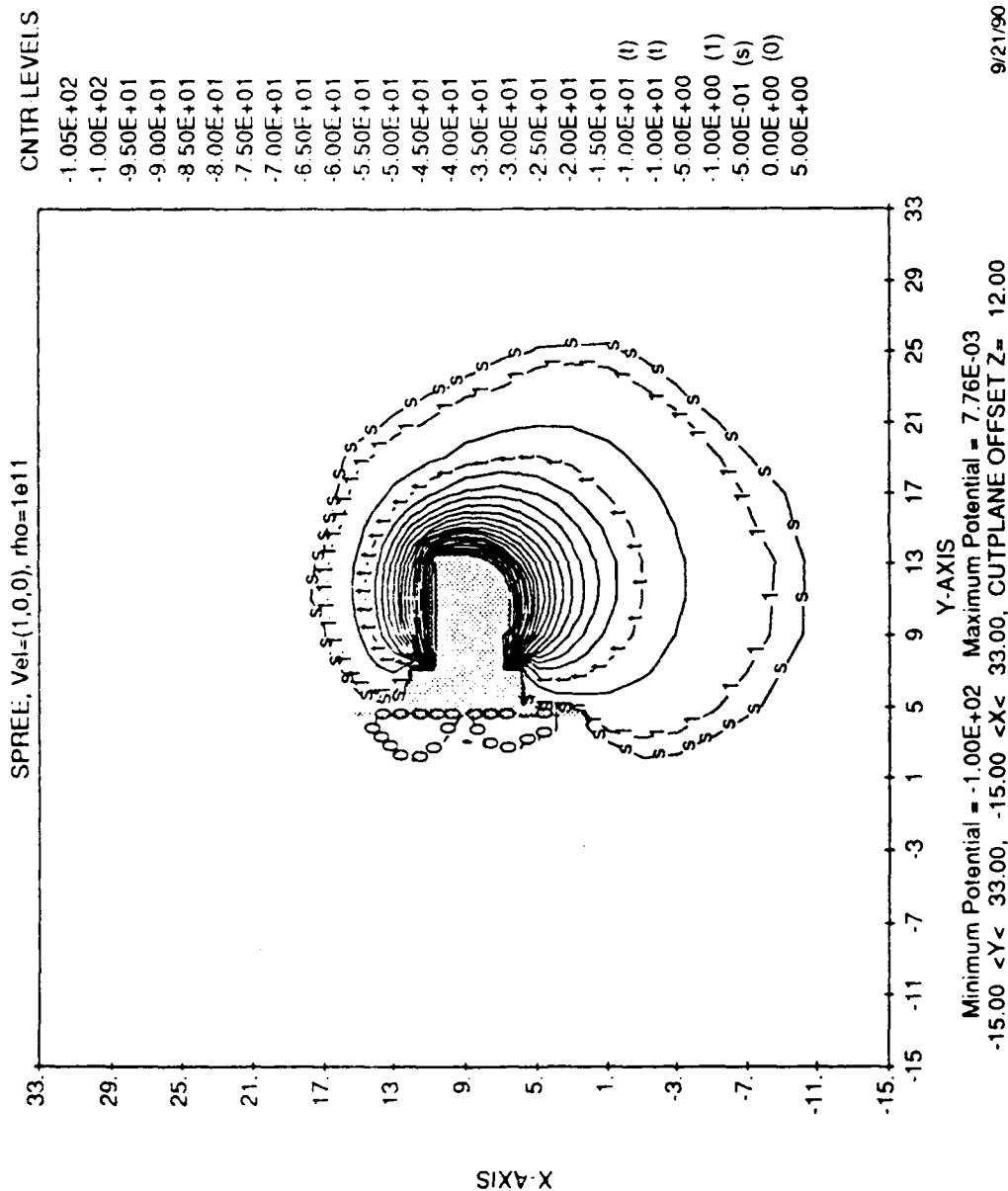
10/17/90 18:46:26



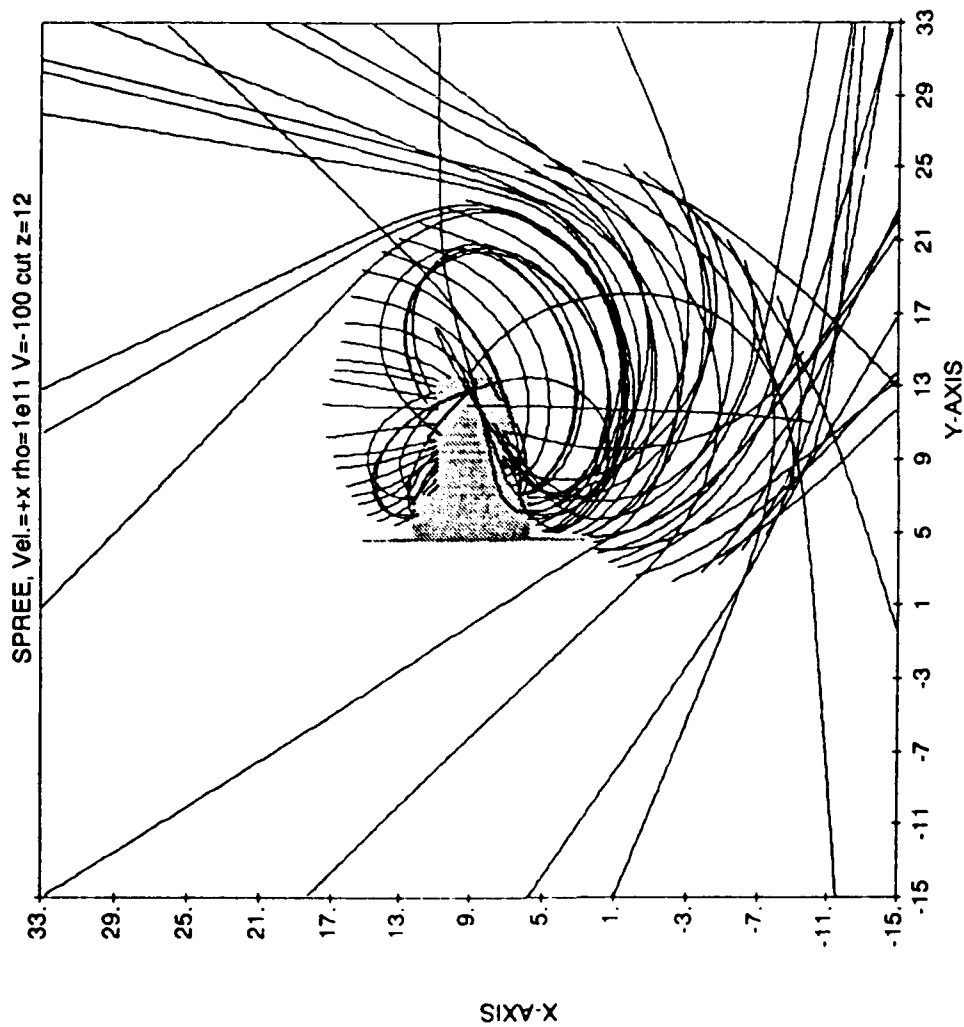
10/17/90 18:46:23



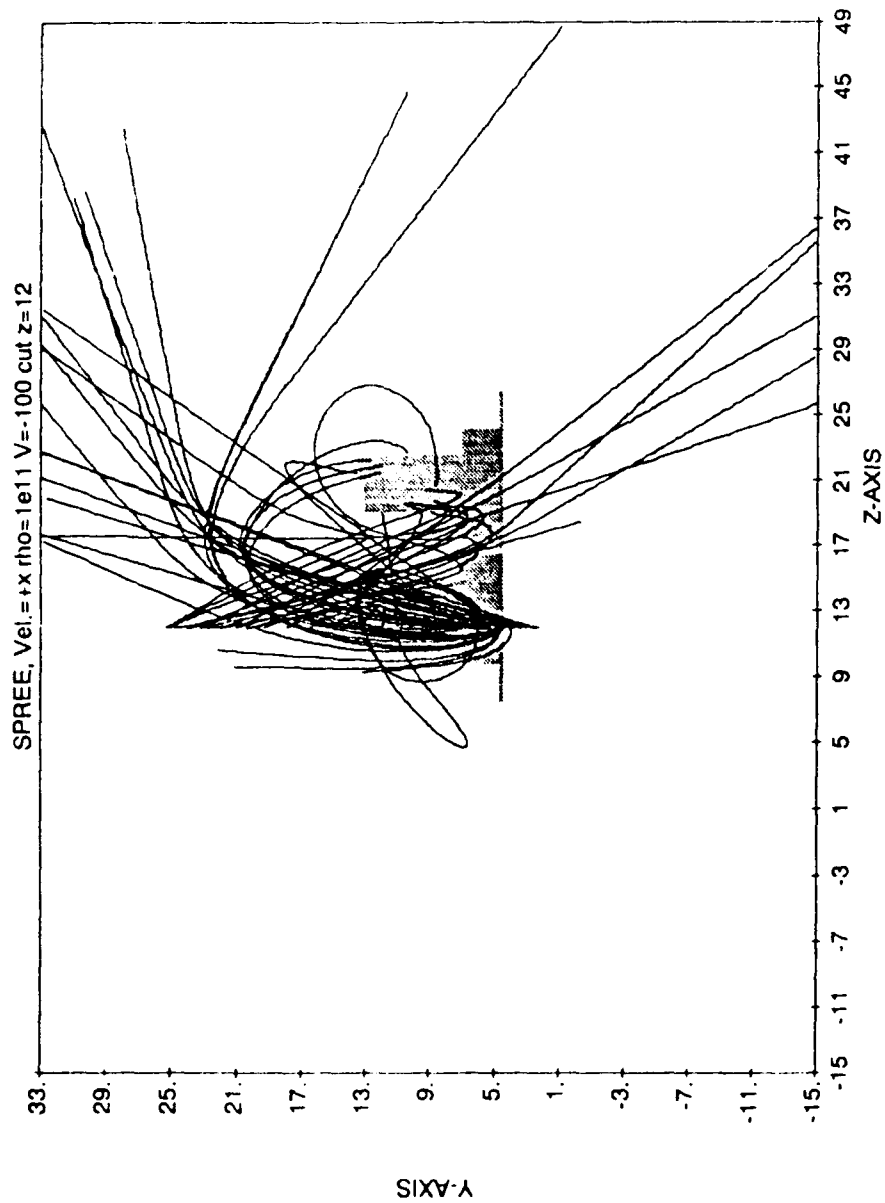
10/17/90 18:46:28



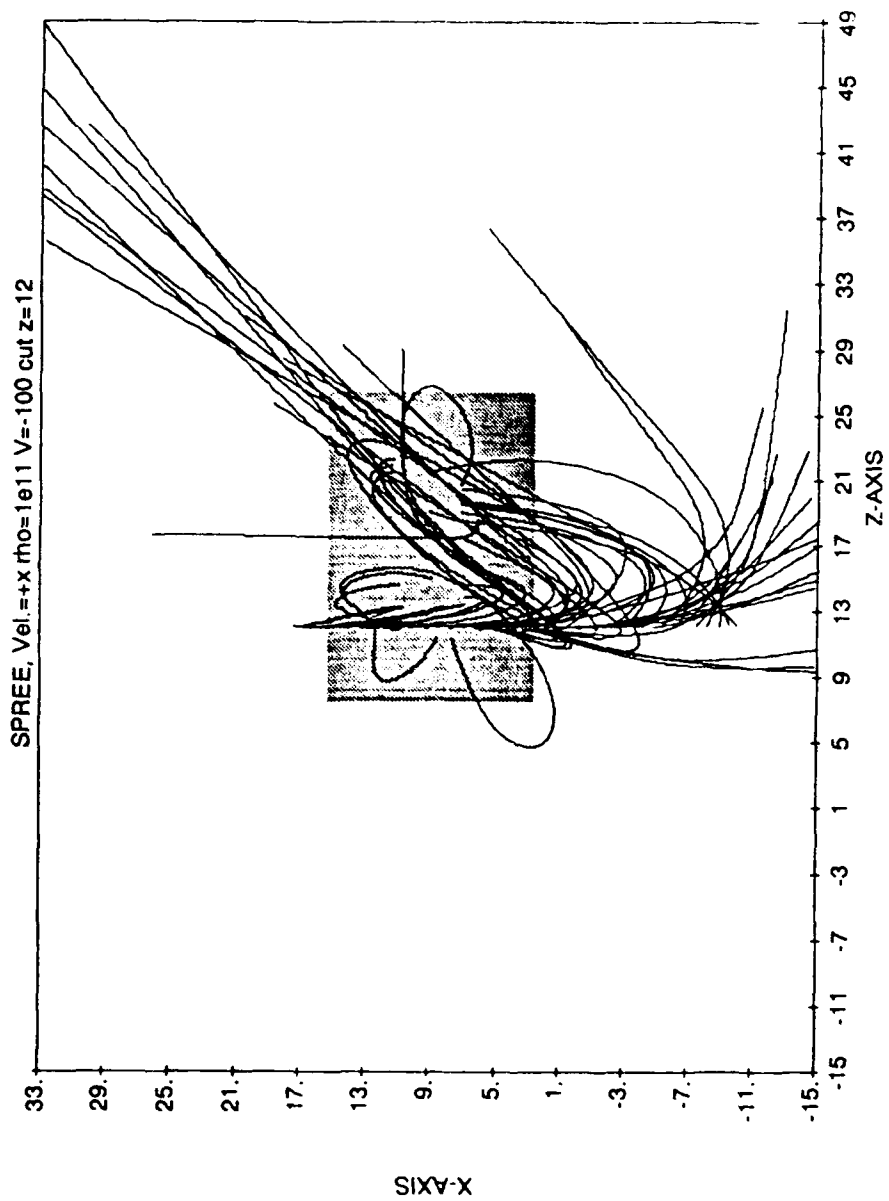
9/21/90 22 05 49



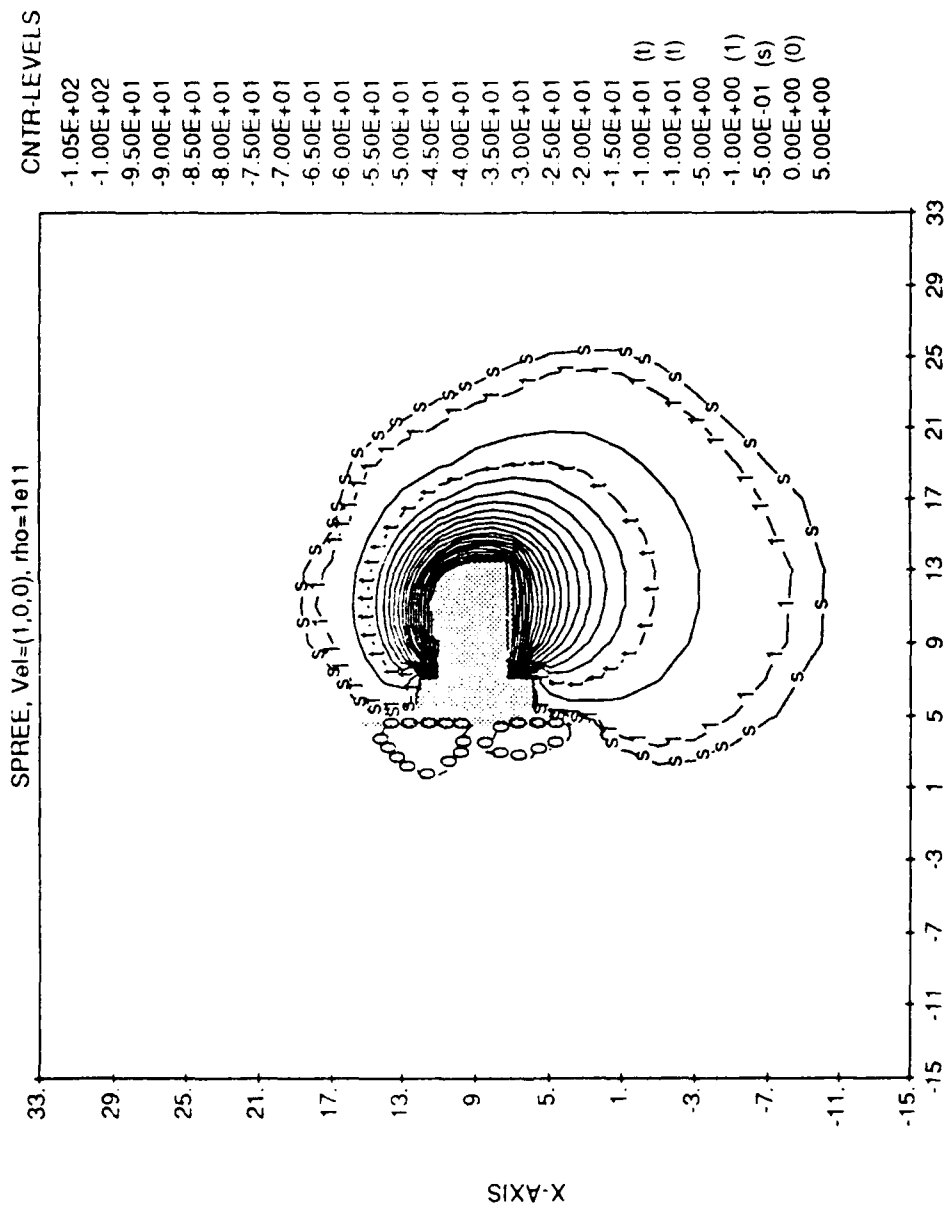
10/17/90 18:50:18



10/17/90 18:50:16

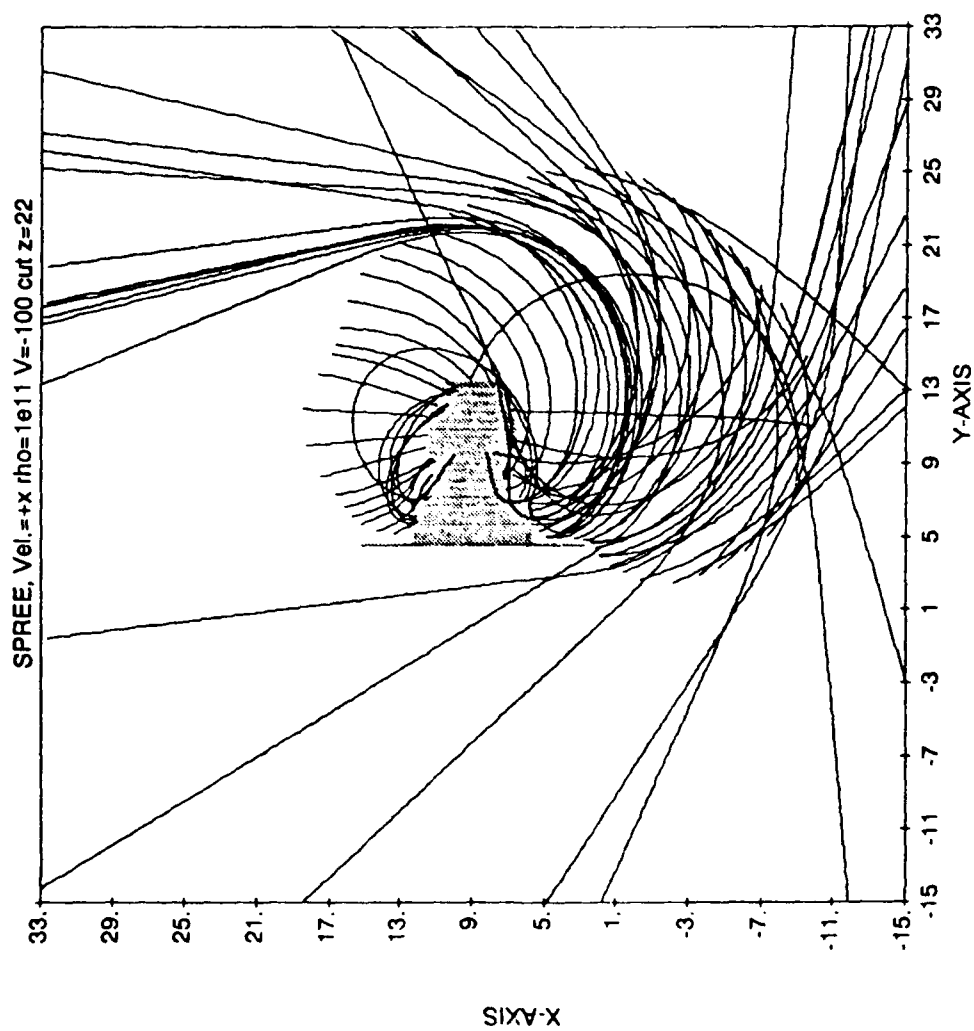


10/17/90 18:50:17

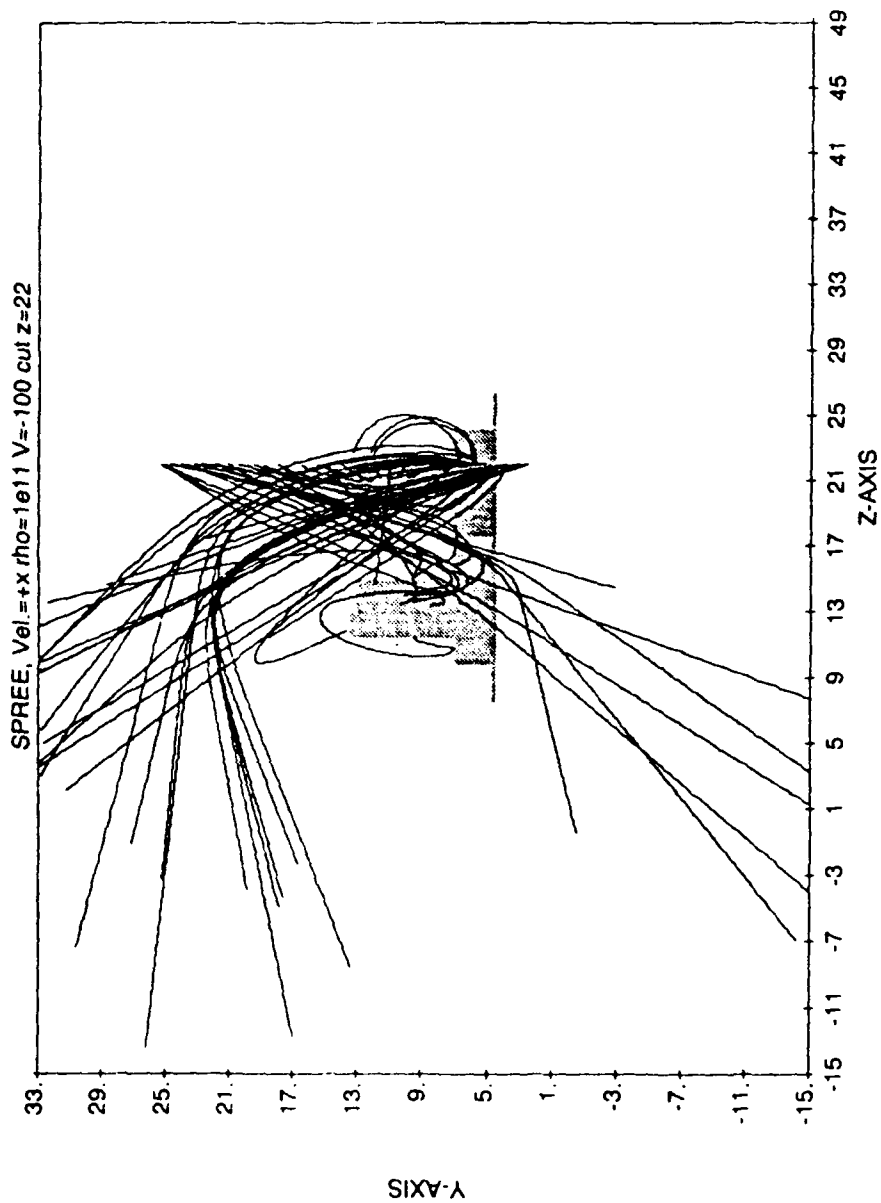


Minimum Potential = -1.00E+02 Maximum Potential = 6.38E-03
 -15.00 <Y< 33.00, -15.00 <X< 33.00, CUTPLANE OFFSET Z= 22.00

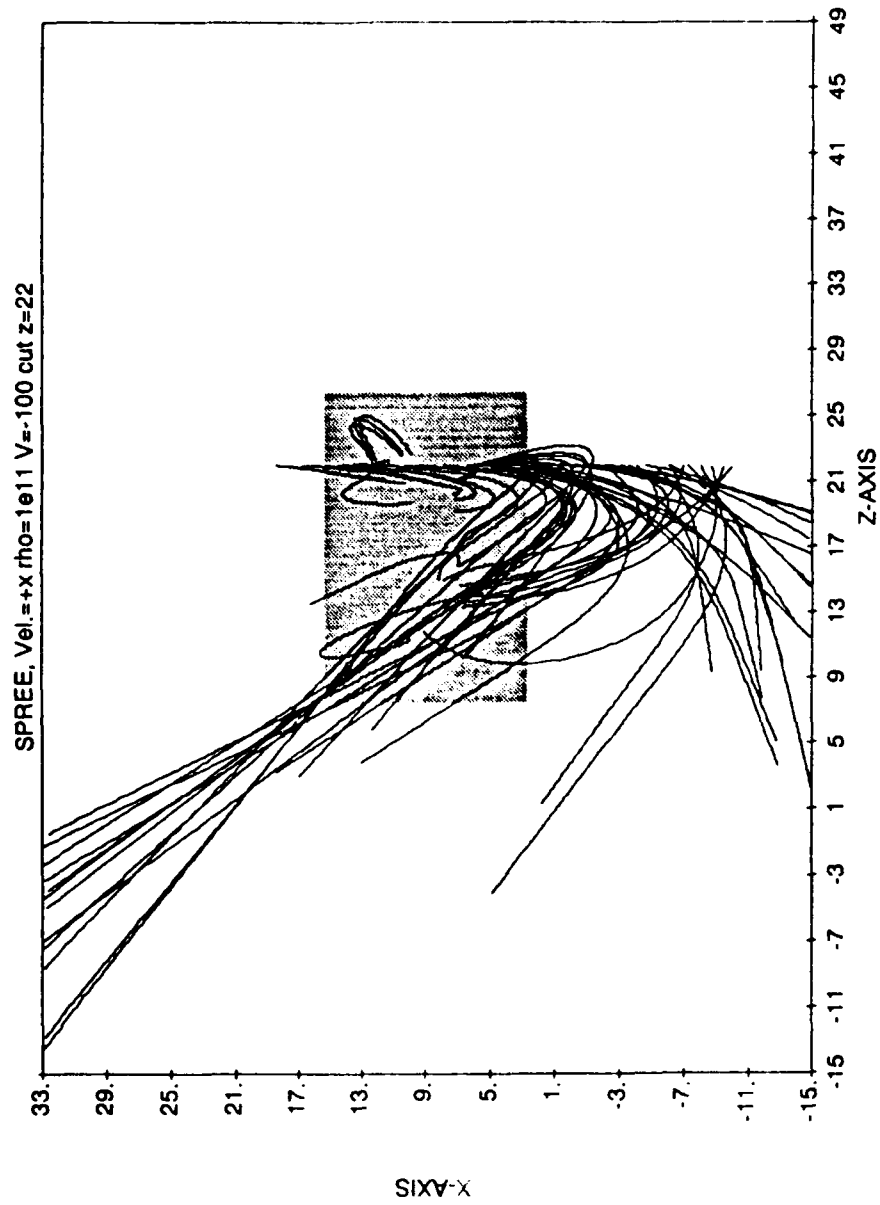
9/21/90 22 05 51



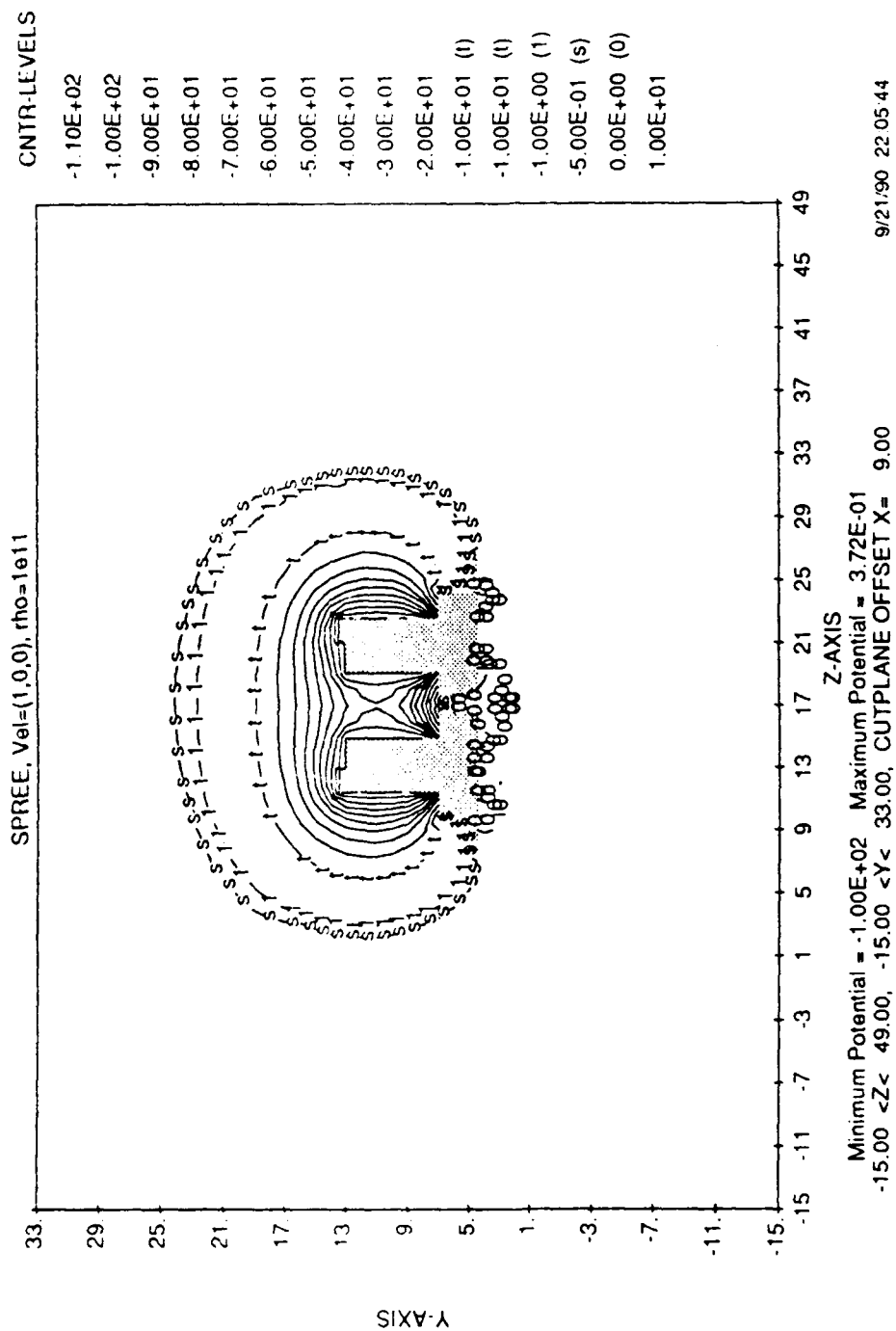
10/17/90 18:52:59



10/17/90 18:52:57

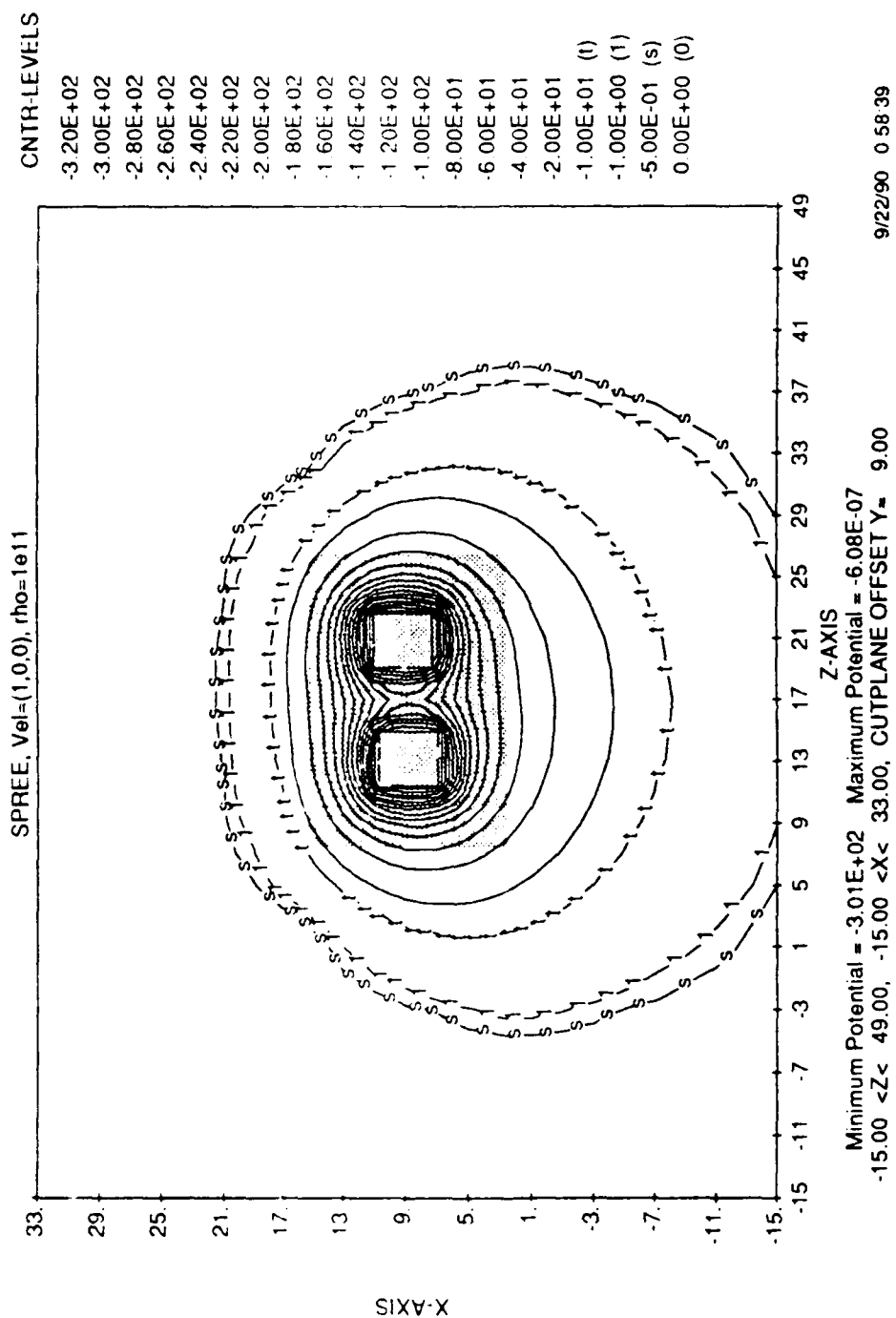


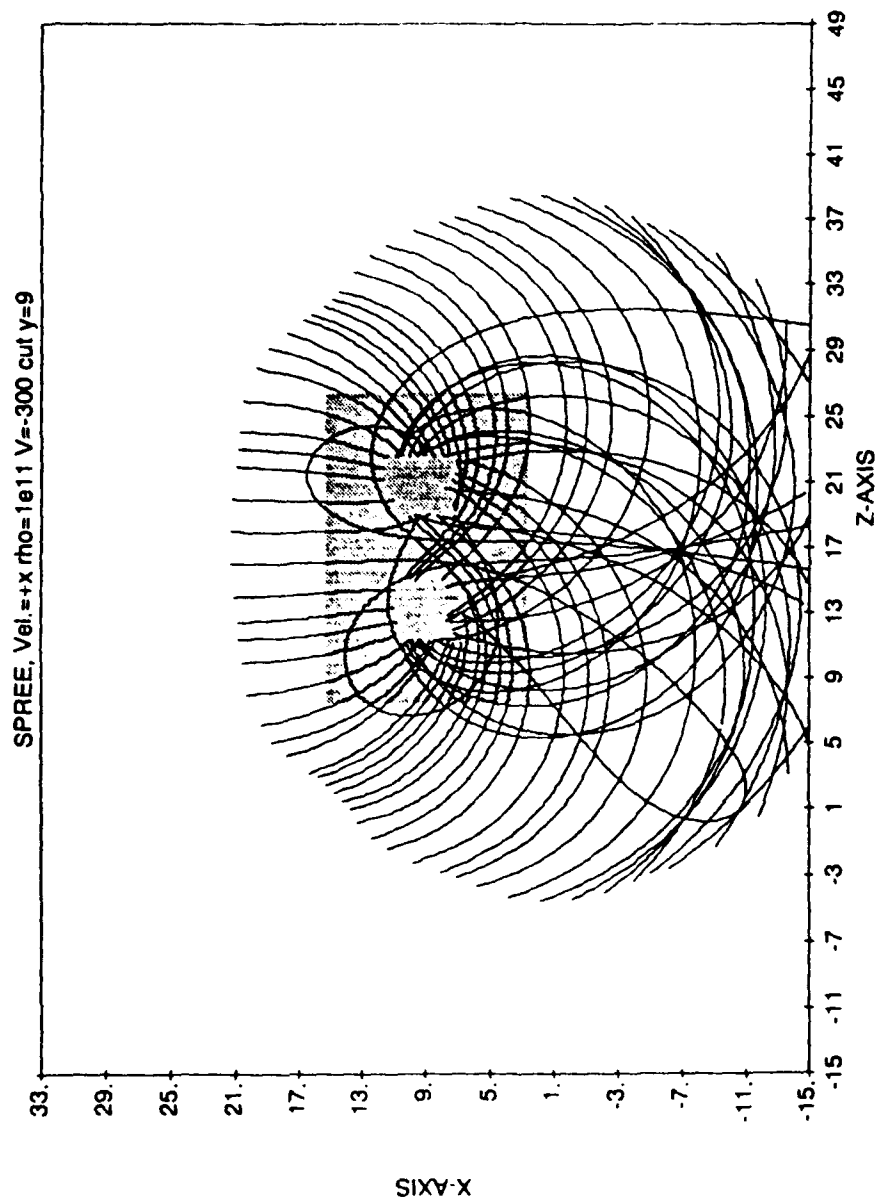
10/17/90 18:52:58



SPREE Case 2

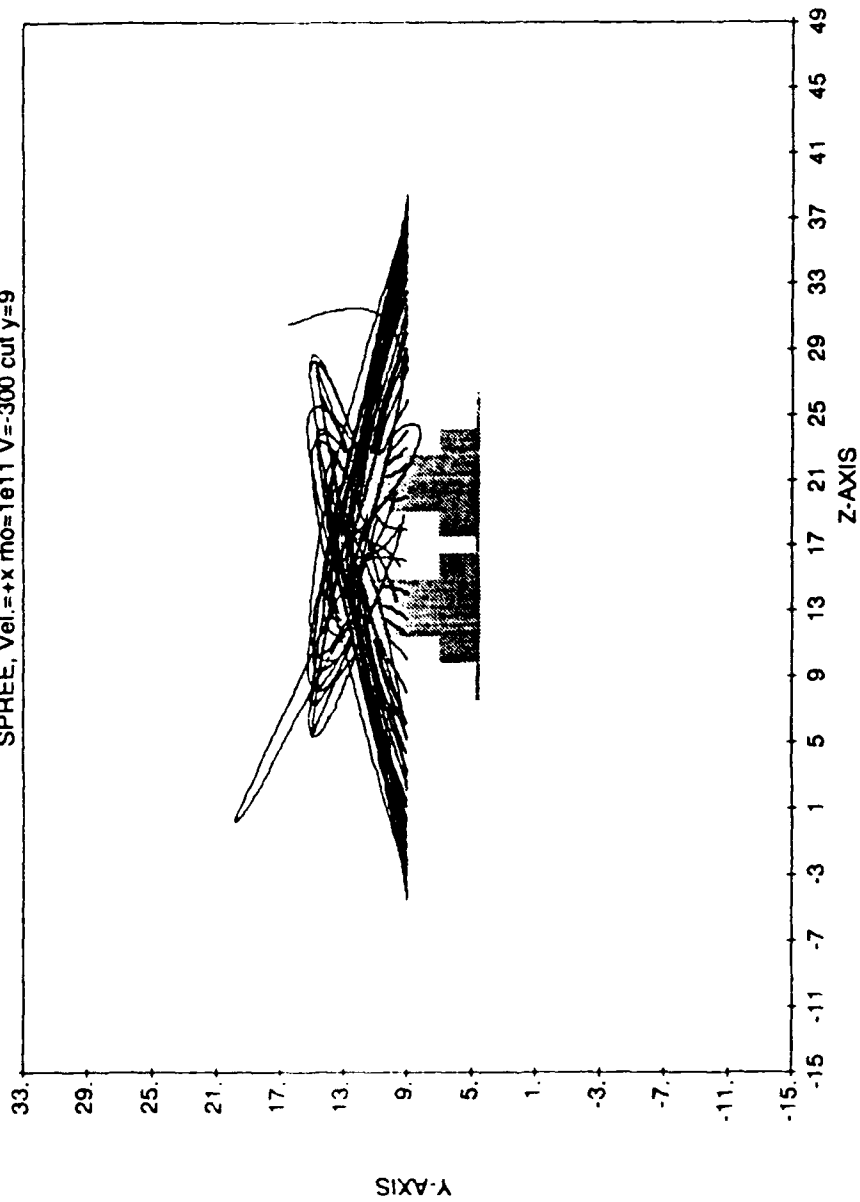
-300 V



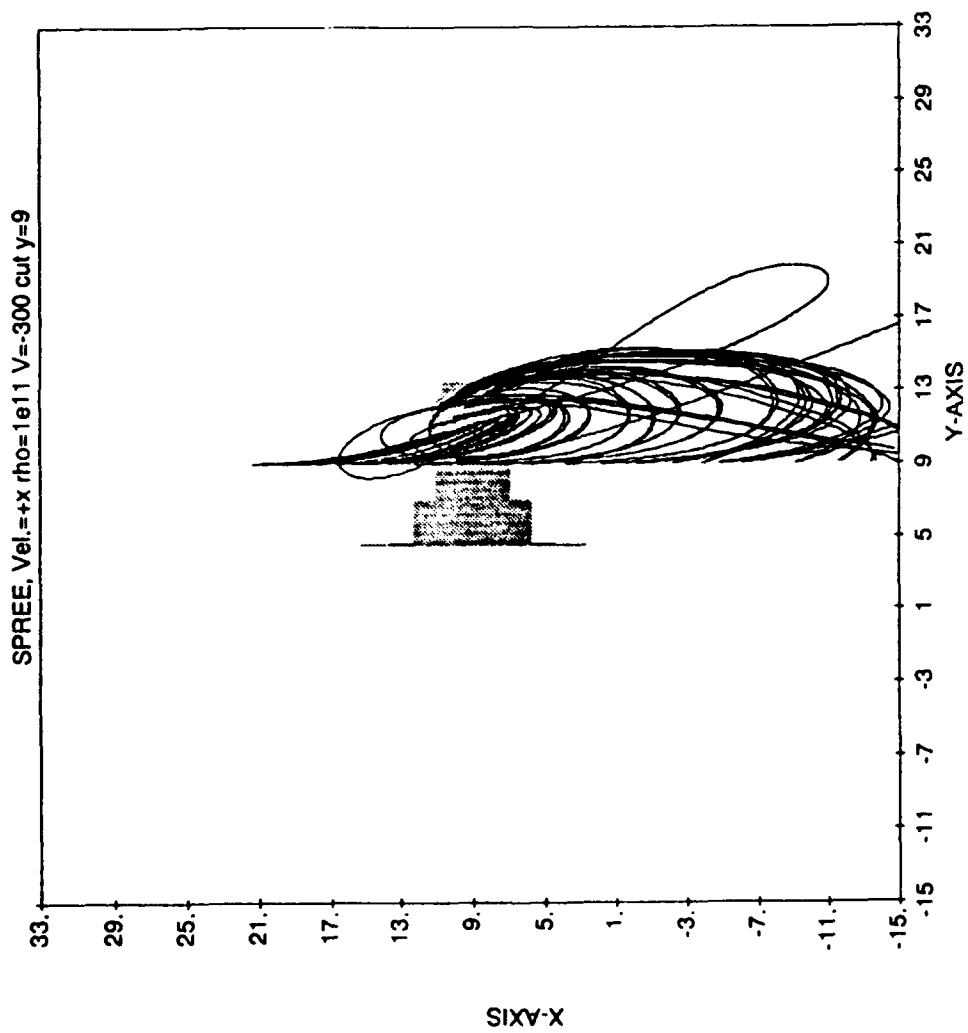


10/17/90 19:23:00

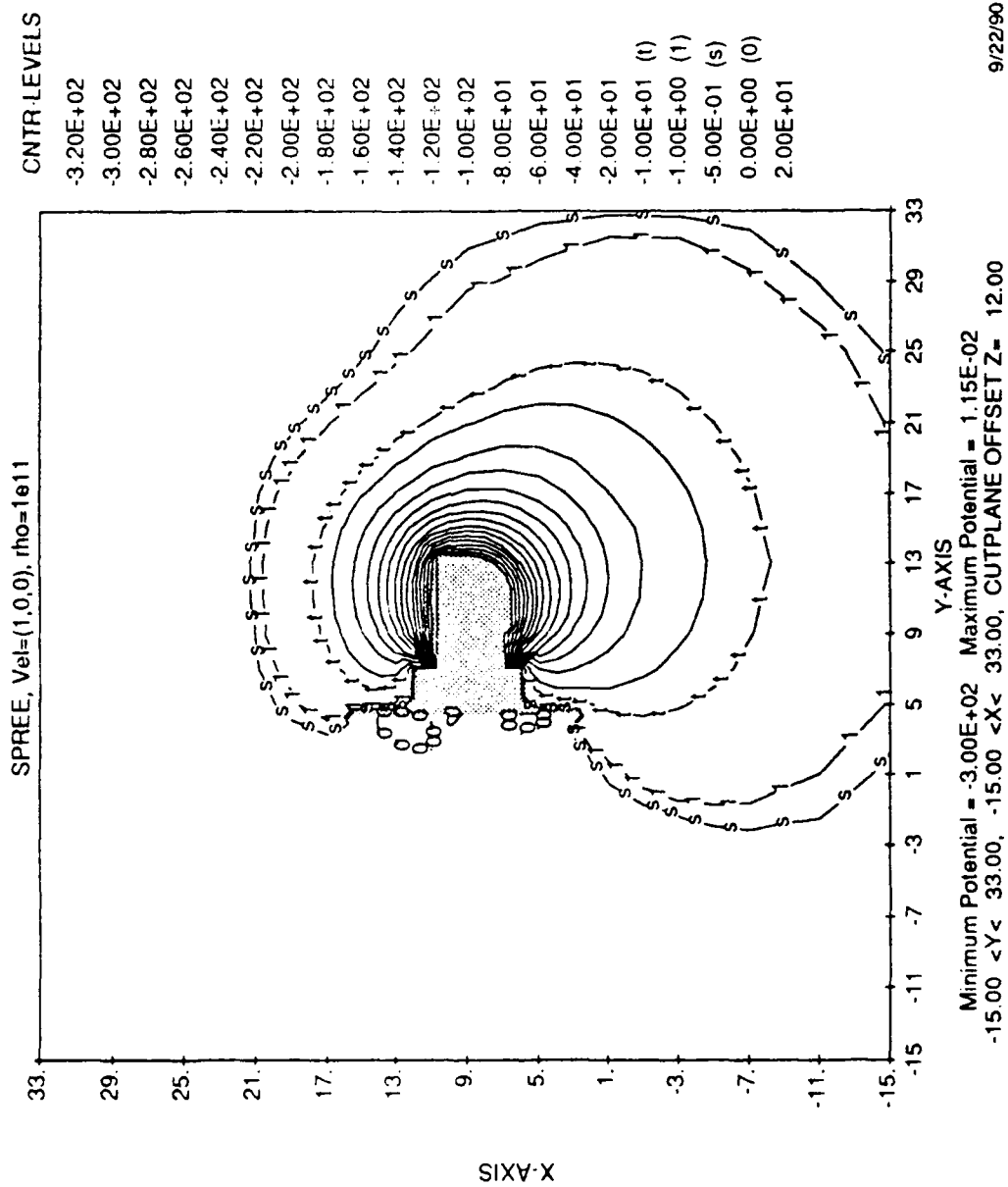
SPREE, Vel.=+x rho=1e11 V=-300 cut y=9

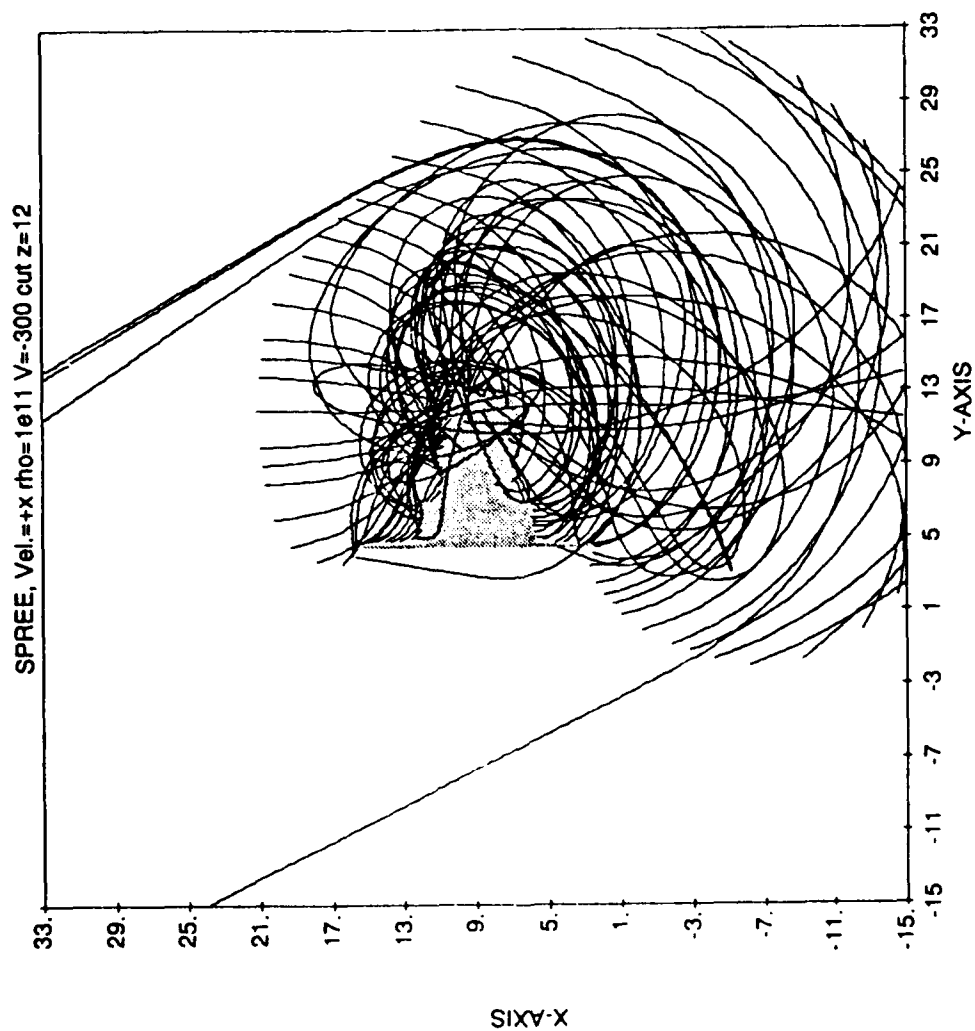


10/17/90 19:22:59

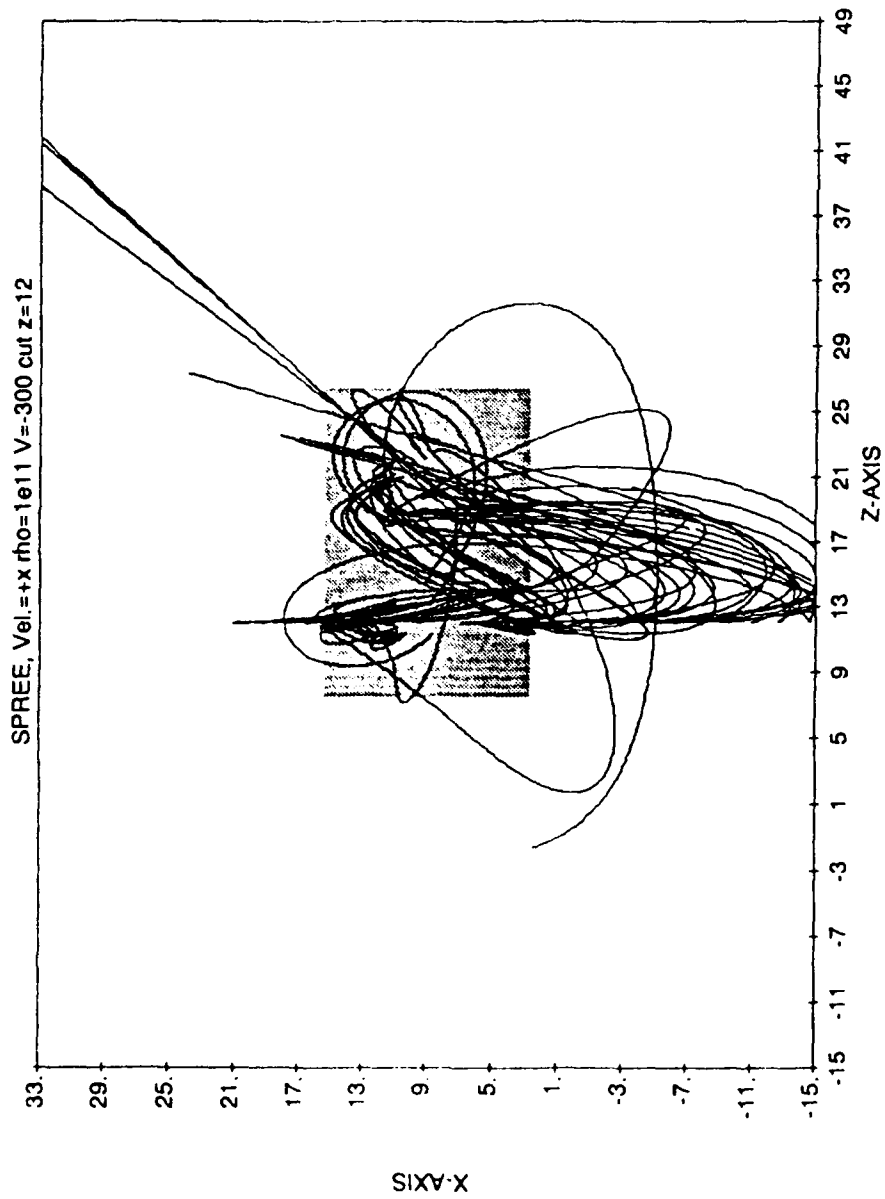


10/17/90 19:23:02

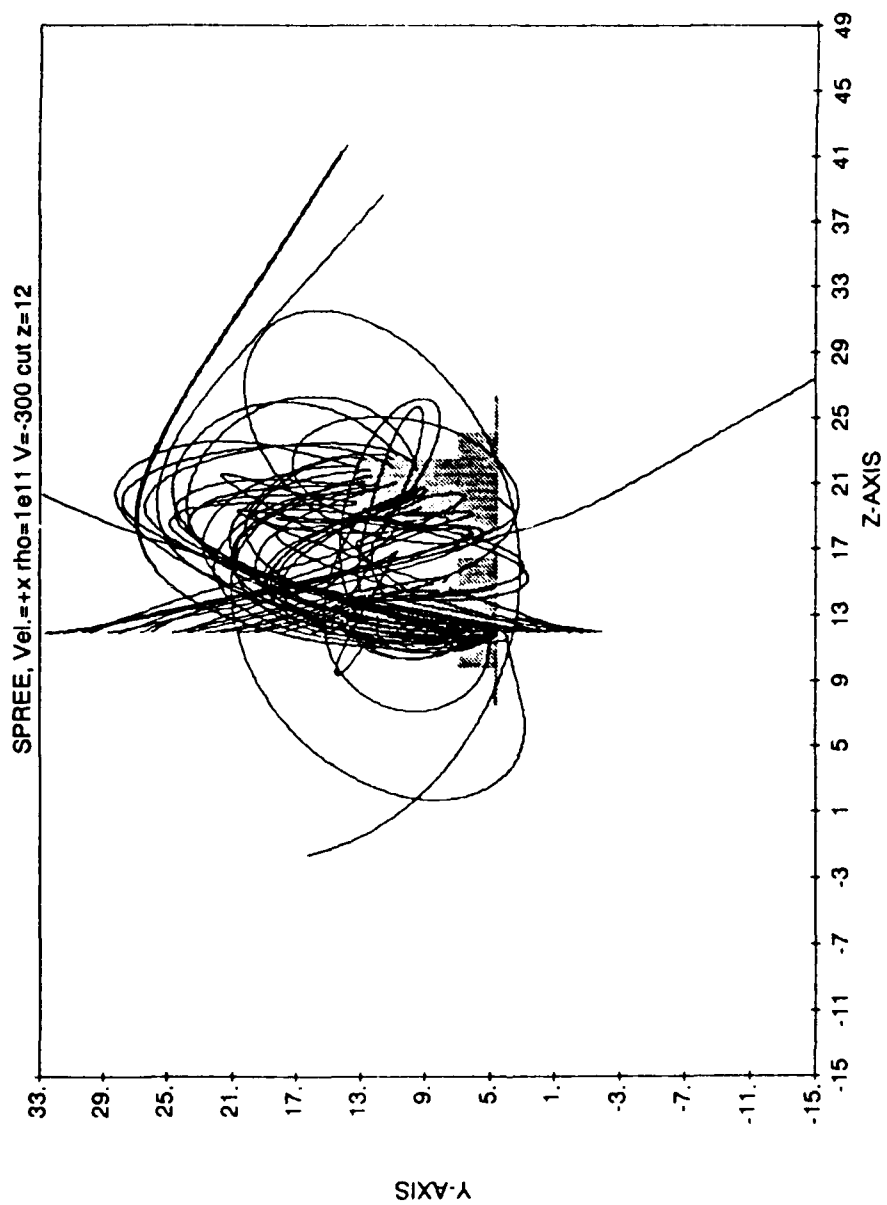




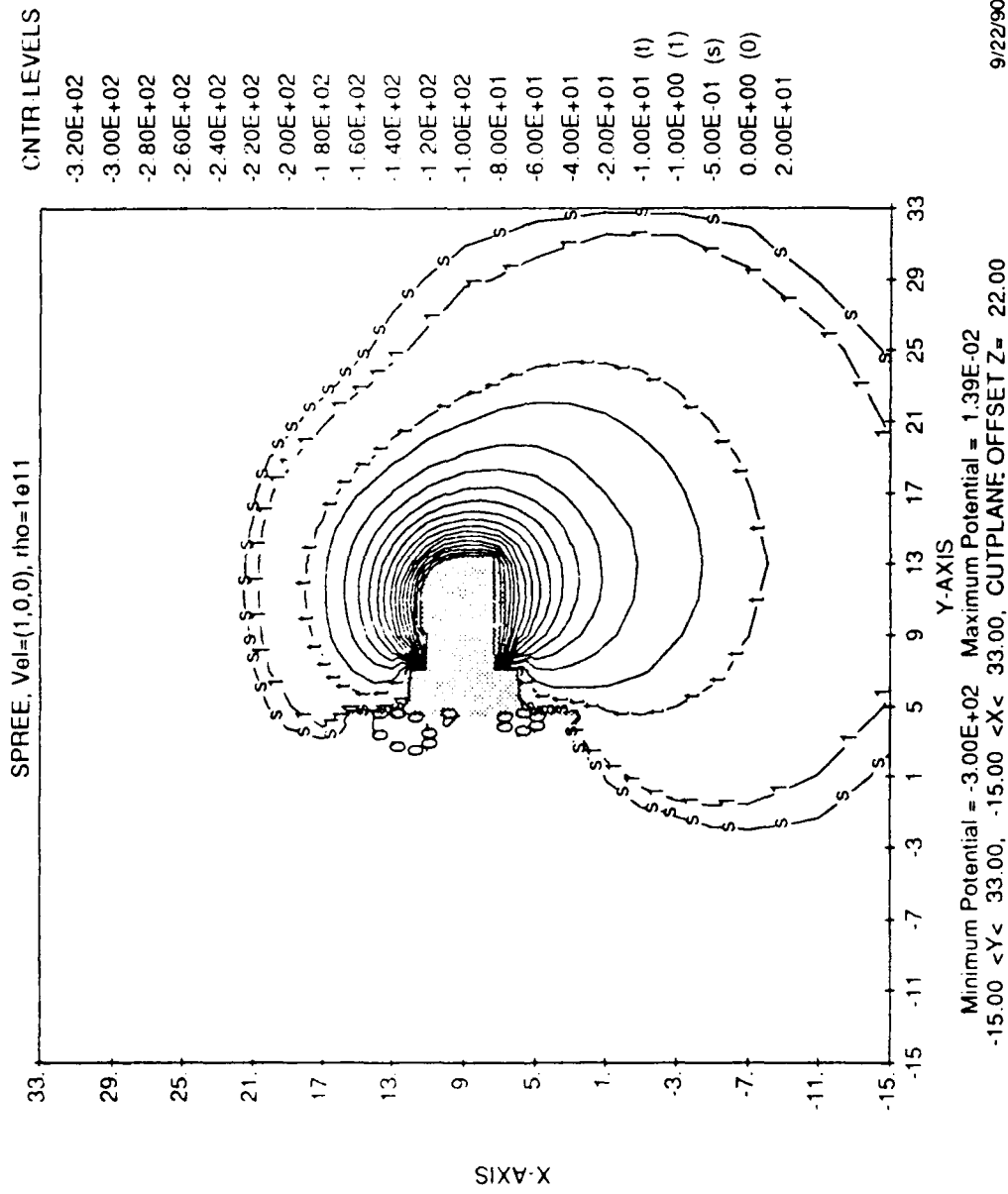
10/17/90 19:28:57



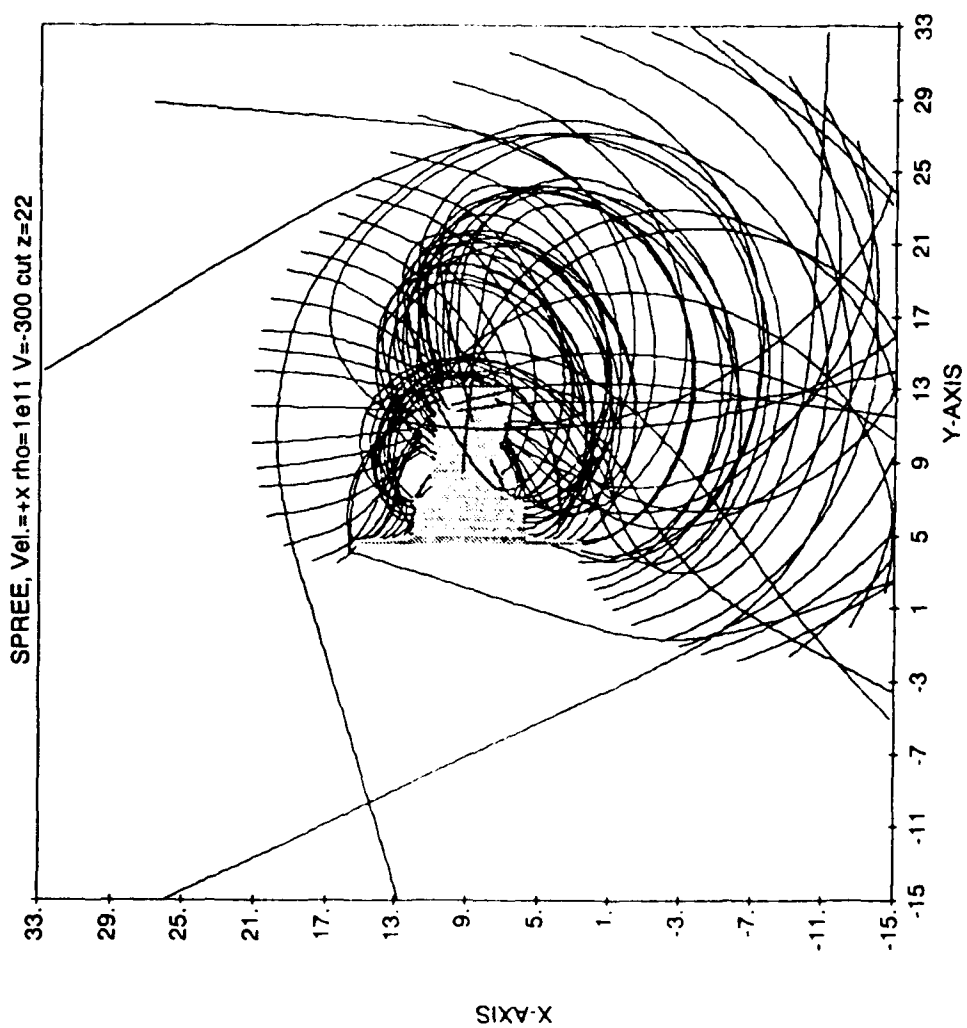
10/17/90 19:28:56



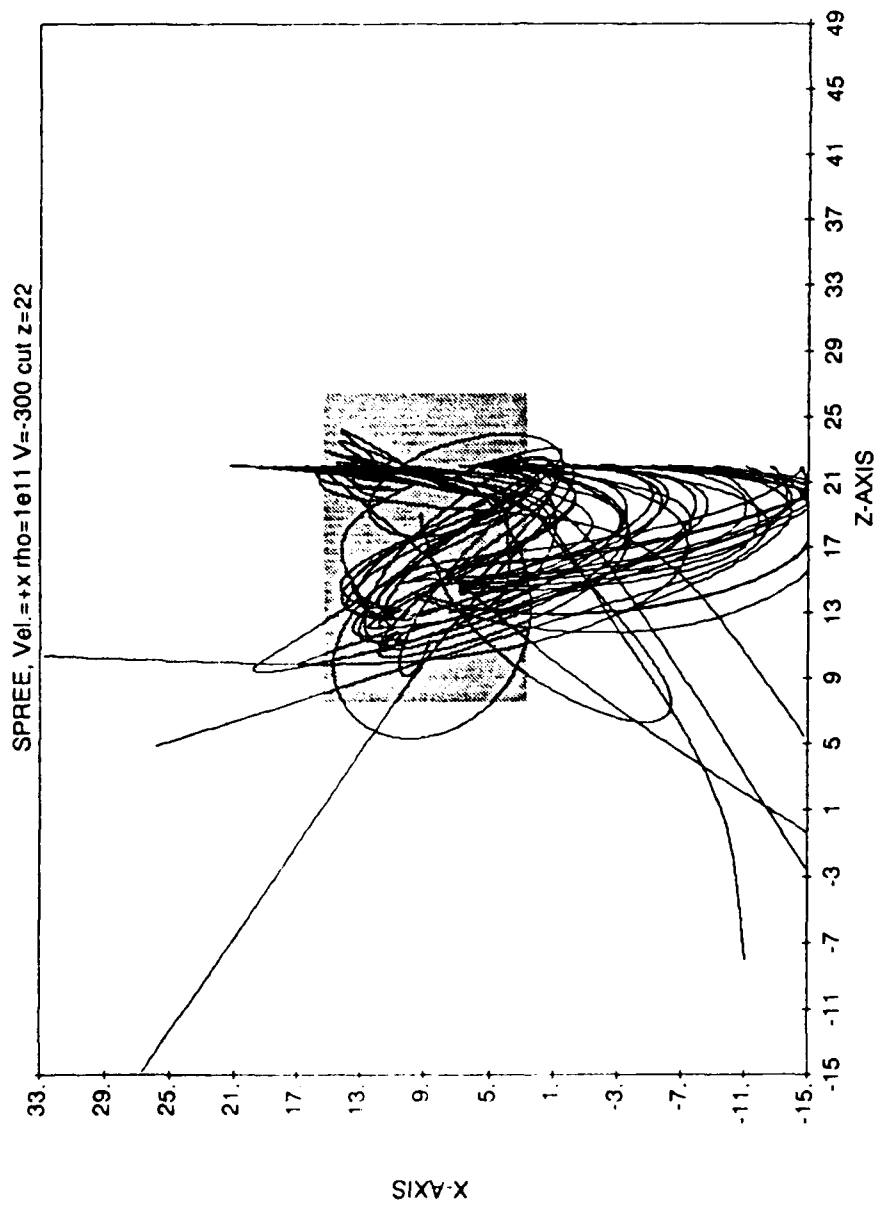
10/17/90 19:28:54



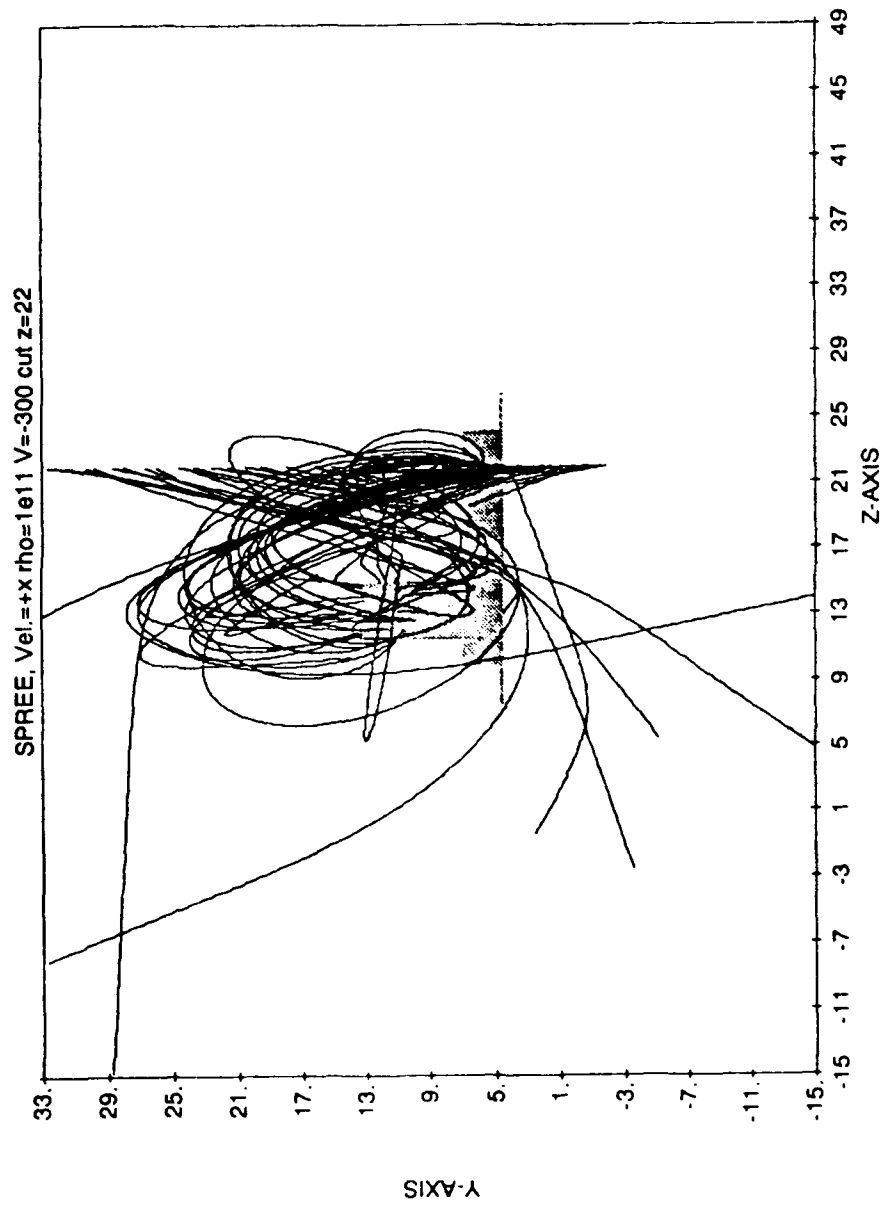
9/22/90 0.58 44



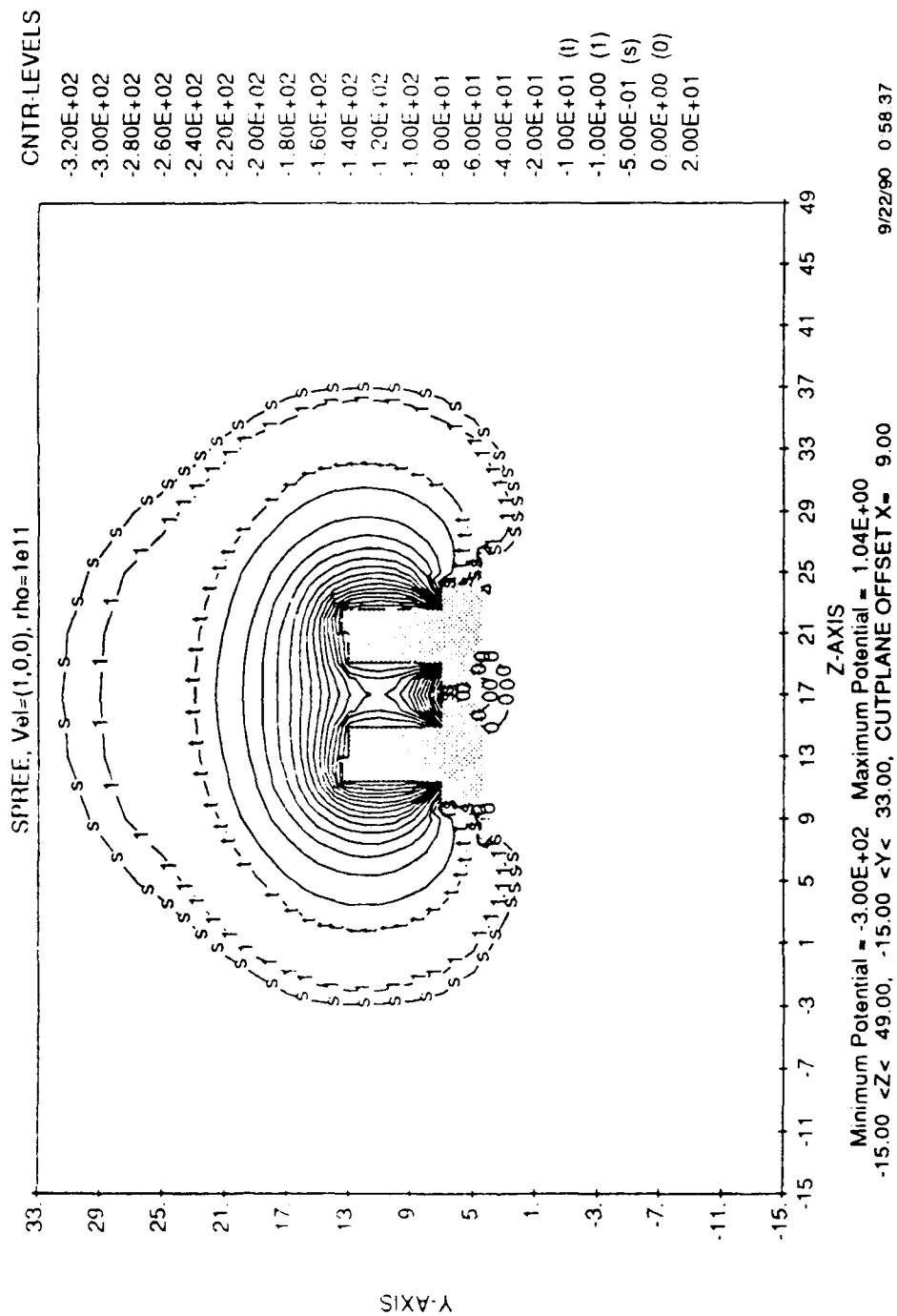
10/17/90 19:37:24



10/17/90 19:37:22

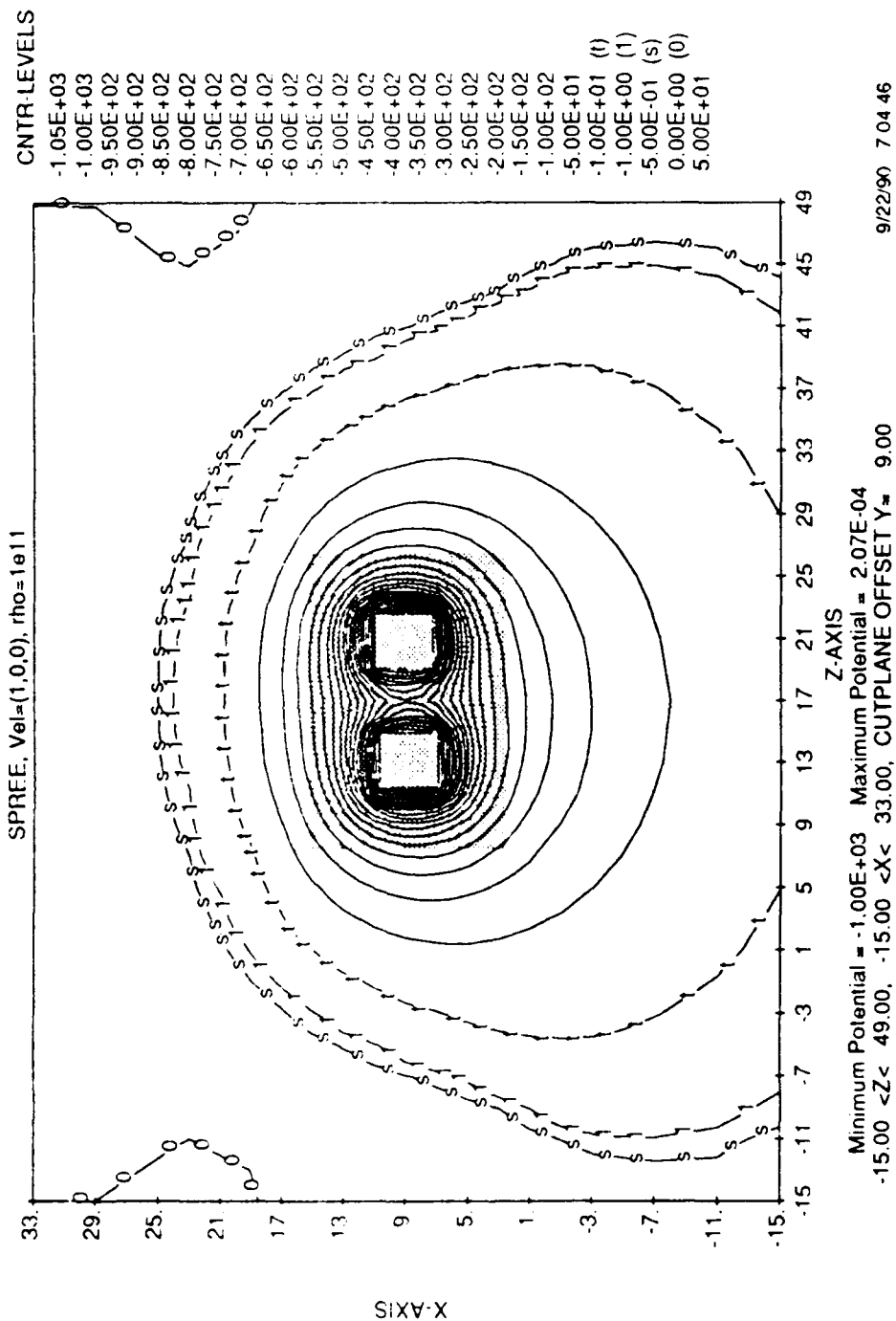


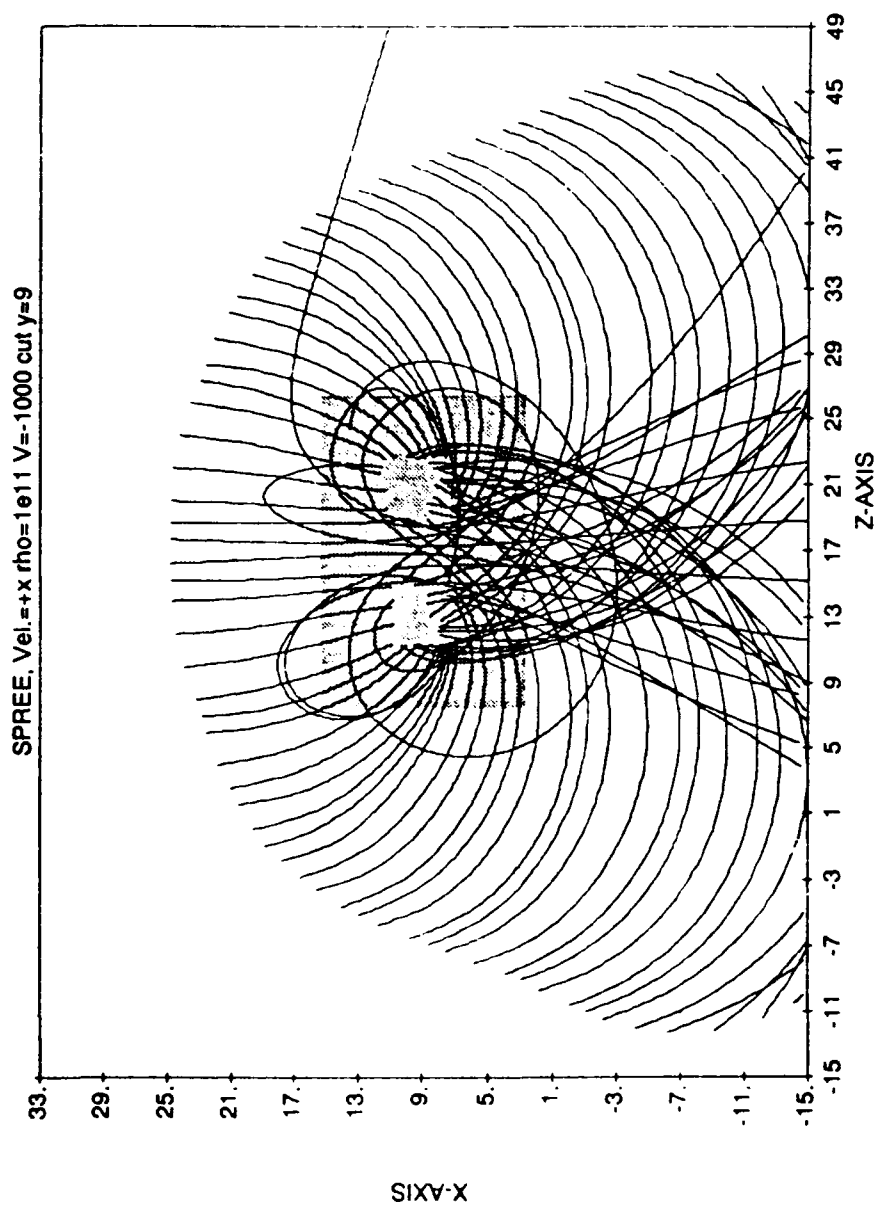
10/17/90 19:37:21



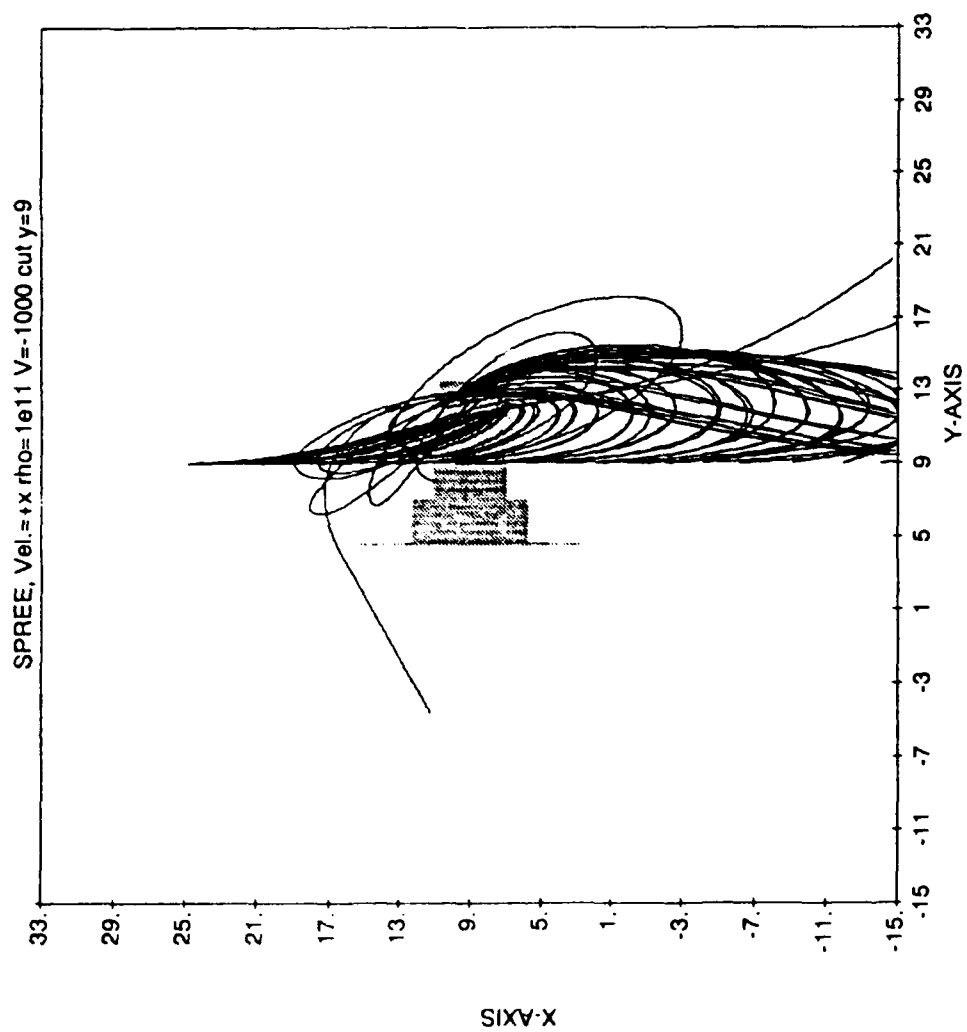
SPREE Case 2

-1000 V

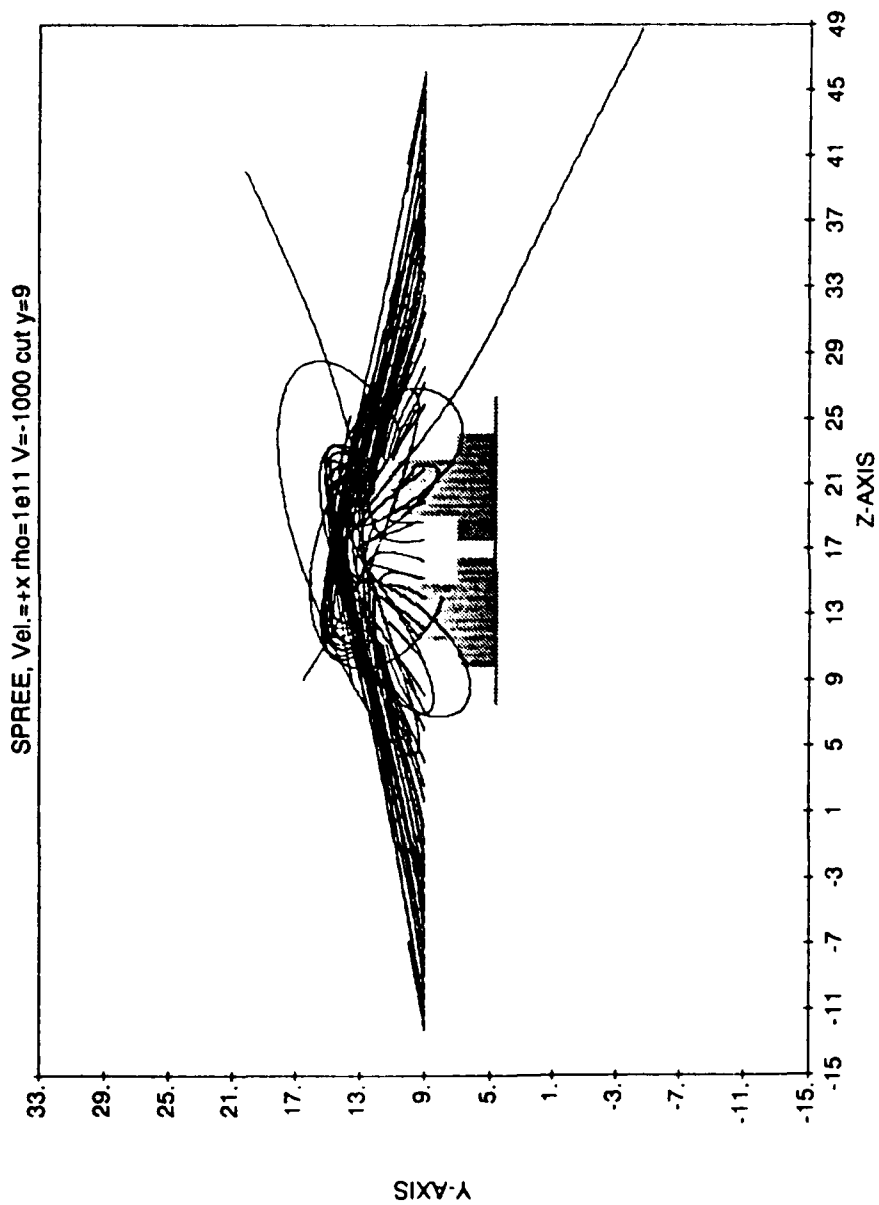




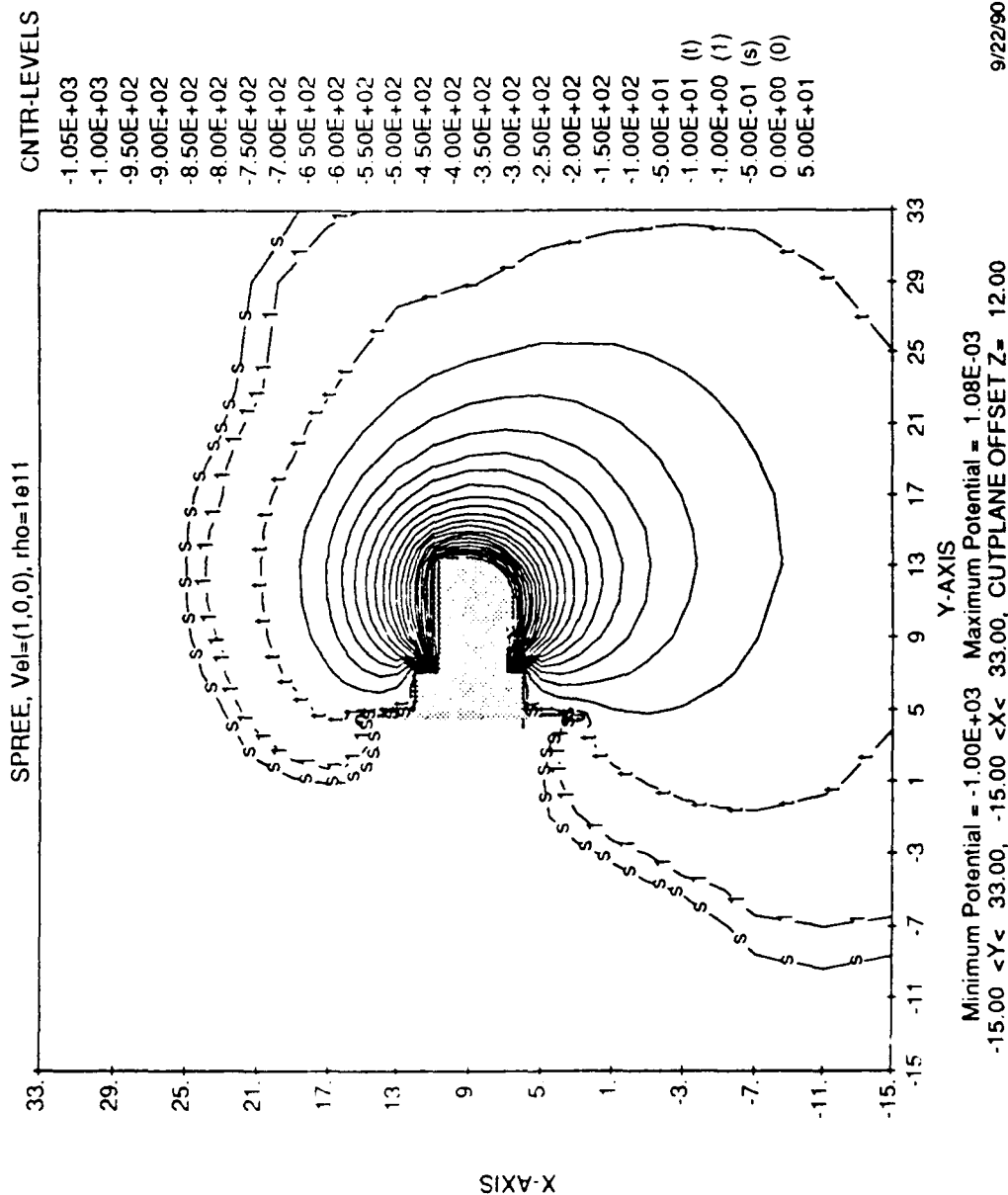
10/17/90 18:57:05

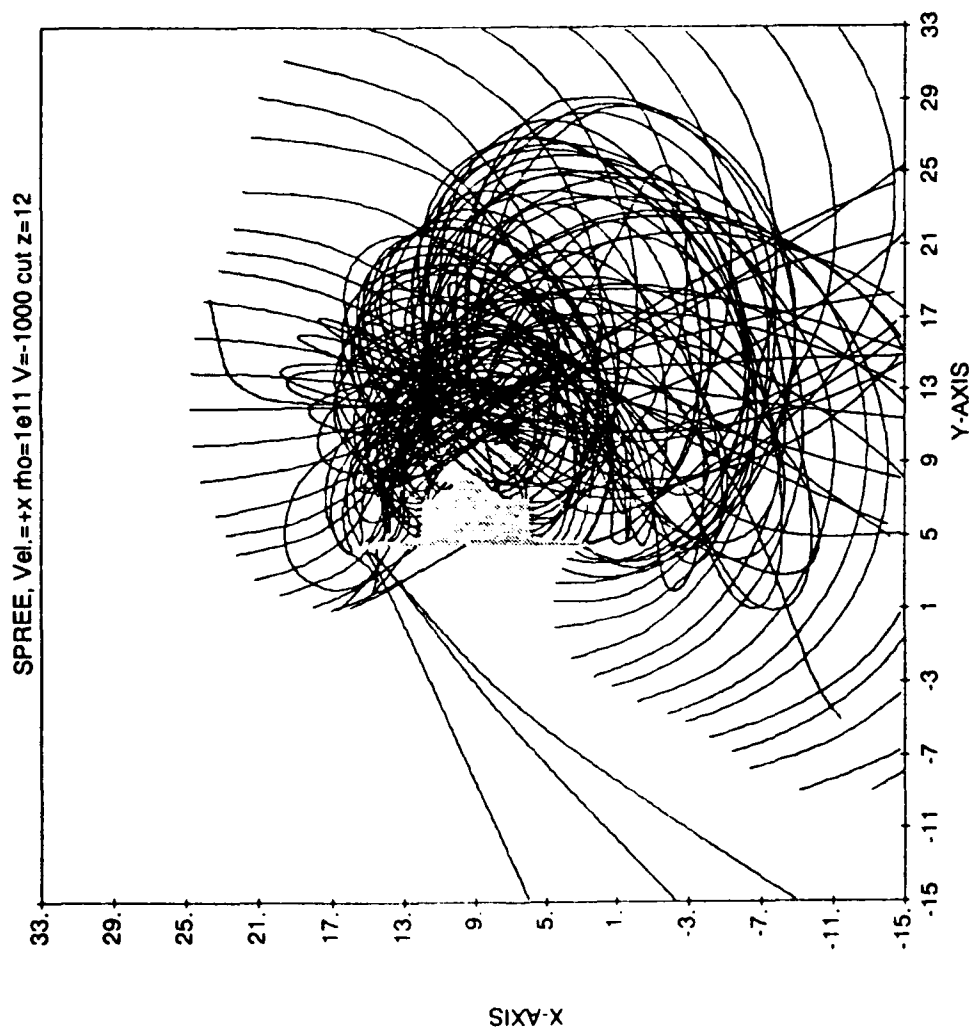


10/17/90 18:57:07

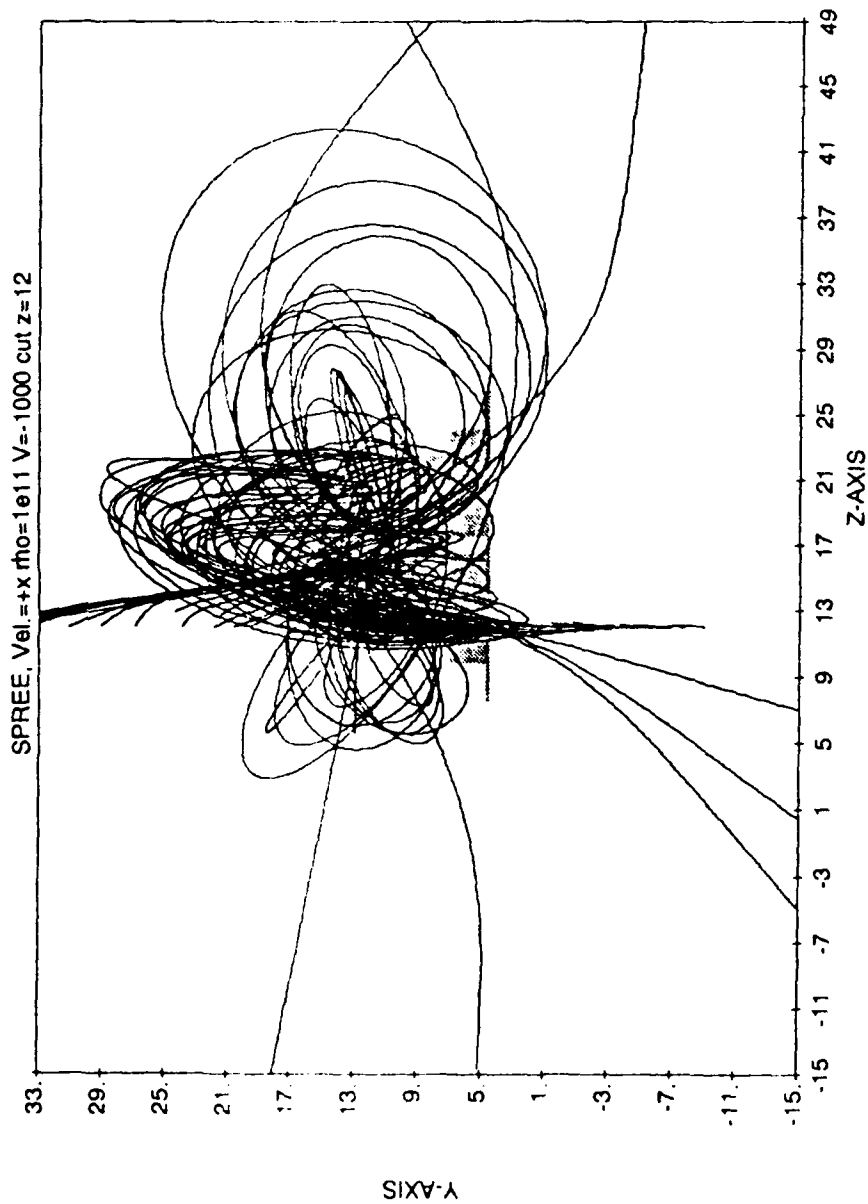


10/17/90 18:56:57

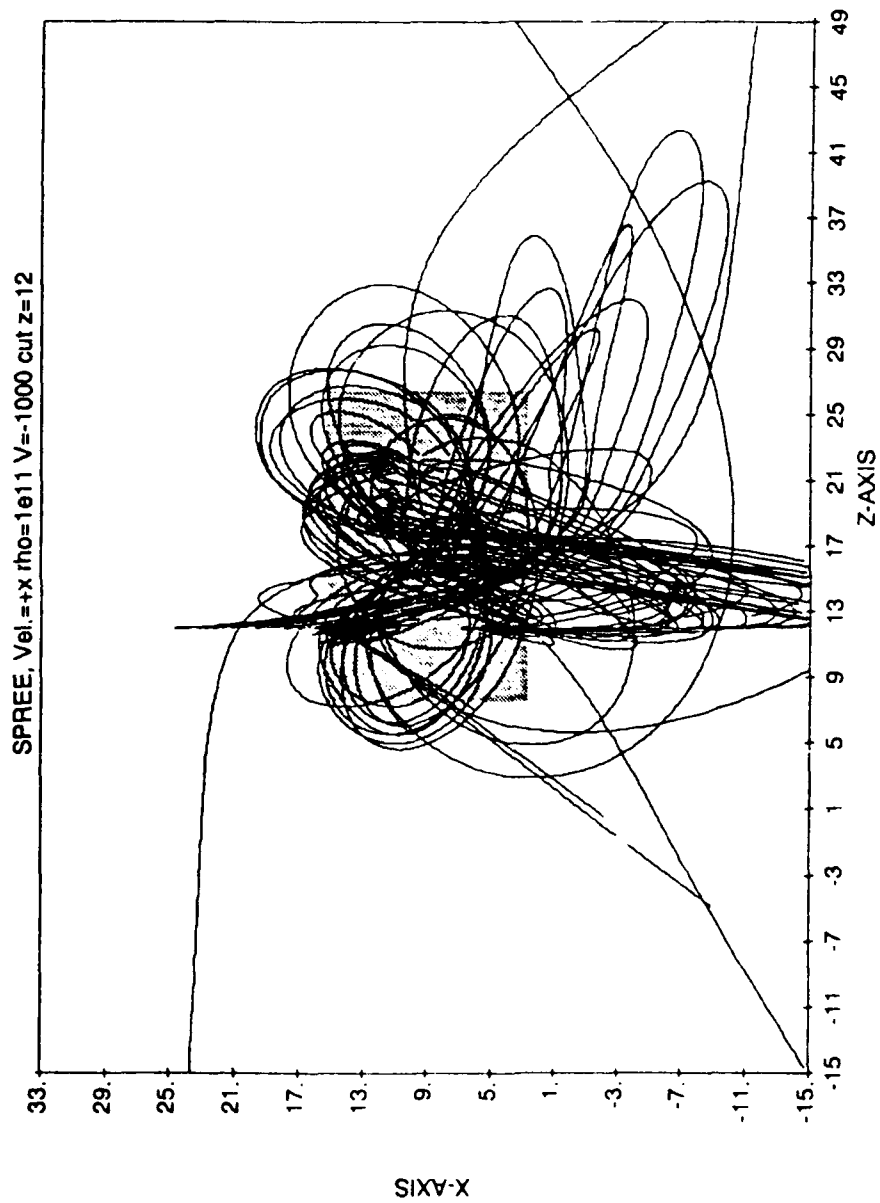




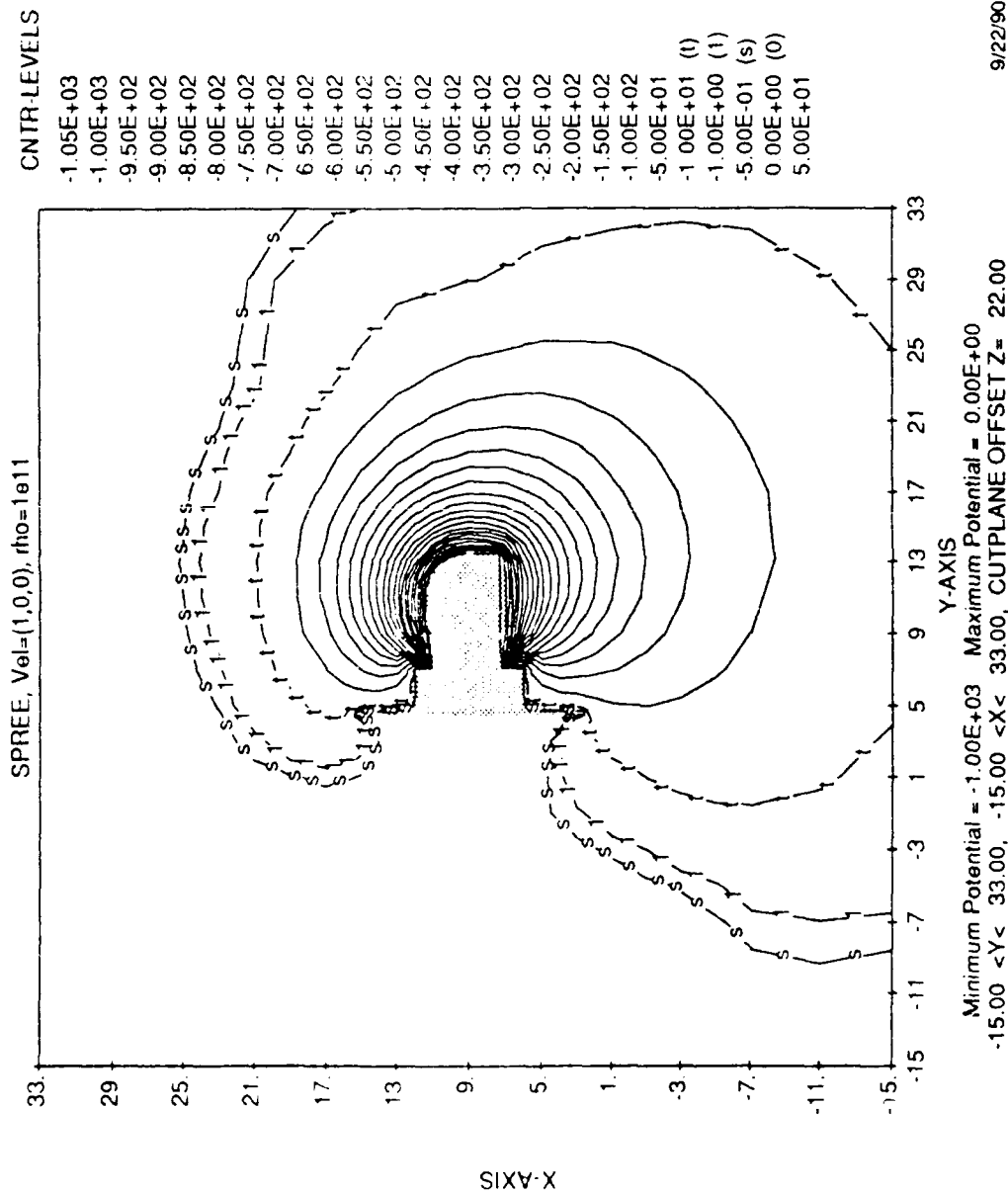
10/17/90 19:07:00



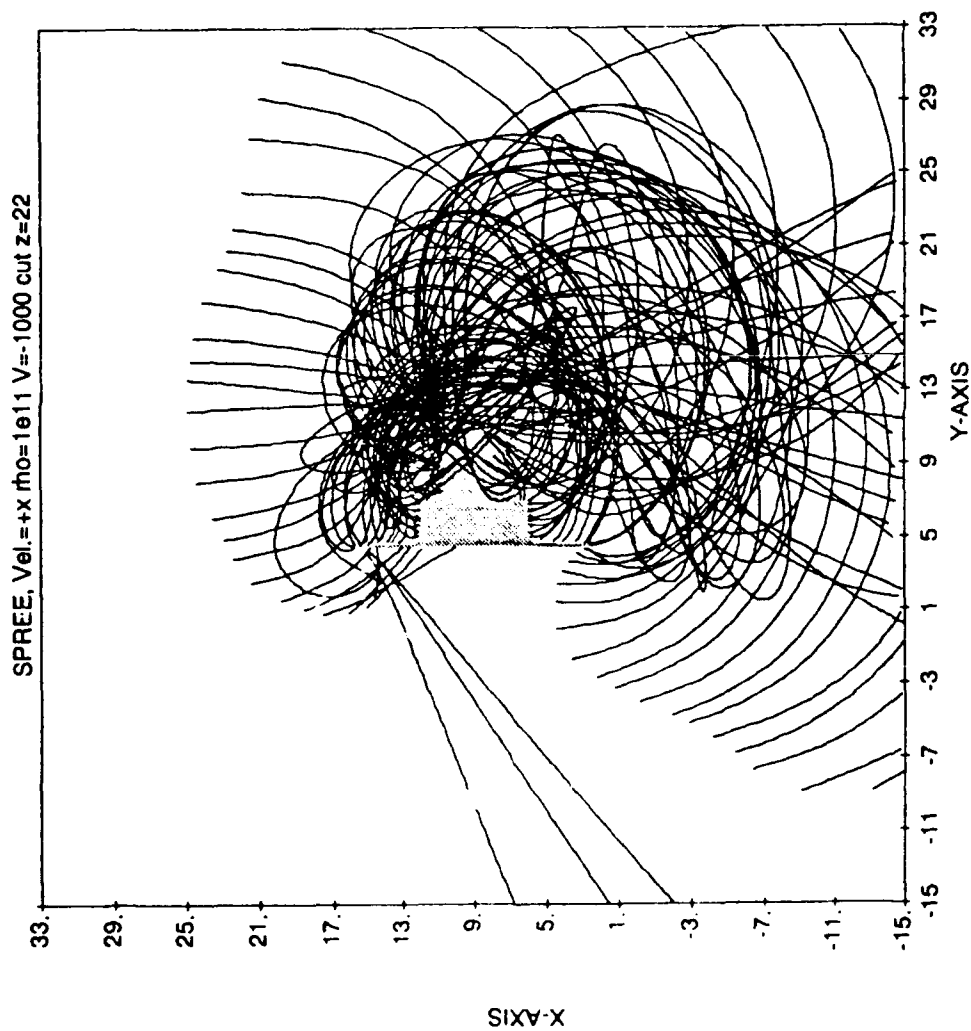
10/17/90 19:06:54



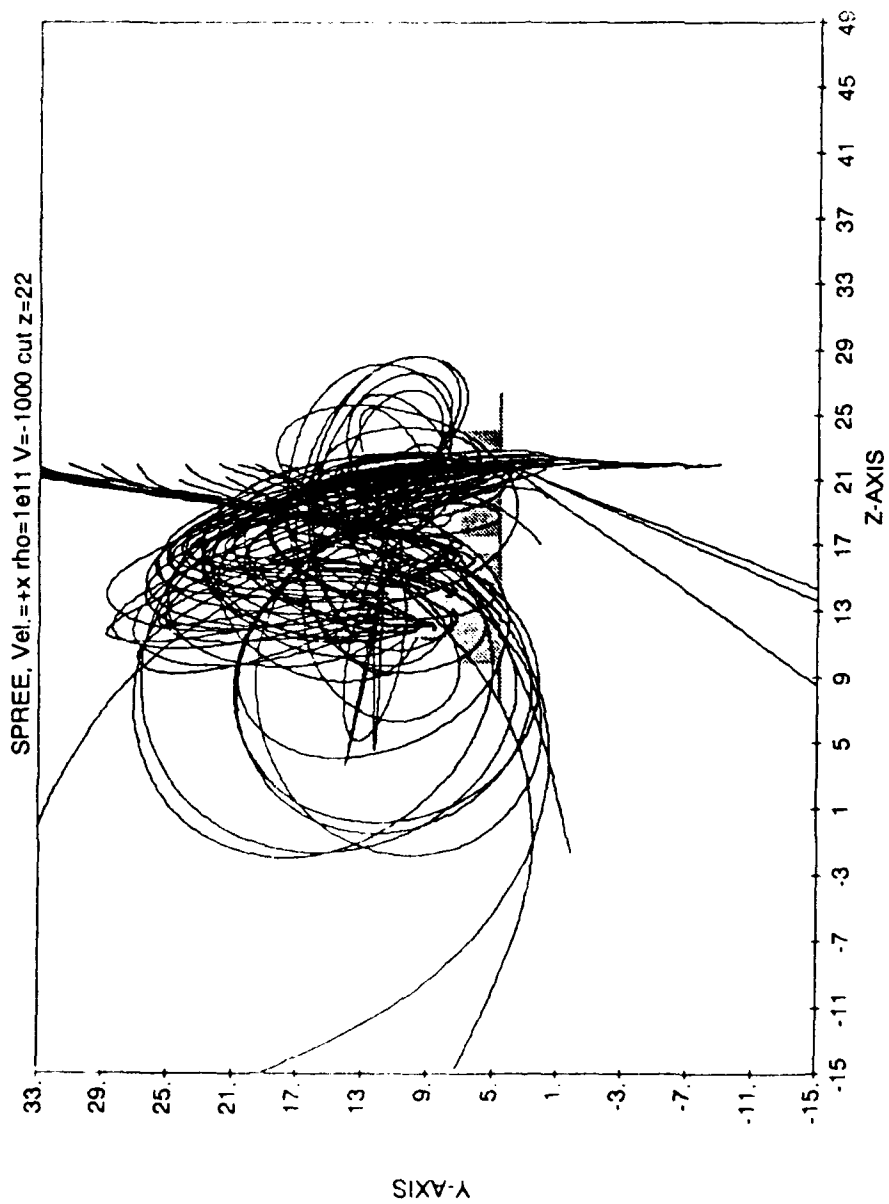
10/17/90 19:06:57



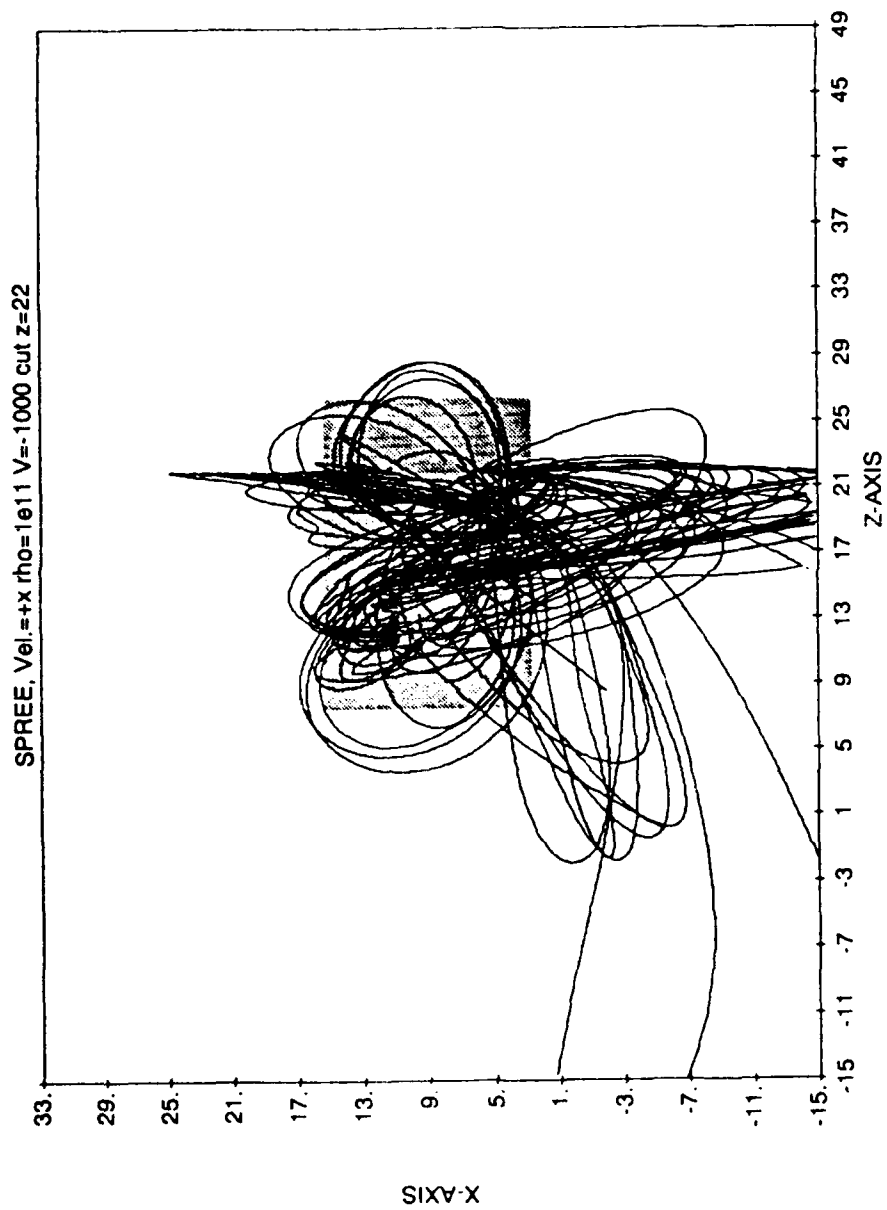
9/22/90 7 04 51



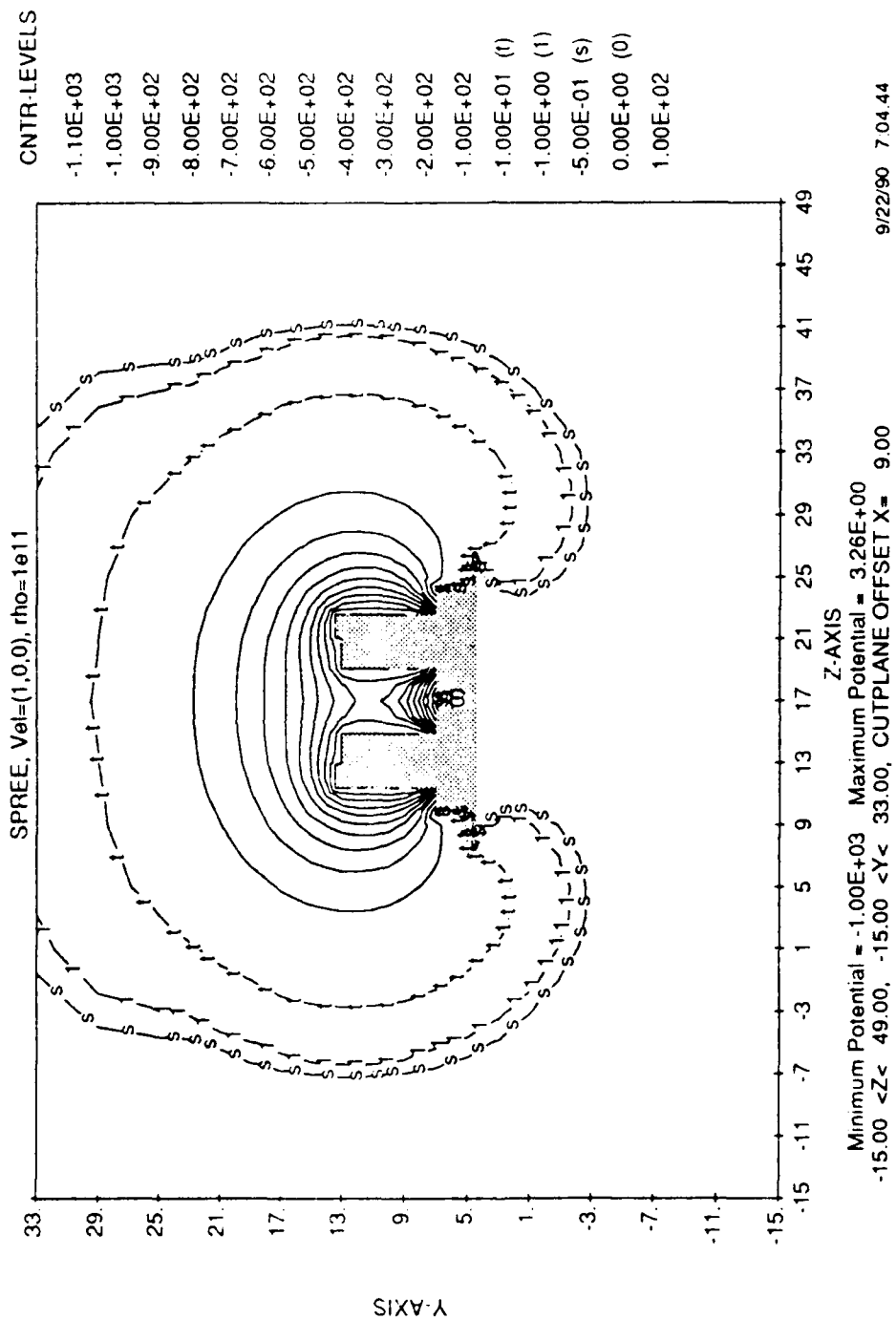
10/17/90 19:18:01



10/17/90 19:17:54



10/17/90 19:17:58



5. OBSTRUCTION OF CURRENT OF SPREE INSTRUMENTS DUE TO RMS AND CAMERA

5.1 OBJECTIVES

This chapter describes the investigation of the degree of obstruction to the SPREE instrument due to the RMS (Remote Manipulation System) and the camera mounted on top of the RMS.

5.2 PROCEDURE

The calculations were done using NASCAP/LEO, which has been modified to treat wake and ram particles more efficiently. The currents calculated were

1. Total current to the SPREE instruments (the two boxes);
2. Total current to each of the detector entrance screens;
3. Current that entered the detector within 10° of the surface normal; and
4. The weighted (by particle current) average angle of particles striking the detector entrance.

5.3 RUN CASES

Ion currents to the detectors were calculated for three cases:

1. SPREE only (repeat previous calculation);
2. SPREE and RMS and nonconducting camera;
3. SPREE and RMS and conducting camera.

5.4 PARAMETERS

Parameters common to all three cases are as follows:

Plasma temperature	0.1	eV
Ion density	10^{11}	m^{-3}
Orbiter velocity	7500	m/s
Inner grid mesh size	0.06	m

In all cases, a potential of -300 V is applied to the surfaces of the detector cases. In case 3, the same potential is applied to the camera surfaces as well.

5.5 ORIENTATIONS

In all cases, the low-Z detector is looking toward its wake and the high-Z detector is looking upstream. Different orientations used in the calculations are shown in table 5.1.

Table 5.1 Detector orientations used in calculations.

Case	$\theta(^{\circ})$	$\phi(^{\circ})$	Velocity(m/s)
1	0	-10	7386,0,-1302
2	10	-10	7274,1302,-1283
3	20	-10	6941,2565,-1224
4	0	0	7500,0,0
5	10	0	7386,1302,0
6	20	0	7048,2565,0
7	0	10	7386,0,1302
8	10	10	7274,1302,1283
9	20	10	6941,2565,1224

The symbols θ and ϕ are defined in figure 5.1.

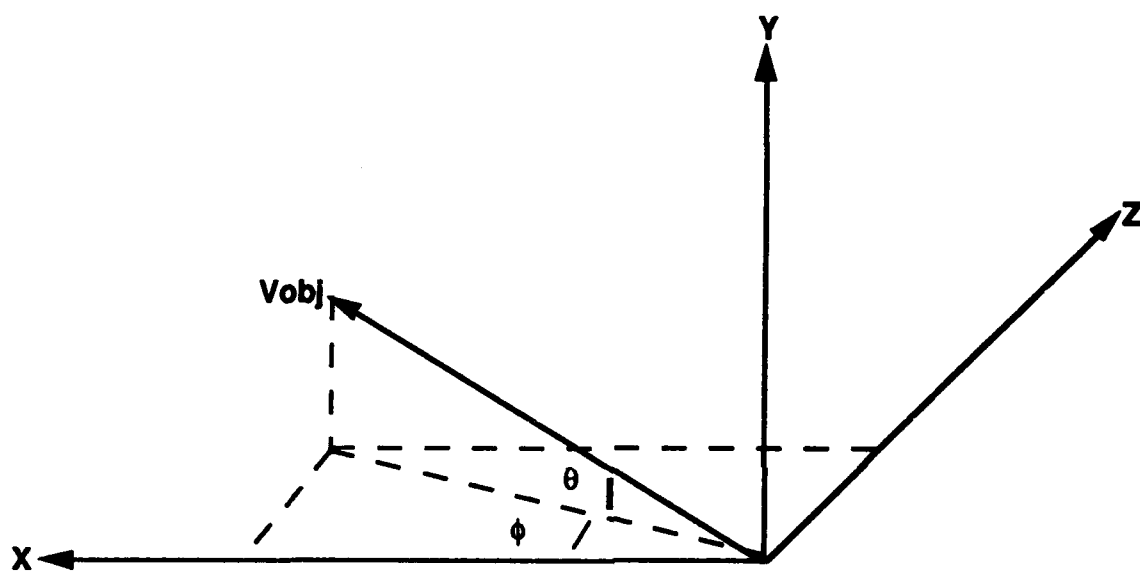


Figure 5.1 Definition of θ and ϕ .

COLOR LEGEND

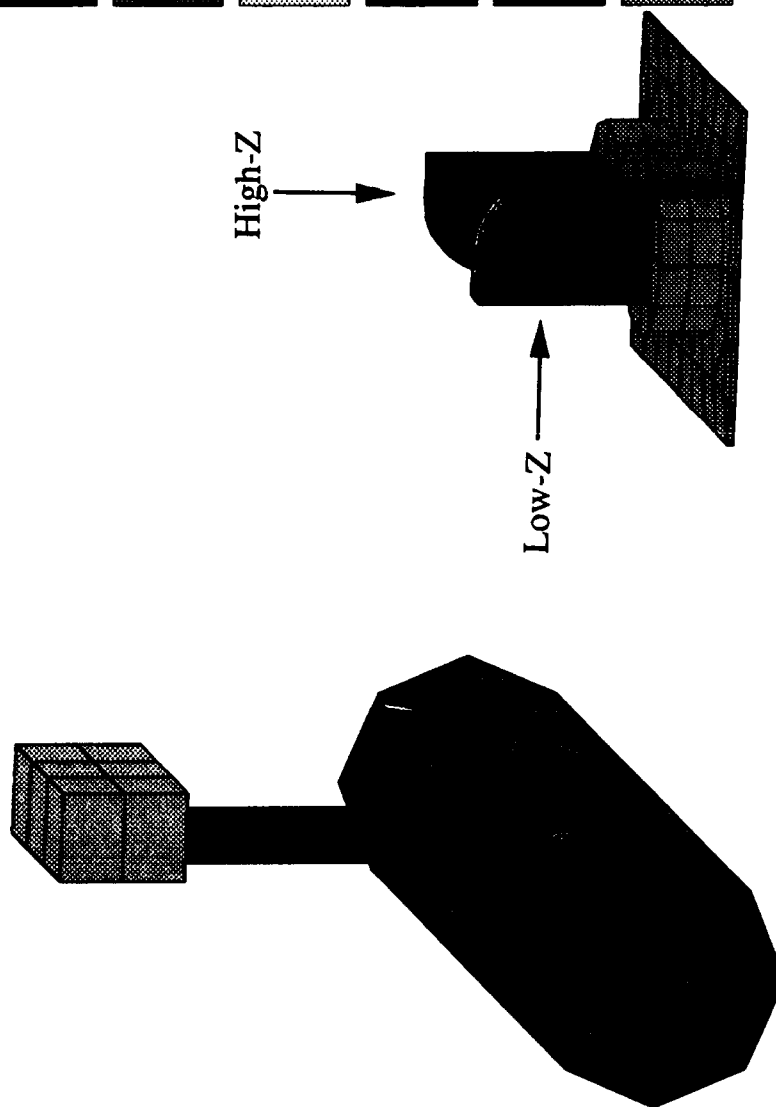
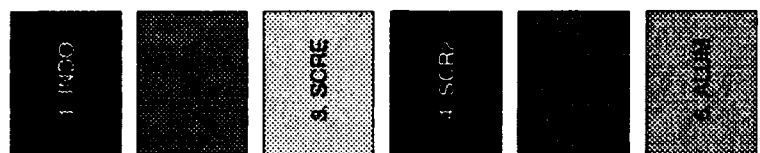


Figure 5.2 PATRAN model of SPREE and RMS and camera.

5.6 RESULTS

All currents are in amperes. The low-Z detector is facing the wake, and the high-Z detector is facing the ram.

Table 5.2 Total currents collected by both detector boxes.

Orientation	θ	ϕ	Case 1	Case 2	Case 3
1	0	-10	2.27e-4	1.75e-4	1.76e-4
2	10	-10	2.14e-4	1.61e-4	1.63e-4
3	20	-10	2.03e-4	1.71e-4	1.30e-4
4	0	0	2.25e-4	1.85e-4	1.86e-4
5	10	0	2.03e-4	1.52e-4	1.51e-4
6	20	0	2.02e-4	1.72e-4	1.31e-4
7	0	10	2.25e-4	1.83e-4	1.83e-4
8	10	10	2.13e-4	1.61e-4	1.58e-4
9	20	10	2.12e-4	1.71e-4	1.38e-4

Table 5.3 Total currents collected at the detector screens.

Orientation	θ	ϕ	Low-Z			High-Z		
			Case 1	Case 2	Case 3	Case 1	Case 2	Case 3
1	0	-10	6.82e-6	7.31e-6	9.52e-6	8.15e-6	7.72e-6	6.86e-6
2	10	-10	6.43e-6	6.39e-6	6.79e-6	5.84e-6	4.77e-6	6.55e-6
3	20	-10	5.69e-6	6.63e-6	4.76e-6	5.76e-6	3.90e-6	5.60e-6
4	0	0	7.17e-6	6.52e-6	8.41e-6	6.06e-6	8.20e-6	7.59e-6
5	10	0	5.41e-6	5.46e-6	4.72e-6	5.79e-6	6.17e-6	6.05e-6
6	20	0	5.16e-6	6.28e-6	4.17e-6	5.25e-6	5.45e-6	6.53e-6
7	0	10	6.06e-6	6.13e-6	6.67e-6	6.32e-6	6.69e-6	6.29e-6
8	10	10	5.37e-6	5.01e-6	2.69e-6	5.68e-6	5.94e-6	4.95e-6
9	20	10	4.52e-6	5.11e-6	4.26e-6	6.09e-6	6.39e-6	3.49e-6

Table 5.4 Total currents entering the detectors within 10° of the surface normal.

Orientation	θ	ϕ	Low-Z			High-Z		
			Case 1	Case 2	Case 3	Case 1	Case 2	Case 3
1	0	-10	1.45e-7	1.42e-8	1.64e-7	5.27e-7	5.20e-7	0.
2	10	-10	1.37e-7	1.08e-8	3.97e-8	5.47e-7	7.06e-7	0.
3	20	-10	1.34e-8	4.04e-9	6.40e-9	6.91e-7	7.87e-7	1.73e-7
4	0	0	3.94e-8	6.06e-9	2.05e-8	4.53e-8	2.61e-7	9.23e-7
5	10	0	1.77e-8	3.05e-10	4.92e-8	1.77e-8	1.63e-7	8.26e-7
6	20	0	3.38e-10	1.10e-9	4.16e-9	2.00e-7	1.09e-7	3.02e-7
7	0	10	1.19e-7	4.15e-8	3.37e-10	3.65e-9	0.	3.73e-7
8	10	10	2.13e-20	3.87e-20	7.53e-8	9.31e-8	0.	9.67e-8
9	20	10	1.37e-9	1.34e-10	2.47e-8	5.65e-8	0.	6.89e-10

Table 5.5 Weighted average angle of the particles striking the detectors.

Orientation	θ	ϕ	Low-Z			High-Z		
			Case 1	Case 2	Case 3	Case 1	Case 2	Case 3
1	0	-10	47.5	50.8	38.9	34.6	36.9	44.5
2	10	-10	47.7	50.0	41.4	27.8	31.0	39.2
3	20	-10	49.1	48.0	45.0	23.8	23.2	38.0
4	0	0	47.2	50.3	42.3	29.1	33.4	50.7
5	10	0	55.4	48.1	42.3	26.5	35.2	34.0
6	20	0	49.9	48.1	48.6	25.9	31.9	35.2
7	0	10	47.0	44.5	39.0	28.0	37.7	51.9
8	10	10	54.9	45.7	40.1	25.2	37.1	48.3
9	20	10	48.3	47.4	40.7	23.8	35.6	52.4

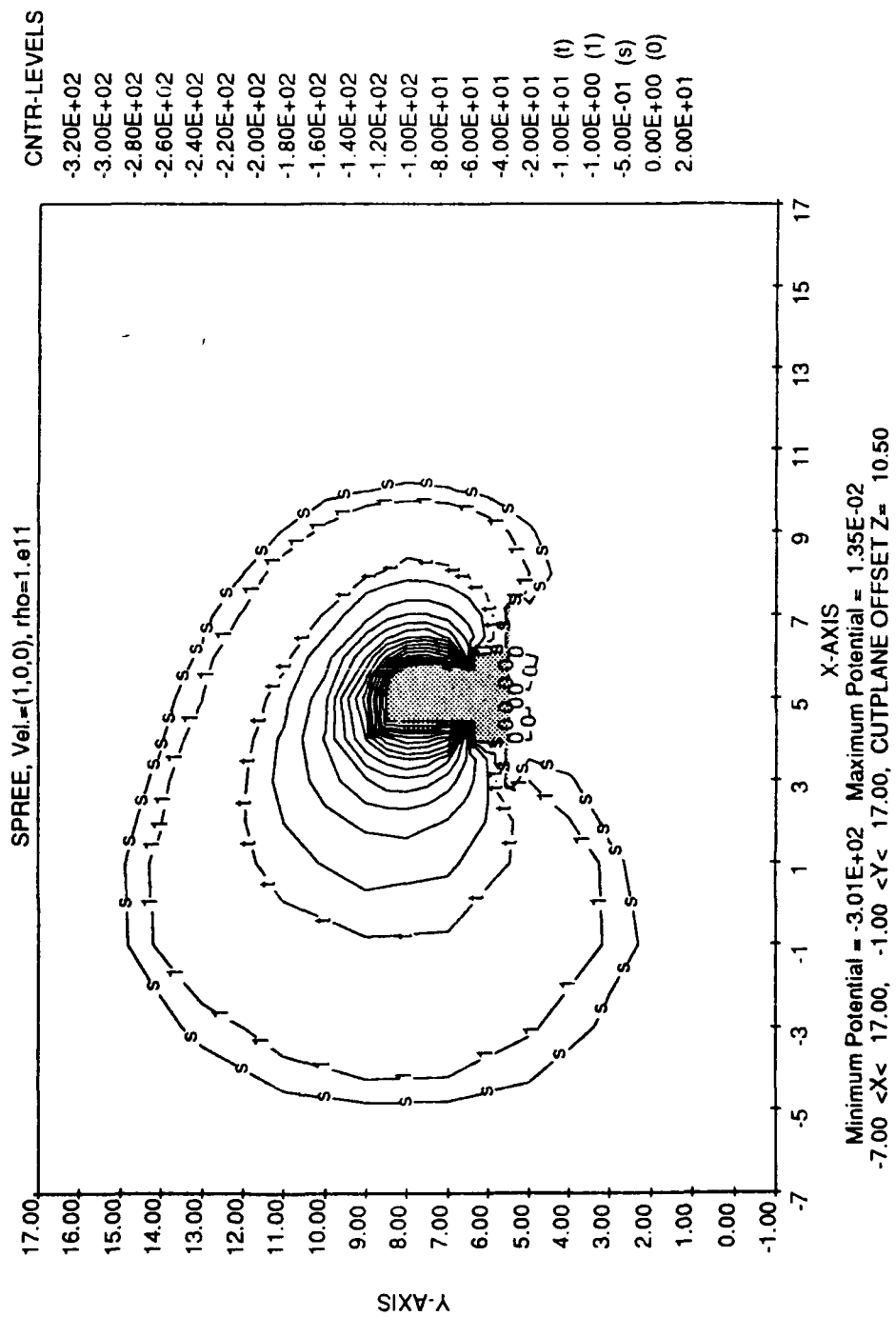
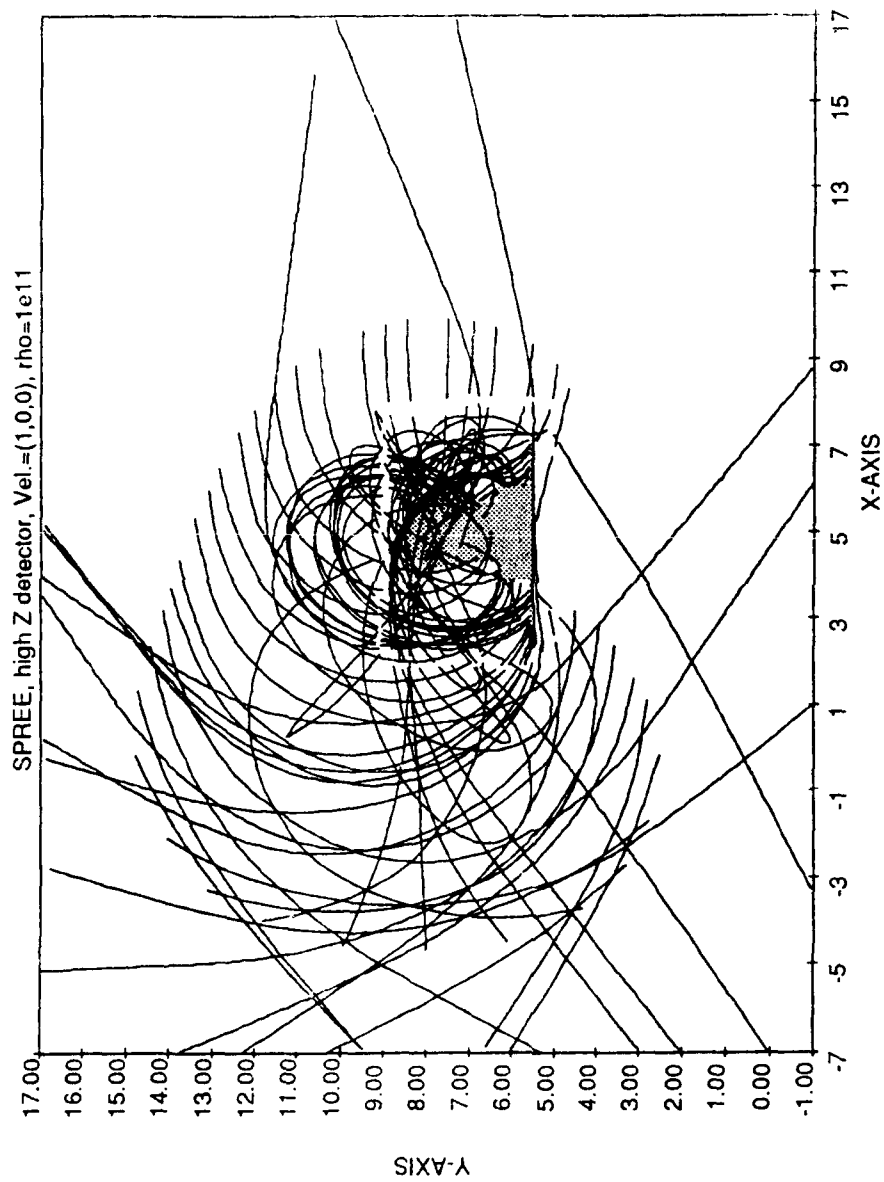
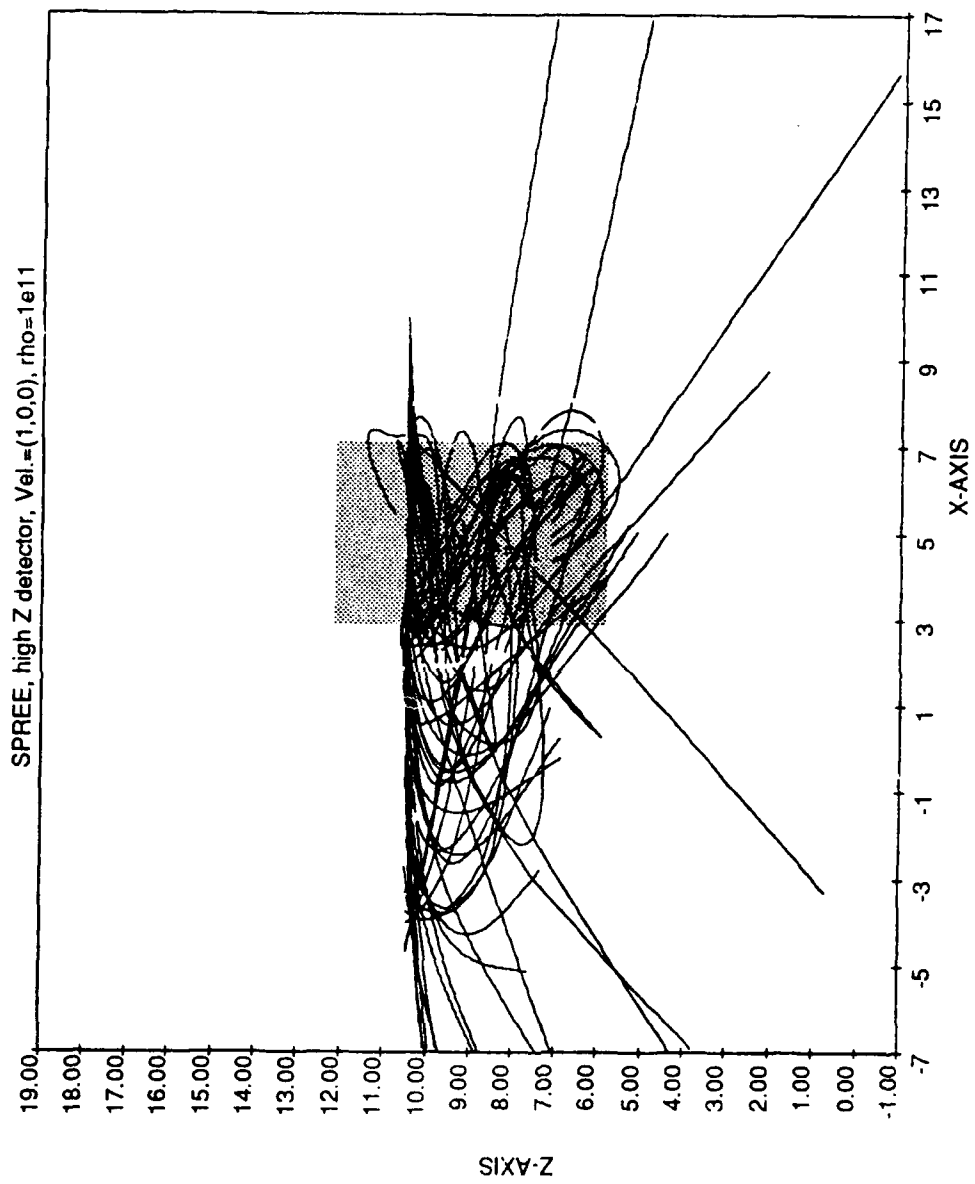


Figure 5.3 Sheath for case 1—SPREE only.

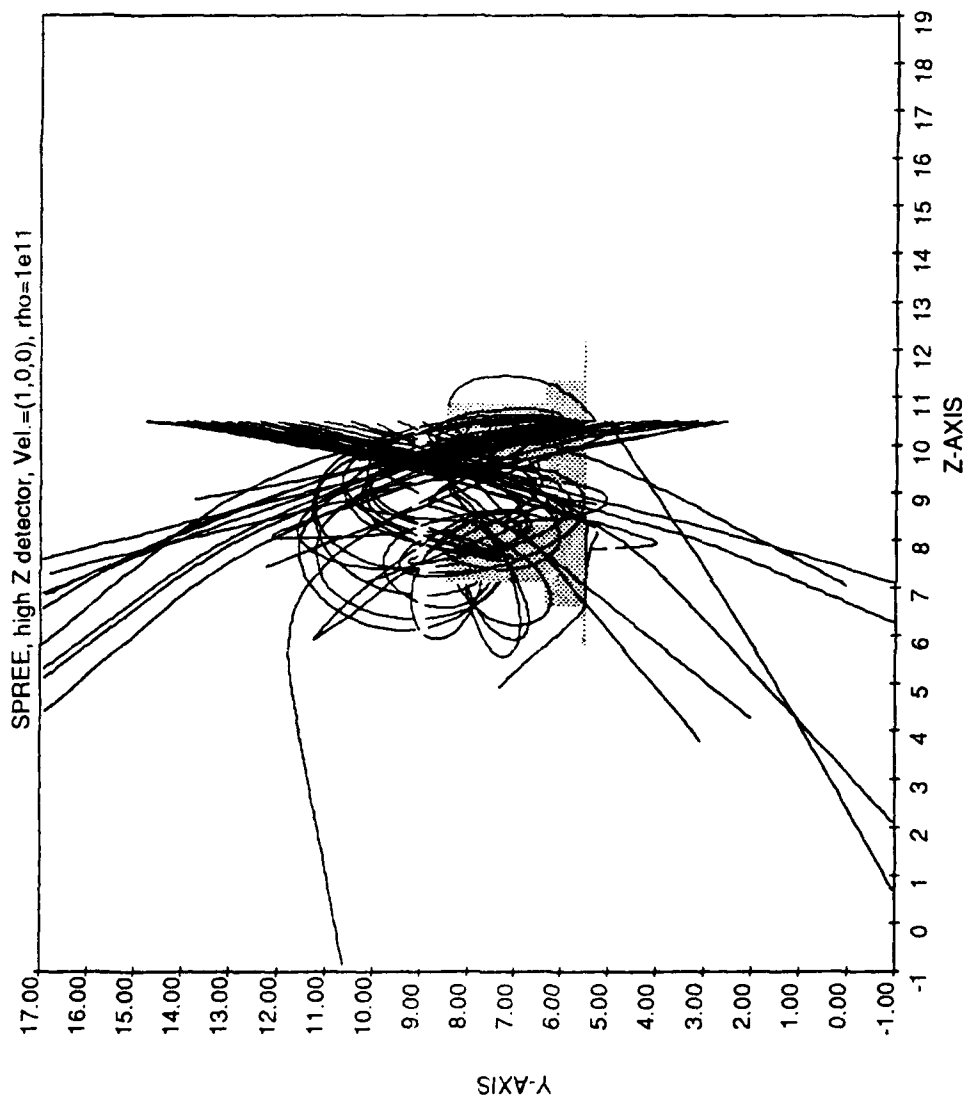


(a)

Figure 5.4 Particle trajectories for case 1—SPREE only—projected on the (a) X-Y plane, (b) Y-Z plane, and (c) X-Z plane.



(b)



(c)

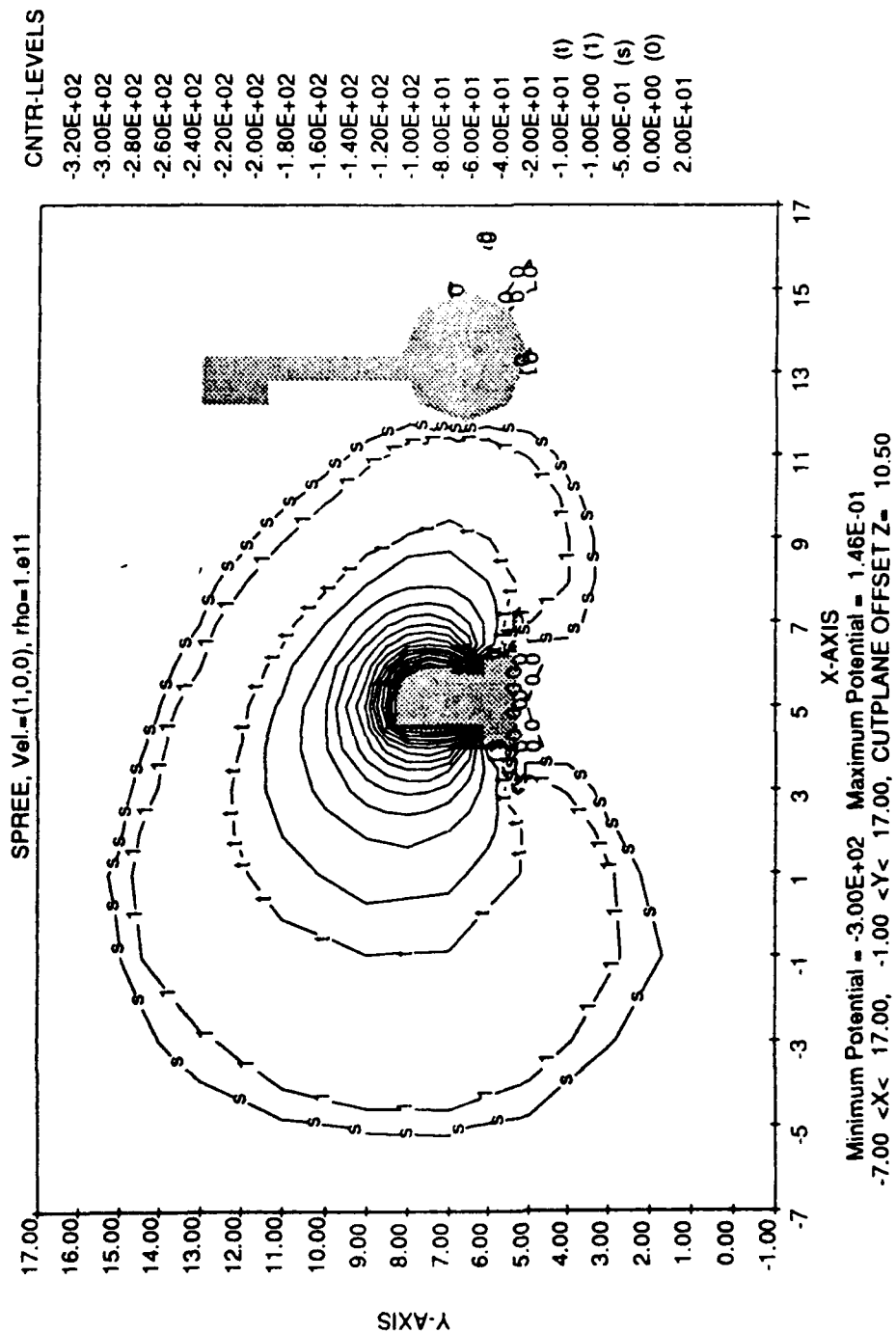
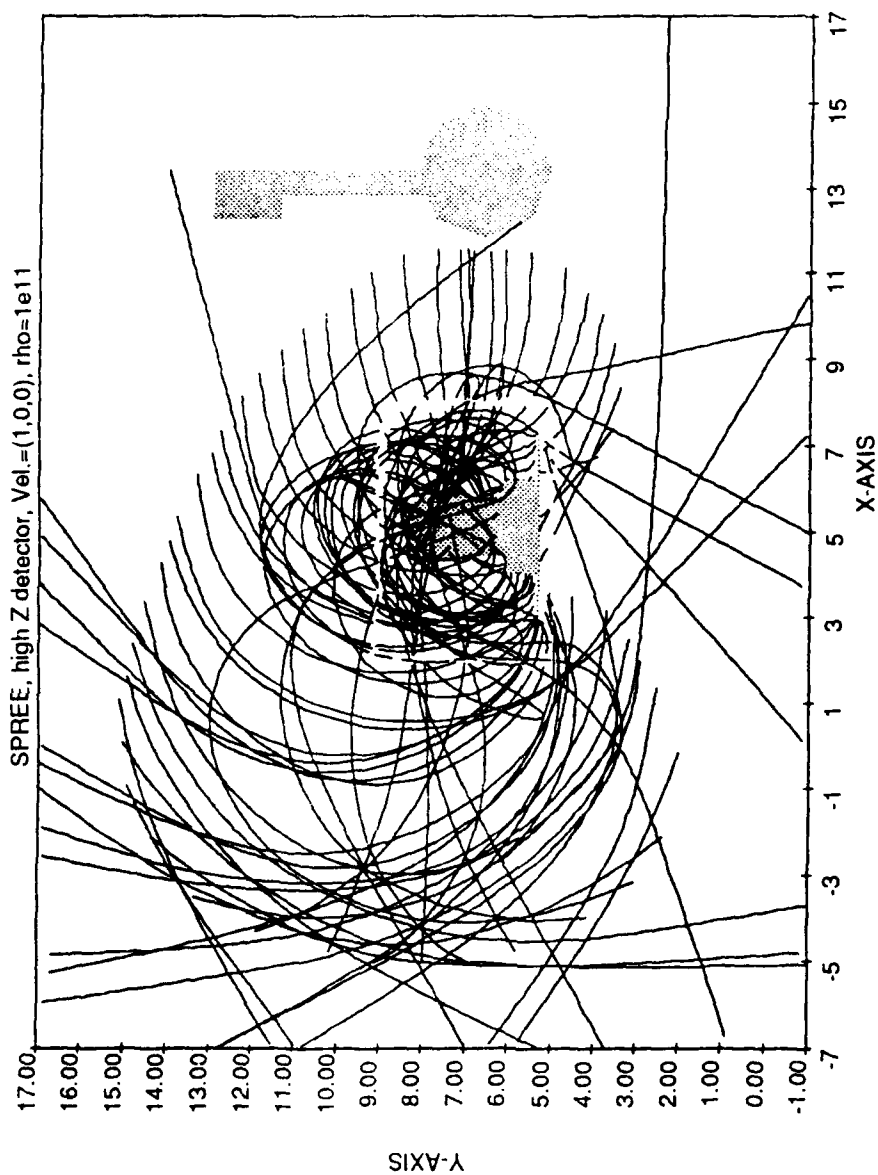
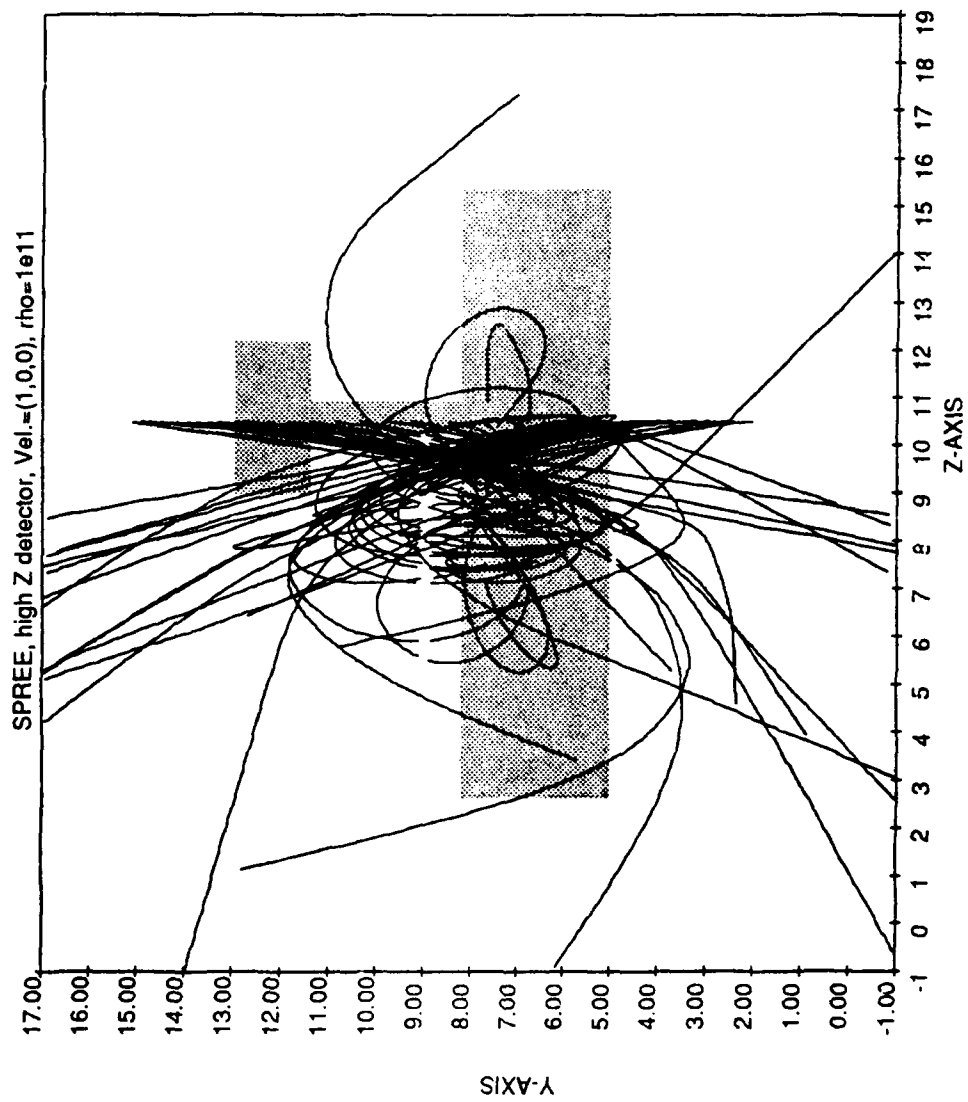


Figure 5.5 Sheath for case 2—SPREE and RMS and nonconducting camera.

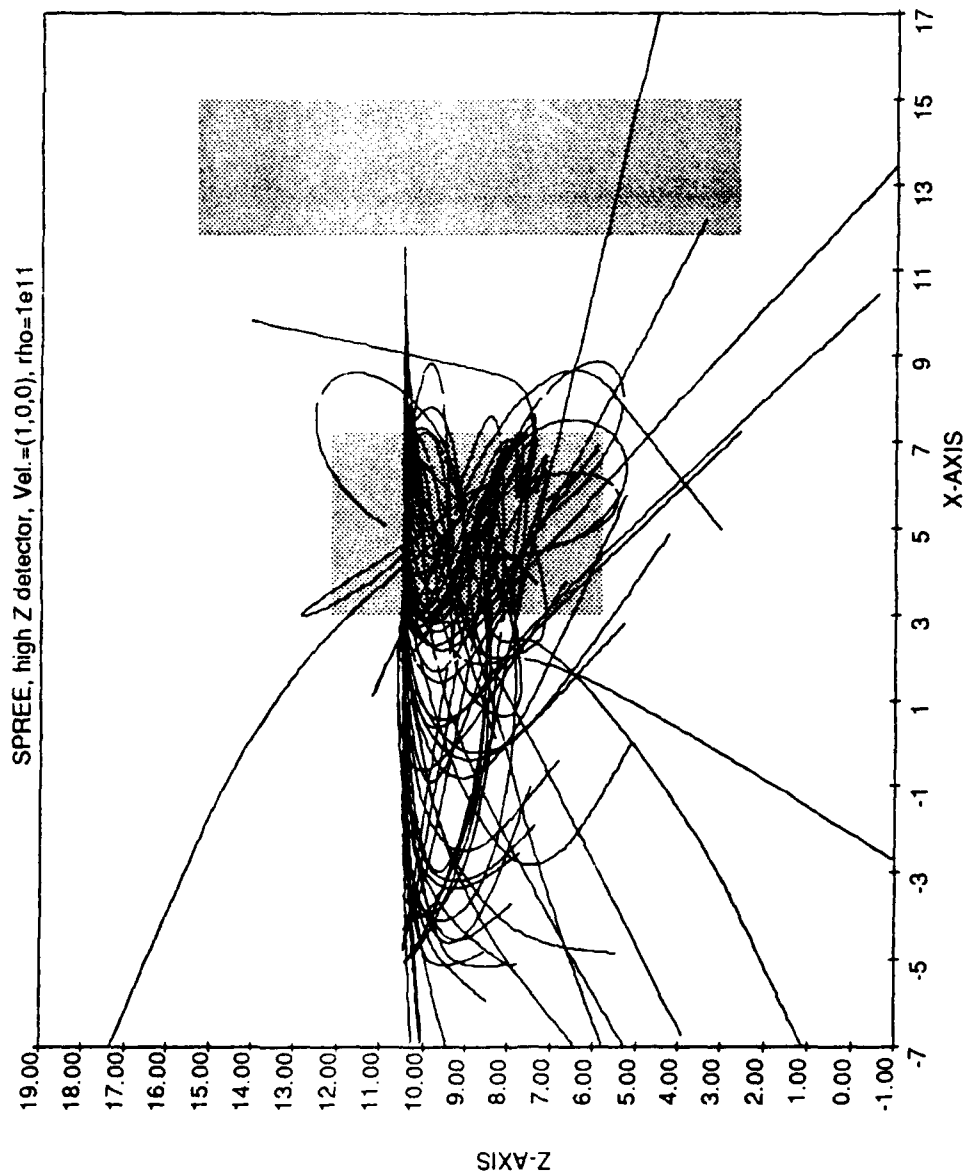


(a)

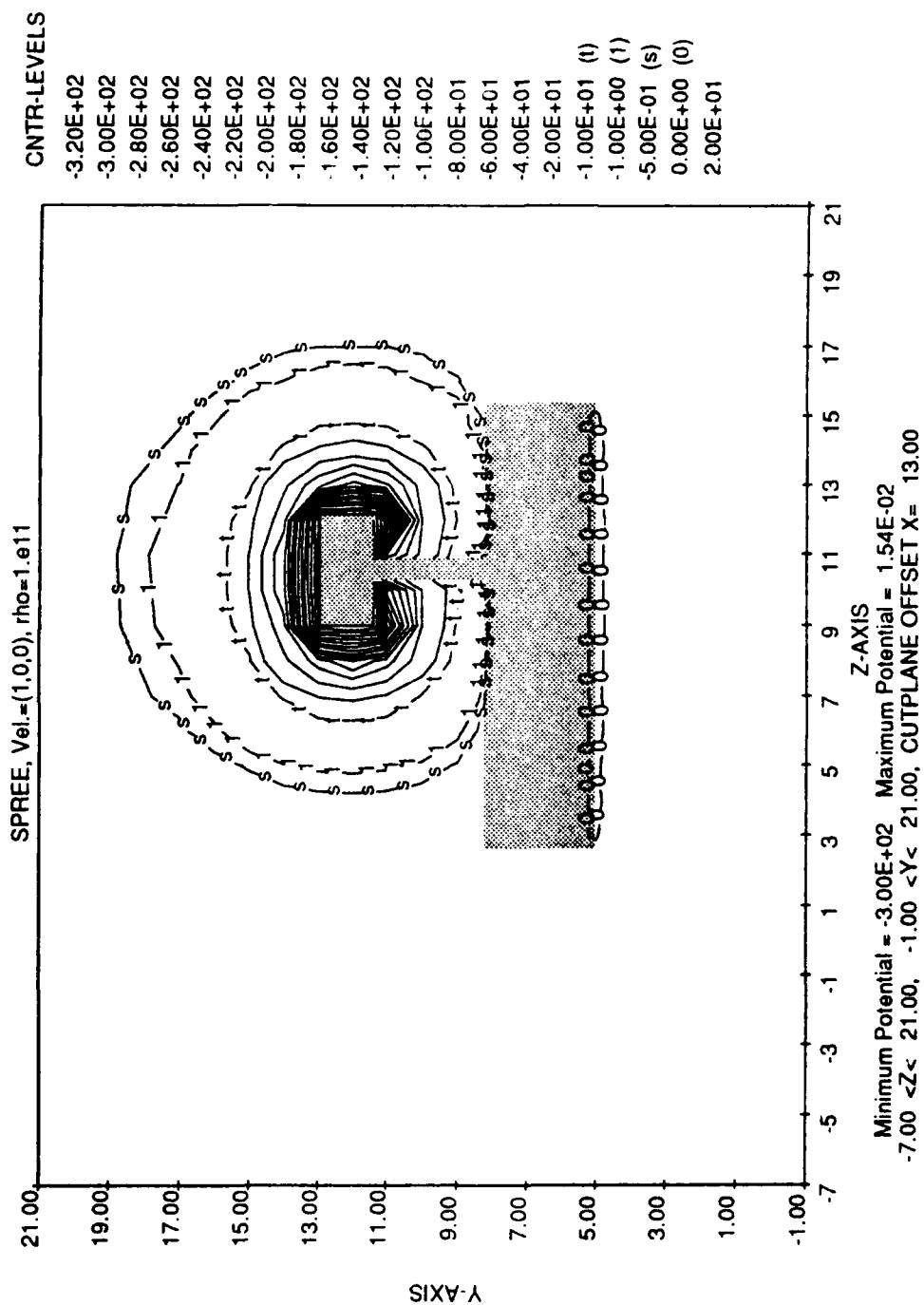
Figure 5.6 Particle trajectories for case 2—SPREE and RMS and nonconducting camera projected on the (a) X-Y plane, (b) Y-Z plane, and (c) X-Z plane.



(b)

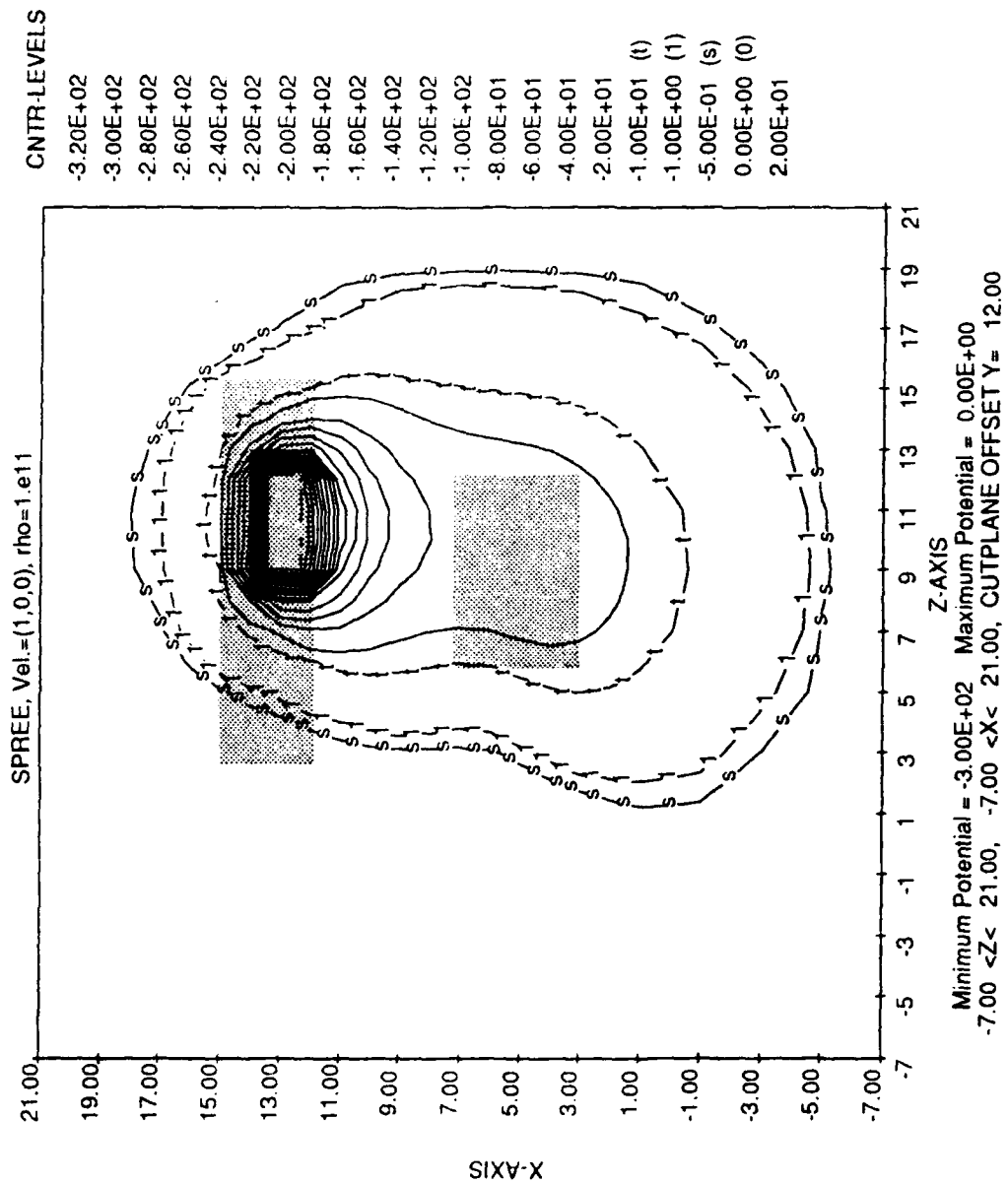


(c)

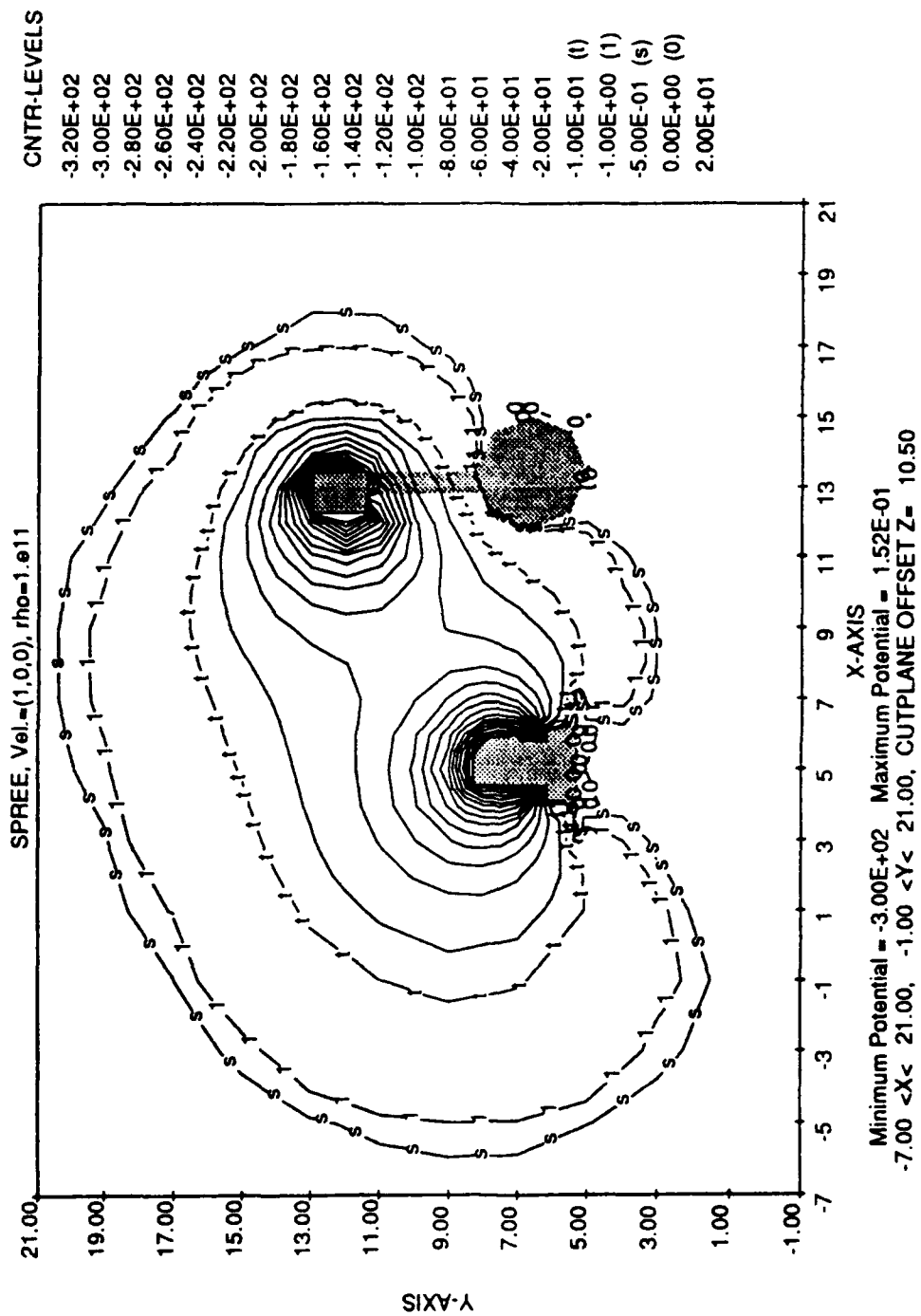


(a)

Figure 5.7 Sheath for case 3—SPREE and RMS and conducting camera. (a) Cutplane at $X = 13$, (b) cutplane at $Y = 12$, and (c) cutplane at $Z = 10.5$.



(b)



(c)

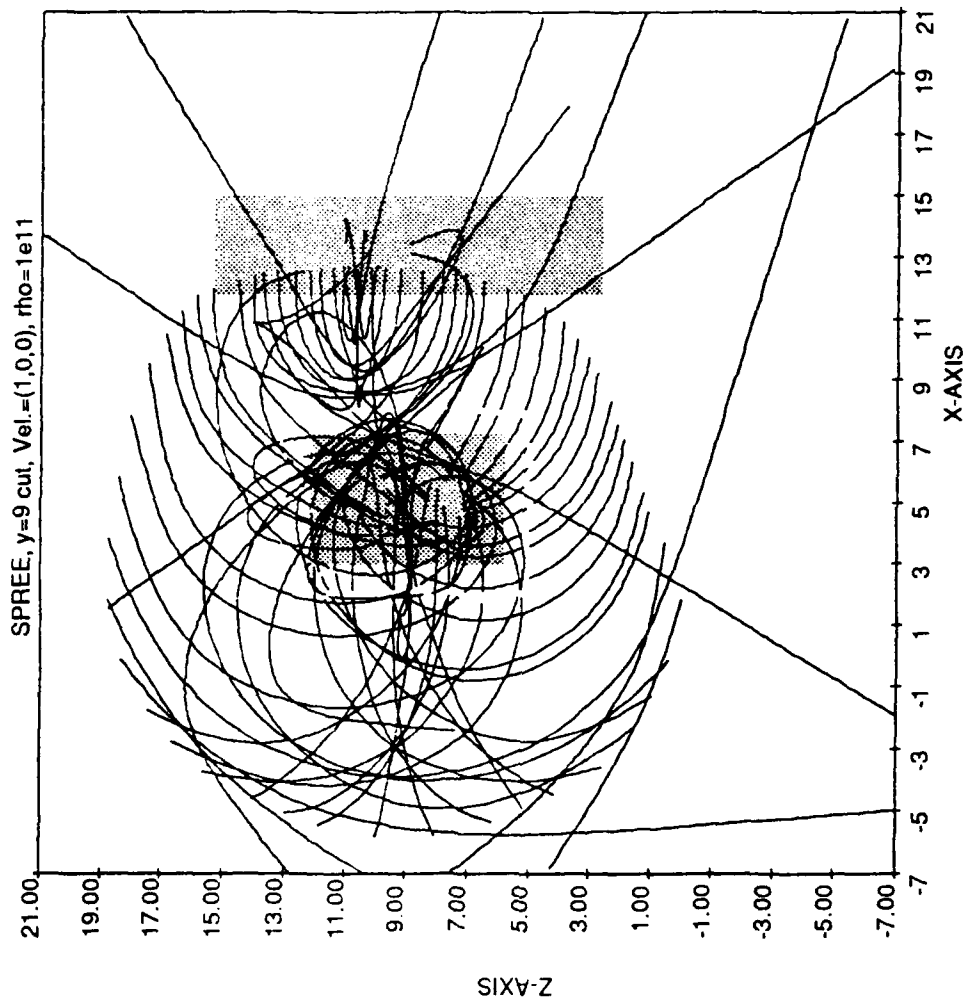


Figure 5.8 Particle trajectories for case 3—SPREE and RMS and conducting camera projected on the X-Z plane.

6. CALCULATIONS OF ION CURRENT COLLECTED BY SHUTTLE ORBITER

This attachment describes the calculations of the collected currents as a function of the orientation of the orbiter with respect to the ram, the potential, and the plasma density.

6.1 ION CURRENT COLLECTED AS A FUNCTION OF ORIENTATION

The calculations were done using NASCAP/LEO, which has been modified to treat wake and ram particles more efficiently.

The following procedure was used in this set of calculations:

1. Select an orientation of the orbiter;
2. Compute the ion wake formed behind the moving shuttle;
3. Calculate the resulting spatial plasma potentials;
4. Push ions from an equipotential plasma sheath to compute the collected current.

This set of calculations was done with the following parameters:

Plasma temperature	0.1	eV
Ion density	10^{12}	m^{-3}
Orbiter velocity	500	m/s
Conductor potential	-300	V

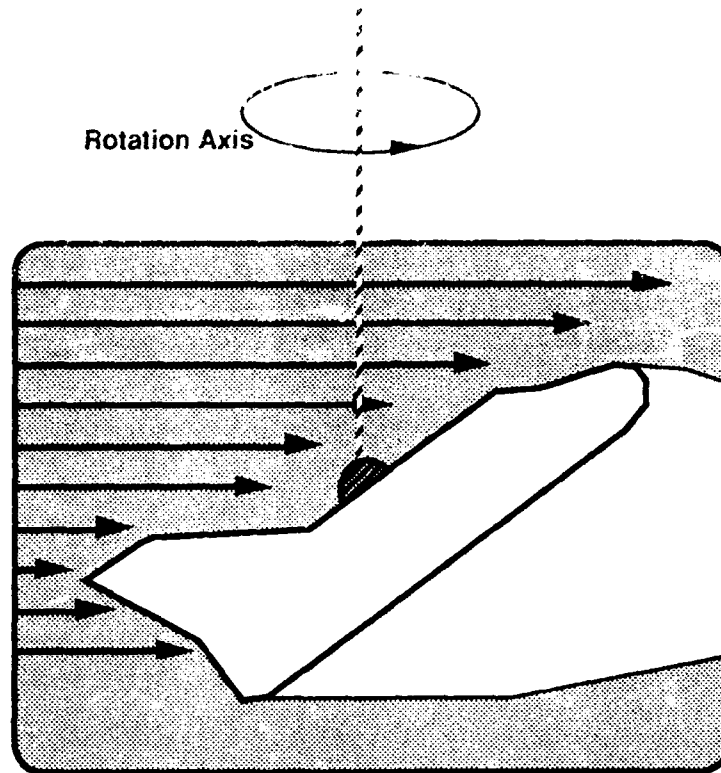


Figure 6.1 Shuttle orientations used in these calculations.

As shown in figure 6.1, the nose of the orbiter was tilted 45° up, and the orbiter was rotated around the vertical axis. The orbiter's belly was facing the ram at 0° rotation and the wake at 180° . The rotation step was 15° . Shuttle velocity vectors (traveling at 7500 m/s) are given in table 6.1:

Table 6.1 Velocity vectors of the shuttle in the different orientations.

Case	Angle($^\circ$)	Velocity(m/s)
1	0	-5303. 0. 5303.
2	15	-5123. 1941. 5123.
3	30	-4593. 3750. 4593.
4	45	-3750. 5303. 3750.
5	60	-2652. 6495. 2652.
6	75	-1373. 7244. 1373.
7	90	0. 7500. 0.
8	105	1373. 7244. -1373.
9	120	2652. 6495. -2652.
10	135	3750. 5303. -3750.
11	150	4593. 3750. -4593.
12	165	5123. 1941. -5123.
13	180	5303. 0. -5303.

Figure 6.2 shows the model of the shuttle used for these calculations.

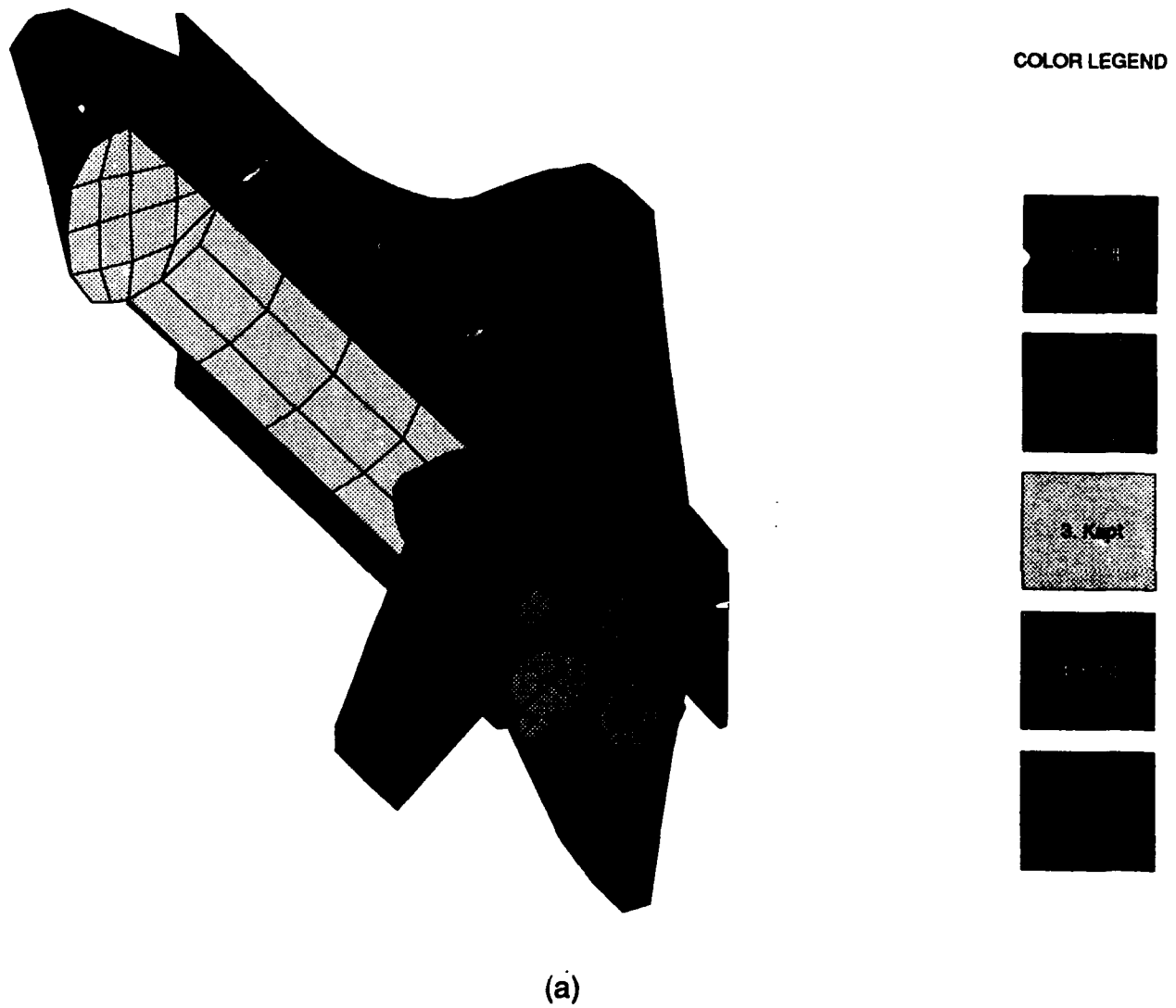
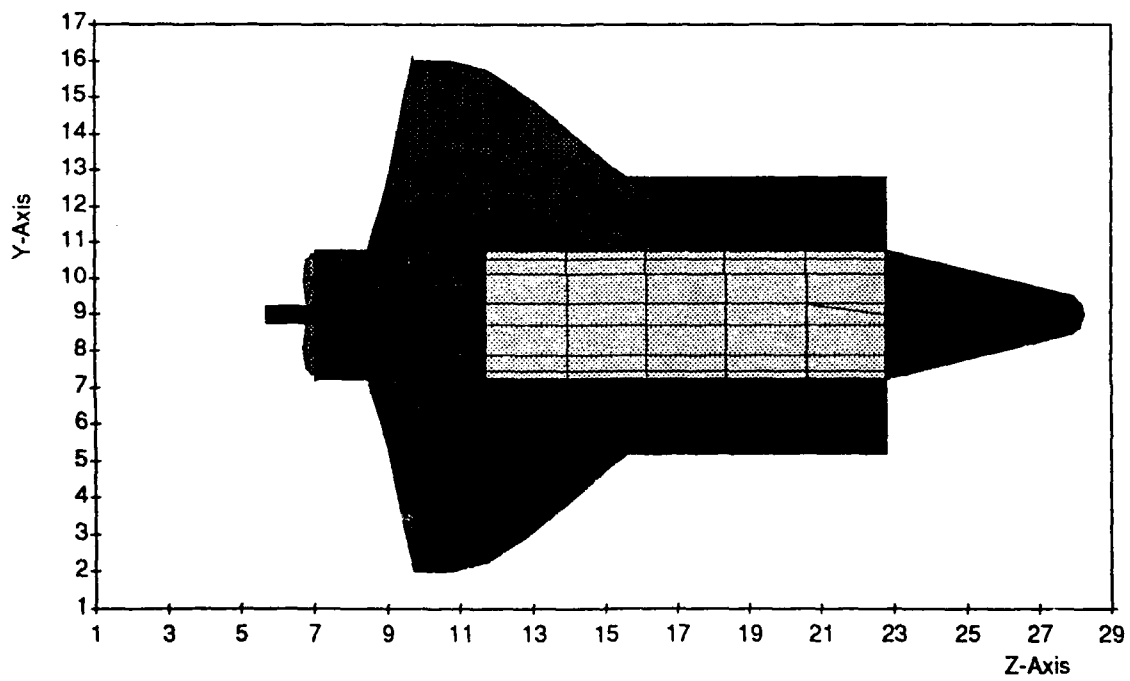


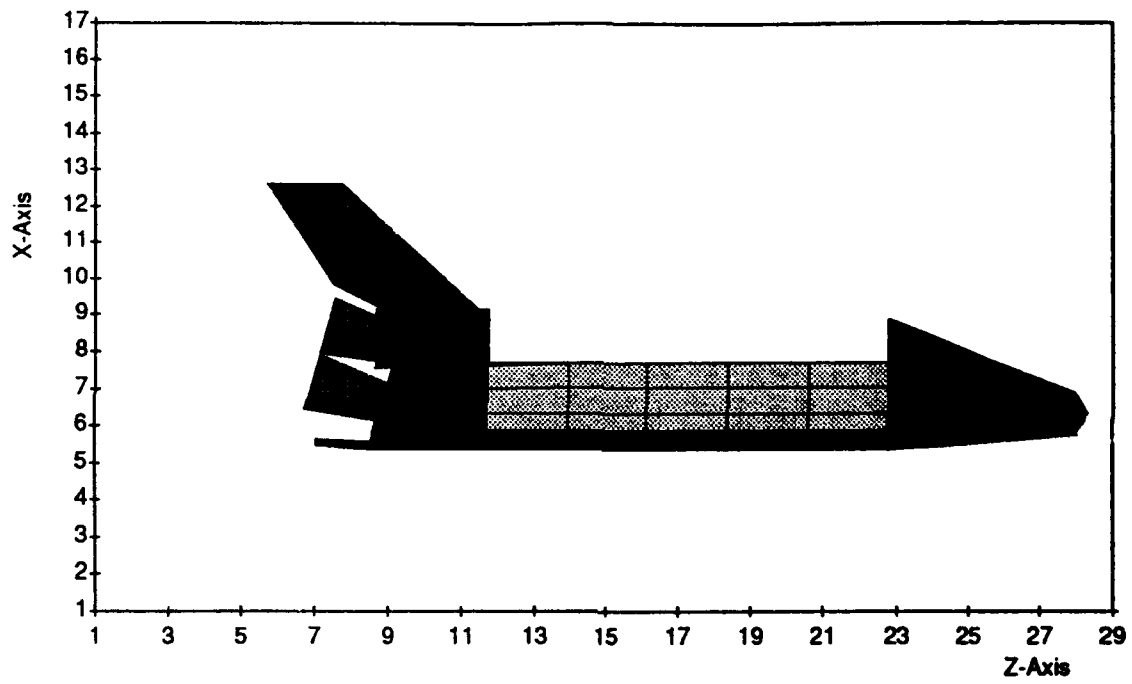
Figure 6.2 Patran model of the shuttle from three directions.

Positive X View



(b)

Positive Y View



(c)

6.2 RESULTS

At 0° angle, the orbiter is traveling with its belly facing the ram directly and the engine nozzles were in the wake. Thus, little current was collected.

As the orbiter rotates, more of the engine nozzles were exposed to the ram side of the orbiter and more current was collected.

At 90°, the orbiter is moving sideways to the ram, and most of the sides of the nozzles were exposed to the ram. The currents to the nozzles' sides peaked at this point and remained steady.

At 180°, the nozzles faced the ram direction, and the currents to the faces of the engine nozzles peaked.

Table 6.2 and figure 6.3 show ion current at different rotation angles. All currents are in amperes.

Table 6.2 Collected current at different orientations.

Case	Angle	Exterior	Nozzle Face	Bay	Inside Doors	Nozzle Doors	Total
1	0	1.1e-6	4.2e-3	0.0e+0	0.0e+0	5.5e-3	9.675e-3
2	15	1.1e-5	4.3e-3	0.0e+0	0.0e+0	4.7e-3	9.086e-3
3	30	2.0e-5	4.3e-3	0.0e+0	0.0e+0	5.7e-3	1.001e-2
4	45	1.8e-5	4.4e-3	0.0e+0	0.0e+0	9.2e-3	1.360e-2
5	60	1.1e-5	6.2e-3	0.0e+0	0.0e+0	1.7e-2	2.347e-2
6	75	5.4e-5	8.0e-3	0.0e+0	0.0e+0	2.6e-2	3.418e-2
7	90	1.4e-4	1.0e-2	0.0e+0	0.0e+0	3.0e-2	4.082e-2
8	105	3.4e-4	1.4e-2	0.0e+0	0.0e+0	3.2e-2	4.655e-2
9	120	6.5e-4	1.9e-2	0.0e+0	0.0e+0	3.3e-2	5.247e-2
10	135	5.9e-4	2.3e-2	0.0e+0	0.0e+0	3.3e-2	5.711e-2
11	150	6.3e-4	2.7e-2	0.0e+0	0.0e+0	3.3e-2	6.071e-2
12	165	5.1e-4	3.0e-2	0.0e+0	0.0e+0	3.2e-2	6.313e-2
13	180	2.7e-4	3.1e-2	0.0e+0	0.0e+0	3.3e-2	6.406e-2

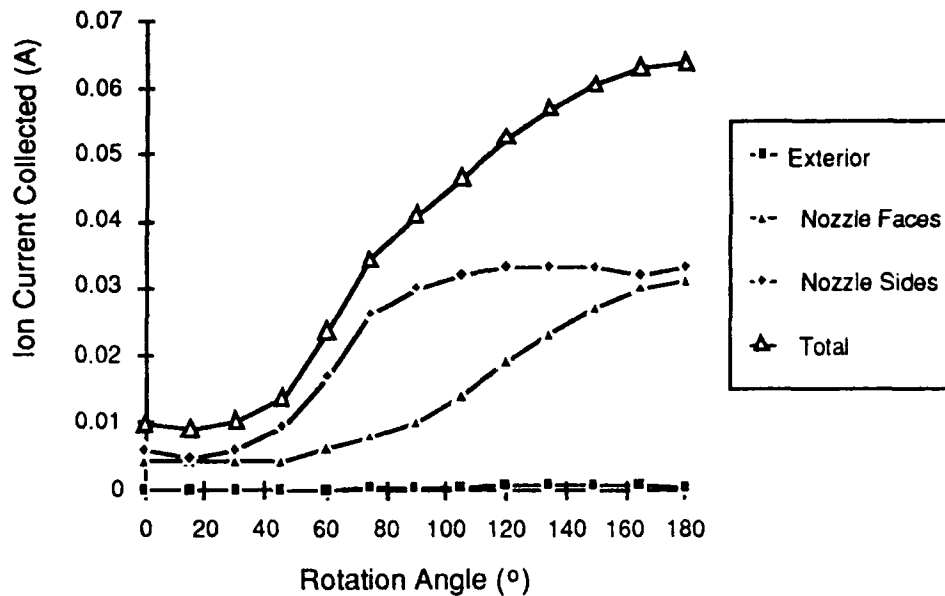


Figure 6.3 Ion currents vs. rotation angles.

6.3 ION CURRENT COLLECTED AS A FUNCTION OF POTENTIAL AND PLASMA DENSITY

The following procedure was used in this set of calculations:

1. Compute the ion wake formed behind the moving shuttle.
2. Calculate the resulting spatial plasma potentials.
3. Push ions from an equipotential plasma sheath to compute the collected current.

The varied parameters are conductor potentials, orientation, and plasma density.

1. Conducting potentials: -10, -100, -300, -1000 V
2. Velocity vectors: (5303,0,-5303) for bay-to-ram direction and (-5303,0,5303) for belly-to-ram direction.

Tables 6.3 through 6.6 give the results of the calculations. All currents are in amperes.

Table 6.3 Ion current collected with bay-to-ram and $10^{11}/\text{m}^3$ plasma density.

Pot.	Tefl	Silv	Kapt	SiO2	Alum	Total
-10	1.2e-04	2.1e-03	0.0e+00	0.0e+00	1.5e-03	3.721e-03
-100	7.9e-05	3.3e-03	0.0e+00	0.0e+00	4.1e-03	7.414e-03
-300	6.5e-05	3.9e-03	0.0e+00	0.0e+00	6.1e-03	1.011e-02
-1000	1.0e-04	4.7e-03	0.0e+00	0.0e+00	9.9e-03	1.466e-02

Table 6.4 Ion current collected with bay-to-ram and $10^{12}/\text{m}^3$ plasma density.

Pot.	Tefl	Silv	Kapt	SiO2	Alum	Total
-10	1.2e-03	2.1e-02	0.0e+00	0.0e+00	1.5e-02	3.703e-02
-100	6.9e-04	2.5e-02	0.0e+00	0.0e+00	2.1e-02	4.618e-02
-300	2.7e-04	3.1e-02	0.0e+00	0.0e+00	3.3e-02	6.406e-02
-1000	4.8e-04	3.8e-02	0.0e+00	0.0e+00	5.1e-02	8.916e-02

Table 6.5 Ion current collected with belly-to-ram and $10^{11}/\text{m}^3$ plasma density.

Pot.	Tefl	Silv	Kapt	SiO2	Alum	Total
-10	1.5e-06	1.8e-06	5.0e-07	2.2e-07	2.5e-05	2.877e-05
-100	3.6e-07	8.7e-04	0.0e+00	0.0e+00	9.3e-04	1.794e-03
-300	6.4e-05	2.1e-03	0.0e+00	0.0e+00	1.8e-03	3.992e-03
-1000	4.3e-05	1e-03	0.0e+00	0.0e+00	4.0e-03	9.160e-03

Table 6.6 Ion current collected with belly-to-ram and $10^{12}/\text{m}^3$ plasma density.

Pot.	Tefl	Silv	Kapt	SiO2	Alum	Total
-10	2.7e-05	1.8e-05	1.0e-07	6.0e-06	2.5e-04	2.992e-04
-100	4.4e-06	2.0e-04	1.8e-09	3.3e-08	7.6e-04	9.617e-04
-300	1.1E-06	4.2E-03	0.0E+00	0.0E+00	5.5E-03	9.675E-03
-1000	3.5E-04	1.5E-02	0.0E+00	3.2E-08	1.6E-02	3.147E-02

7. NEUTRAL DENSITIES ABOUT TSS-1 SUBSATELLITE

We used EPSAT to examine the plasma environment and sheath structure of the subsatellite when the subsatellite is at the highest potential it reaches with the electron gun on. The perveance of the gun is taken to be 3.8×10^{-6} , and the net resistance of the subsatellite paint, tether wire, and shunt is taken to be $10 \text{ M}\Omega$.

Figure 7.1 shows the subsatellite potential as a function of time. The peak potential is 3610 V at 1125 s into the mission. The plasma environment at this time is shown in figure 7.2, and the potentials are shown in figure 7.3. Table 7.1 shows the variation in potential with time near the peak potential time. Table 7.2 shows the Parker-Murphy (magnetic-limited) and space-charge-limited radii and collected currents at the peak potential.

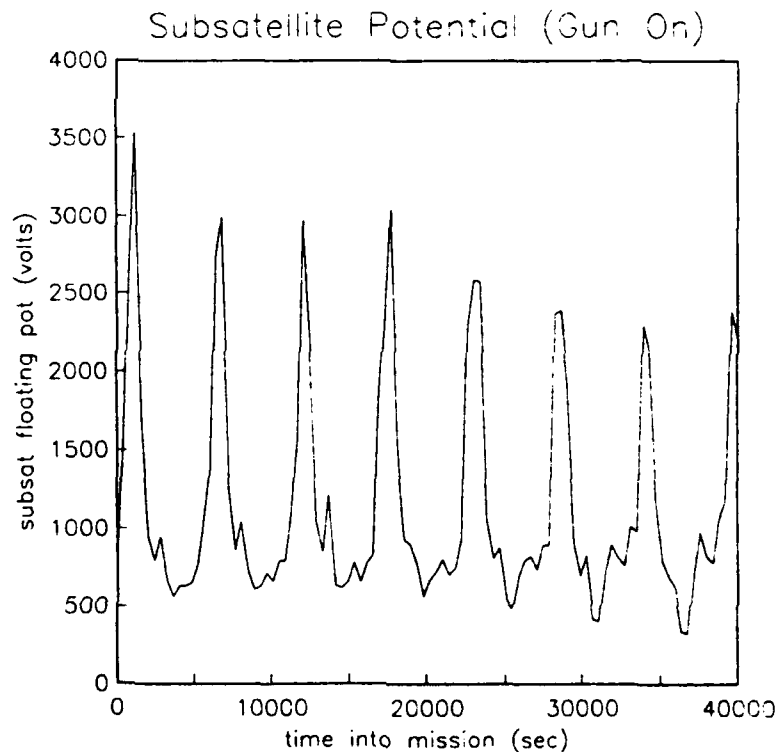


Figure 7.1 The subsatellite potential as a function of time. The perveance of the gun is 3.8×10^{-6} , and the net resistance of the subsatellite paint, tether wire, and shunt is $10 \text{ M}\Omega$.

		Ambient Plasma	Update DoTable HELP! Problem: spree	
Mission Dates			Orbital Position	
Start Date		Absolute Date	Altitude:	400.41
Year: 1991		Year: 1991	Longitude:	66.30
Day: 335		Day: 335	Latitude:	26.68
Univ Time: 0		Univ Time: 1125	Sunspot:	104.
Time into Mission				
1125.0				
Plasma Environment From IRI86				
Species	Density			
o+	3.465E+10			
h+	3.762E+10	Electron Temperature: 8.166E-02		
he+	4.180E+09	Ion Temperature: 7.597E-02		
o2+	0.000E+00			
co+	0.000E+00			
e-	7.645E+10			

Figure 7.2 EPSAT screen that shows the plasma environment at the high potential point in the orbit.

View Parameters		Floating Potentials		Update DoTable HELP! Problem: spree				

Time into Mission		Orbital Position		----- Plasma Environment Summary -----				
Altitude: 400.41		Species Density		Min Max				
1125.0 Longitude: 66.30		o+		3.47E+10 5.11E+10 1.90E+12				
Latitude: 26.68		h+		3.76E+10 5.52E+10 1.03E+12				
Magnetic Field (B)		Velocity		e-				
X: 0.04 X: 7680.40		Temperatures		Thermal Currents				
Y: 0.28 Y: 0.00		Ion: 7.6E-02		Ion: 8.328E-06				
Z: -0.24 Z: 4.92		Electron: 8.2E-02		Electron: -5.844E-04				
Mag: 3.7E-01 Mag: 8.7E+03								

Object Name	Object X	Object Y	Object Z	Object Radius	Bias Voltage	V X B Voltage	Floating Potential	Current
nose	-14.0	0.0	2.0	3.6	0.000E+00	0.000E+00	-335.9	0.
body	0.0	0.0	4.0	4.8	0.003E+00	4.231E-01	-335.4	0.
wing	0.0	0.0	0.5	1.4	0.000E+00	-3.214E-01	-336.2	0.
tail	7.5	0.0	10.0	2.4	0.000E+00	1.803E+00	-334.1	0.
engines	10.5	0.0	4.0	3.6	0.000E+00	4.217E-01	-335.5	2.987E-02
spree	0.0	0.0	8.5	0.7	0.000E+00	1.379E+00	-334.5	6.027E-04
epsat	0.0	0.0	2.0e4	0.7	0.000E+00	4.250E+03	3609.	-3.047E-02

Figure 7.3 EPSAT floating potential screen. This screen summarizes the environment, the potentials on each object, and the collected current for each object.

Table 7.1 Variation of floating potential with time.

Time (s)	Subsatellite Potential (V)
1100	3607
1123	3610
1200	3549
1300	3271
1400	2779

Table 7.2 Current collected by the subsatellite at 3609 V in the above environment.

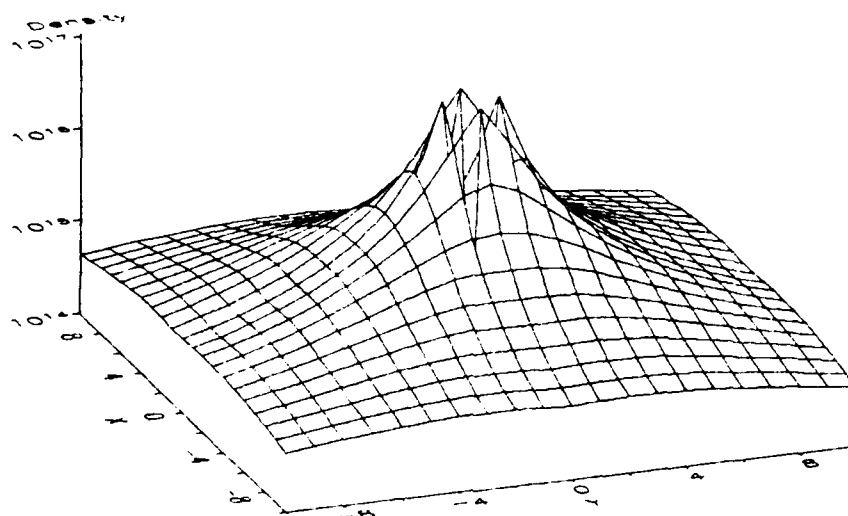
	Collection Radius (m)	Current Collected (A)
Parker-Murphy (Magnetic-Limited)	2.88	-0.0305
Space-Charge-Limited	6.13	-0.276

We also used EPSAT to examine the neutral densities and the likelihood of bulk ionization under conditions of high outgassing, the 2 N in-line thruster, and the 2.5 kg/hr leak.

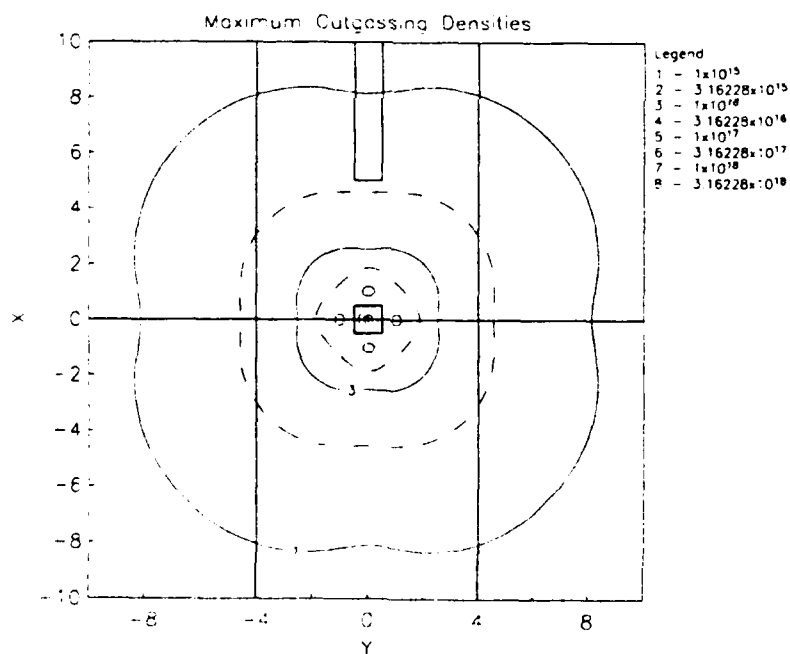
In order to determine if enough neutral atoms will be outgassed from the subsatellite to present a risk of bulk ionization, we examined outgassing densities for the case where all the surfaces emit 0.5 W m^{-2} . This is the outgassing rate of G-10 after exposure to air and provides an upper bound. Figures 7.4(a) and (b) show the neutral densities about the subsatellite due to outgassing at this high rate.

Figure 7.5 is the neutral column density EPSAT screen. The screen shows that the column density of outgassed neutrals from a point just outside the subsatellite (a 1.02 m cube) to a point 2.88 m away (the Parker-Murphy radius) is 1.6×10^{17} . With a cross section of 3×10^{-20} , the ionization fraction (number of ionizations as a fraction of the number needed to cause ionization) is 0.0048. EPSAT (ionization screen) estimates the ionization fraction to be 0.15 when the space-charge sheath size is used as the average path length. Since breakdown is expected when the ionization fraction approaches 1 and the outgassing rate used is orders of magnitude higher than expected, no bulk ionization is expected from outgassing alone.

Maximum Outgassing Neutrals



(a)



(b)

Figure 7.4 Neutral densities about the subsatellite from outgassing at 0.5 W m^{-2} , which is a maximal rate. (a) is a 3-dimensional plot, and (b) is a contour plot. The units of position are meters and of density are molecules per cubic meter.

		Neutral Column Density		Update DoTable HELP! Problem:spree	
Time into Mission 1125.0	Absolute Date Year: 1991 Day: 335 Univ Time: 1125	Orbital Position Altitude: 400.41 Longitude: 66.30 Latitude: 26.68		Total Ambient Neutral Density 1.200E-14	
Column Parameters Length: 2.88 Origin Direction X: 0.51 Theta: 90.0 Y: 0. Phi: 0.0 Z: 2.00E+04		Column Display Display Length 2.88 Top View (XY Plane) Front View (YZ Plane) Right Side View (XZ Plane)		Integration Parameters Number of Points 50 Spacing of Points Log	
Point Density Along Column Distance from Column Origin 1.27		Density 2.758E+16		Column Density 1.613E+17	

Figure 7.5 EPSAT neutral column density screen for outgassing only.

We used the EPSAT nozzle model to model one nozzle of the 2 N in-line thruster on the subsatellite. Figure 7.6 shows the parameters used in the model. Figures 7.7 show the gas density about the subsatellite with operation of one nozzle of the 2 N in-line thruster only. We computed column densities for the thruster gas. The computations are shown in figure 7.8. The column density for a 2.88 m column offset from the axis of the nozzle by 0.51 m is 5×10^{20} . The column density for a 2.88 m column normal to the axis of the nozzle starting 0.51 m from the nozzle is 6×10^{17} .

Change Nozzle		Nozzle		Update DoTable HELP!	
Nozzle Name: In_Line_2N		Analysis		Problem: spree	

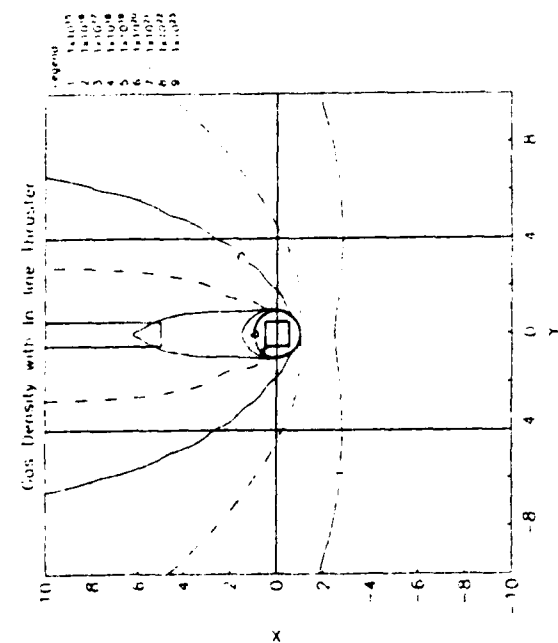
Nozzle	---- Nozzle Direction ----			Neutral Relative	
Position	Spher. Angles	Unit Vector		Species Abundance	
X: 0.0	Theta: 90.0	X: 1.0	Add Species	-----	
Y: 0.0	Phi: 0.0	Y: 0.0	Delete Species	n2	1.00
Z: 20000.0		Z: 0.0			

Input Parameters					
Length: 1.700E-02		Stagnation Temp: 1.730E+02			
Exit Radius: 4.560E-03		Stagnation Press: 1.700E+06			
Exit Mach Number: 6.940E+00					

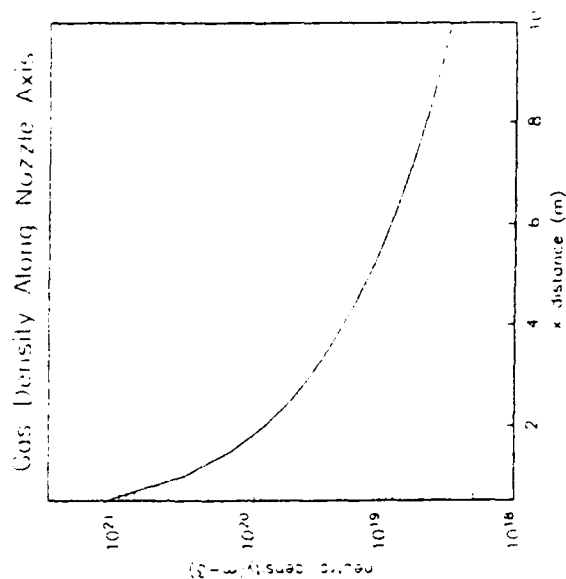
Derived Parameters					
Throat Radius: 4.555E-04		Number Flow Rate: 5.998E+22			
Thrust: 1.91		Mass Flow Rate: 2.790E-03			
Area Ratio: 100.		Gamma: 1.40			

Density From the Nozzle					
Origin	Spherical Coord		Cartesian Coord		
X: 0.	Rho: 0.	X: 0.	Total Neutral		
Y: 0.	Theta: 0.	Y: 0.	Density		
Z: 2.000E+04	Phi: 0.	Z: 2.000E+04	1.931E+24		

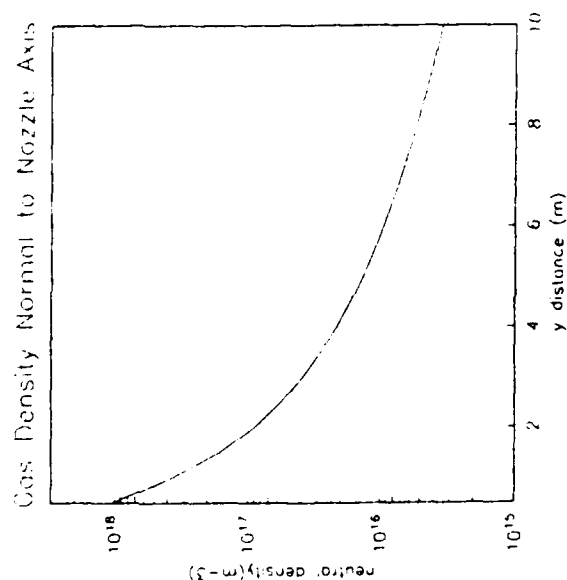
Figure 7.6 Nozzle model screen showing parameters used to model one nozzle of the 2 N in-line thruster.



(a)



(b)



(c)

Figure 7.7 Gas densities due to one nozzle of the 2 N in-line thruster. (a) is a contour plot. (b) and (c) show the gas density along the thruster axis and normal to the nozzle axis. All distances are in meters and all gas densities are in molecules per cubic meter.

		Neutral Column		Update DoTable HELP!
		Density		Problem:spre

Time into		Absolute Date		Orbital Position
Mission		Year:	1991	Altitude: 400.41
1125.0		Day:	335	Longitude: 66.30
		Univ Time:	1125	Latitude: 26.68

Column Parameters		Column Display		Integration Parameters
Length: 2.88		Display Length		
Origin	Direction		2.88	
X: 0.51	Theta: 90.0		Top View (XY Plane)	
Y: 0.	Phi: 0.0		Front View (YZ Plane)	
Z: 2.00E+04			Right Side View (XZ Plane)	

Point Density Along Column				
Distance from	Density		Column Density	
Column Origin	9.744E+19		5.180E+20	
1.27				

(a)

		Neutral Column		Update DoTable HELP!
		Density		Problem:spre

Time into		Absolute Date		Orbital Position
Mission		Year:	1991	Altitude: 400.41
1125.0		Day:	335	Longitude: 66.30
		Univ Time:	1125	Latitude: 26.68

Column Parameters		Column Display		Integration Parameters
Length: 2.88		Display Length		
Origin	Direction		2.88	Number of Points
X: 0.	Theta: 90.0		Top View (XY Plane)	50
Y: 0.51	Phi: 90.0		Front View (YZ Plane)	Spacing of Points
Z: 2.00E+04			Right Side View (XZ Plane)	Log

Point Density Along Column				
Distance from	Density		Column Density	
Column Origin	1.158E+17		6.299E+17	
1.27				

(b)

Figure 7.8 Column density screens for the computation of the column density (a) along the nozzle axis and (b) normal to the nozzle axis.

Nozzle parameters for the other thruster nozzles were also determined. EPSAT screens describing each of the nozzles are shown in figure 7.9 through 7.12.

Change Nozzle		Nozzle		Update DoTable HELP!	
Nozzle Name: In_Line_1N		Analysis		! Problem: spree	

Nozzle		---- Nozzle Direction ----		Neutral Relative	
Position		Spher. Angles	Unit Vector	Species Abundance	
X: 0.0	Theta: 90.0	X: 1.0	Add Species	-----	
Y: 0.0	Phi: 0.0	Y: 0.0	Delete Species	n2	1.00
Z: 20000.0		Z: 0.0			
----- Input Parameters -----					
Length: 1.200E-02		Stagnation Temp: 1.730E+02			
Exit Radius: 3.230E-03		Stagnation Press: 1.700E+06			
Exit Mach Number: 6.940E+00					
----- Derived Parameters -----					
Throat Radius: 3.226E-04		Number Flow Rate: 3.009E+22			
Thrust: 0.959		Mass Flow Rate: 1.400E-03			
Area Ratio: 100.		Gamma: 1.40			
----- Density From the Nozzle -----					
Origin	Spherical Coord		Cartesian Coord		
X: 0.	Rho: 0.	X: 0.	Total Neutral		
Y: 0.	Theta: 0.	Y: 0.	Density		
Z: 2.000E+04	Phi: 0.	Z: 2.000E+04	1.931E+24	Leak	
Parameters					

Figure 7.9 EPSAT screen showing nozzle parameters for one nozzle of the 1 N in-line thruster.

Change Nozzle		Nozzle		Update DoTable	HELP!
Nozzle Name: In_Plane		Analysis		Problem: spree	

Nozzle	---- Nozzle Direction ----			Neutral Relative	
Position	Spher. Angles	Unit Vector	Species Abundance		
X: 0.0	Theta: 90.0	X: 1.0	Add Species	-----	
Y: 0.0	Phi: 0.0	Y: 0.0	Delete Species	n2	1.00
Z: 20000.0		Z: 0.0			
----- Input Parameters -----					
Length:	1.250E-02	Stagnation Temp:	1.730E+02		
Exit Radius:	1.000E-02	Stagnation Press:	4.300E+05		
Exit Mach Number:	6.630E+00				
----- Derived Parameters -----					
Throat Radius:	1.105E-03	Number Flow Rate:	9.926E+22		
Thrust:	2.83	Mass Flow Rate:	4.152E-03		
Area Ratio:	61.9	Gamma:	1.40		
----- Density From the Nozzle -----					
Origin	Spherical Coord	Cartesian Coord			
X: 0.	Rho: 0.	X: 0.	Total Neutral		
Y: 0.	Theta: 0.	Y: 0.	Density		
Z: 2.000E+04	Phi: 0.	Z: 2.000E+04	6.002E+23		

Figure 7.10 EPSAT screen showing nozzle parameters for one nozzle of the in-plane thruster.

```

Change Nozzle | Nozzle | Update DoTable HELP!
Nozzle Name: Out_of_Pla | Analysis | Problem: spree
-----
Nozzle | ---- Nozzle Direction ---- | Neutral Relative
Position | Spher. Angles | Unit Vector | Species Abundance
X: 0.0 | Theta: 90.0 | X: 1.0 | Add Species
Y: 0.0 | Phi: 0.0 | Y: 0.0 | Delete Species n2 1.00
Z: 20000.0 | Z: 0.0
-----
Input Parameters
Length: 1.955E-02 Stagnation Temp: 1.730E+02
Exit Radius: 1.150E-02 Stagnation Press: 1.150E+06
Exit Mach Number: 8.730E+00
-----
Derived Parameters
Throat Radius: 6.823E-04 Number Flow Rate: 9.106E+22
Thrust: 2.95 Mass Flow Rate: 4.236E-03
Area Ratio: 284. Gamma: 1.40
-----
Density From the Nozzle
Origin | Spherical Coord | Cartesian Coord
X: 0. | Rho: 0. | X: 0. Total Neutral
Y: 0. | Theta: 0. | -> Y: 0. Density
Z: 2.000E+04 | Phi: 0. | Z: 2.000E+04 4.529E+23

```

Figure 7.11 EPSAT screen showing nozzle parameters for the out-of-plane thruster.

```

Change Nozzle | Nozzle | Update DoTable HELP!
Nozzle Name: Yaw | Analysis | Problem: spree
-----
Nozzle | ---- Nozzle Direction ---- | Neutral Relative
Position | Spher. Angles | Unit Vector | Species Abundance
X: 0.0 | Theta: 90.0 | X: 1.0 | Add Species
Y: 0.0 | Phi: 0.0 | Y: 0.0 | Delete Species n2 1.00
Z: 20000.0 | Z: 0.0
-----
Input Parameters
Length: 2.990E-02 Stagnation Temp: 1.730E+02
Exit Radius: 1.150E-02 Stagnation Press: 2.700E+05
Exit Mach Number: 9.250E+00
-----
Derived Parameters
Throat Radius: 5.964E-04 Number Flow Rate: 1.634E+22
Thrust: 0.531 Mass Flow Rate: 7.599E-04
Area Ratio: 372. Gamma: 1.40
-----
Density From the Nozzle
Origin | Spherical Coord | Cartesian Coord
X: 0. | Rho: 0. | X: 0. Total Neutral
Y: 0. | Theta: 0. | -> Y: 0. Density
Z: 2.000E+04 | Phi: 0. | Z: 2.000E+04 8.097E+22

```

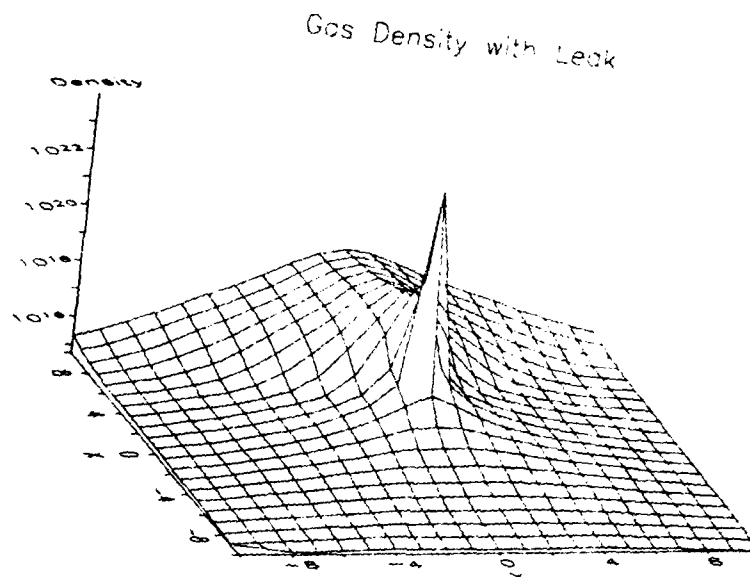
Figure 7.12 EPSAT screen showing nozzle parameters for one nozzle of the yaw thruster.

A 2 1/2 kg per hour leak in one of the thrusters has been reported. The parameters of the 1 N in-line thruster, with a lower pressure, define a nozzle that loses gas at this rate. The EPSAT screen describing this nozzle is shown in figure 7.13. Note that this nozzle gives rise to 0.5 N of thrust. Figure 7.14 shows the neutral densities about the subsatellite due to this leak. At the high potential point, EPSAT computes the ionization fraction to be 2718, which is much greater than 1. Therefore, the leak is expected to cause a bulk discharge.

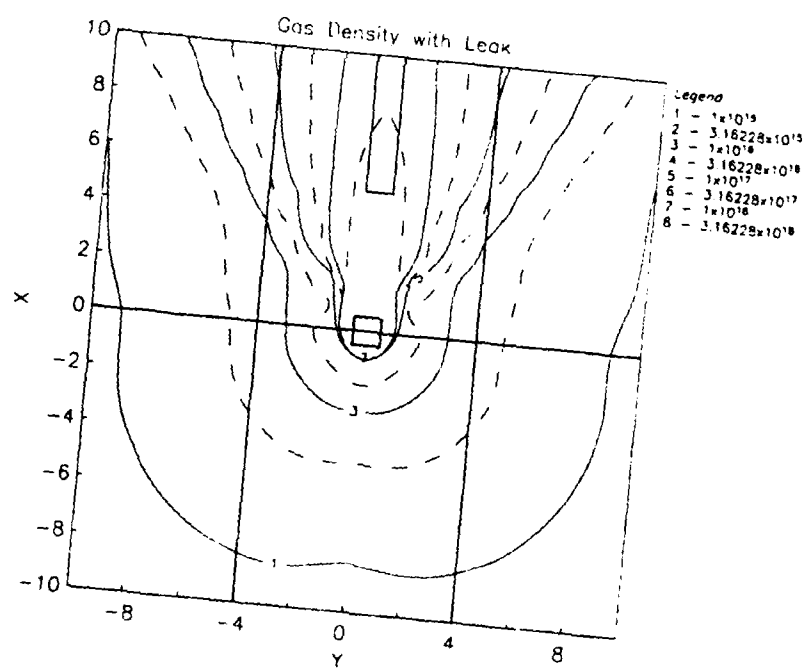
Change Nozzle		Nozzle		Update DoTable HELP!	
Nozzle Name: Leak		Analysis		Problem: spree	

Nozzle		---- Nozzle Direction ----			Neutral Relative
Position		Spher. Angles	Unit Vector		Species Abundance
X: 0.0	Theta: 90.0	X: 1.0	Add Species	-----	
Y: 0.0	Phi: 0.0	Y: 0.0	Delete Species	n2	1.00
Z: 20000.0		Z: 0.0			
----- Input Parameters -----					
Length: 1.200E-02		Stagnation Temp: 1.730E+02			
Exit Radius: 3.230E-03		Stagnation Press: 8.500E+05			
Exit Mach Number: 6.940E+00					
----- Derived Parameters -----					
Throat Radius: 3.226E-04		Number Flow Rate: 1.505E+22			
Inlet: 0.479		Mass Flow Rate: 6.999E-04			
Area Ratio: 100.		Gamma: 1.40			
----- Density from the Nozzle -----					
Origin	Spherical Coord		Cartesian Coord		
X: 0.	Rho: 0.	X: 0.	Total Neutral		
Y: 0.	Theta: 0.	Y: 0.	Density		
Z: 2.000E+04	Phi: 0.	Z: 2.000E+04	9.654E+23		

Figure 7.13 EPSAT screen showing nozzle parameters used to describe the thruster leak.



(a)



(b)

Figure 7.14 Neutral densities due to "leak". (a) is a 3-dimensional plot, and (b) is a contour plot.